Reliability based design methodology incorporating residual strength prediction of structural fiber reinforced polymer composites under stochastic variable amplitude fatigue loading

Nathan L. Post

Dissertation submitted to the Faculty of the
Virginia Polytechnic Institute and State University
in partial fulfillment of the requirements for the degree of

Doctor of Philosophy
in
Engineering Mechanics

Scott W. Case, Co-Chair
John J. Lesko, Co-Chair
Michael Hyer
Surot Thangjitham
Judy Riffle

March 18, 2008
Blacksburg, Virginia

Keywords: FRP, Random Loading, Probability of failure, Spectrum, LRFD

Reliability based design methodology incorporating residual strength prediction of structural fiber reinforced polymer composites under stochastic variable amplitude fatigue loading

Nathan L. Post

ABSTRACT

The research presented in this dissertation furthers the state of the art for reliability-based design of composite structures subjected to high cycle variable amplitude (spectrum) fatigue loads. The focus is on fatigue analyses for axially loaded fiber reinforced polymer (FRP) composites that contain a significant proportion of fibers in the loading direction and thus have fiber-direction dominated failure. The four papers presented in this dissertation describe the logical progression used to develop an improved reliability-based methodology for fatigue-critical design. Throughout the analysis extensive experimental fatigue data on several material systems was used to verify the assumptions and suggest the path forward.

A comparison of 12 fatigue model approaches from the literature showed that a simple linear residual strength approach (Broutman and Sahu) provides an improvement in fatigue life prediction compared to the Palmgren-Miner rule, while more complex residual strength models did not consistently improve on Broutman and Sahu. Evaluation of the effect of load history randomness on fatigue life was made using experimental results for spectra in terms of the first order autocorrelation of the stress events. For approximately reversed Rayleigh distributed fatigue loading, load sequence was not critical in the material behavior. Based on observations of empirical data and evaluation of the micro-mechanics deterioration and failure phenomena of FRP composites under fatigue loading, a new residual strength model for the tension and compression under any load history was proposed. Then this model was implemented in a stochastic framework and a method was proposed to enable calculation of the load and resistance factor design (LRFD) parameters for realistic reliabilities with relatively few computations. The proposed approach has significant advantages over traditional lifetime-damage-sum-based reliability analysis and provides a significant step toward enabling more accurate reliability-based design with composite materials.

This research was conducted with support from the National Science Foundation Interdisciplinary Graduate Education Research and Traineeship (Award # DGE-0114346) and the Office of Naval Research (Award # N00014-06-1-0812). Note: The opinions expressed herein are the views of the author and should not be interpreted as the views of the Naval Surface Warfare Center or the Department of the Navy, nor of the National Science Foundation.

Acknowledgments

I gratefully acknowledge the continuing support, inspiration, and direction provided by my advisors Dr. Scott Case and Dr. Jack Lesko, without which this dissertation and the papers included would not have been possible. I thank my other committee members Dr. Michael Hyer, Dr. Surot Thangjitham and Dr. Judy Riffle for reviewing my dissertation. Thanks to Jason Cain, Hazen White, Brian Clements and Adam Vittum, who had direct parts in making this research happen, and all the other Materials Response Group students who are always available to help out in the lab or discuss a research issue. And, of course, none of this would be possible without Beverly Williams handling paperwork and travel arrangements, Joyce Smith helping with the Graduate School paper work, and Mac McCord who has always managed to keep the MTS load-frames going. Also thanks to Florian Riebel for teaching me LaTeX which was used to compile this document.

I also send a big thank you to my parents Irwin Post and Diane Post, grandparents Dan and Frieda Post, and friends Laurel Travis and Michael Taaffe, for providing valuable insight during technical discussions, copy editing, and most of all for their moral support that gave me the strength to complete this dissertation.

Contents

List of Figures

List of Tables

Chapter 1

Introduction

The research presented in this dissertation furthers the state of the art for reliability-based design of composite structures subjected to high cycle variable amplitude (spectrum) fatigue loads. The focus is on fatigue analysis for axially loaded fiber reinforced polymer (FRP) composites that contain a significant proportion of fibers in the loading direction and thus exhibit fiber direction dominated failure. Present fatigue models and reliability analysis for composites are evaluated and a new residual strength model is proposed that represents the tensile and compressive residual strength of a composite under any load sequence. Finally a reliability-based design framework implementing the new model is proposed. Throughout this research, extensive experimental data sets have been used to develop empirical theories and evaluate the models results.

The body of this dissertation is presented as four separate papers that have been or will be submitted to academic journals as indicated at the beginning of each chapter. Chapter 2 presents a comprehensive review of available models in the literature for calculating the fatigue life of FRP composite materials under spectrum fatigue loading and serves as the primary literature review for the dissertation. Additional literature references relevant to the specific topics discussed in subsequent chapters are provided in each paper. In addition to being a review article, the first paper also provides the results of analyzes that compare the predictive performance of 12 models for spectrum fatigue life predictions in four material systems. Chapter 3 focuses on the issue of the significance of load order on the damage and resulting residual strength of composites subjected to spectrum fatigue. In this paper, the statistical first order autocorrelation is proposed as a measure of load ordering in a spectra. Chapter 4 develops a new residual strength model for the variable amplitude fatigue of composites that calculates the tensile and compressive residual strength as a function of any given load history. The model is tested using experimental spectrum fatigue data for two material systems and several load histories. In Chapter 5 a reliability based design methodology is developed using the new residual strength model to determine appropriate load and resistance factor design (LRFD) knockdowns for a desired reliability under stochastically

described spectrum fatigue loading. An appendix that describes the experimental methods used for generating the Virginia Tech data set (labeled VT8084) is provided and the data is publicly available as a second appendix in the form of a Microsoft Excel spreadsheet.

Note to the reader: Since each chapter was written as a separate journal article, they reference the other chapters in this dissertation as articles in the bibliography. Reference [1] refers to Chapter 2, reference [2] refers to Chapter 3, reference [3] refers to Chapter 4 and reference [4] refers to Chapter 5. The dissertation and its appendix which contains the VT8084 data set are also referenced in the individual papers as [5]. In addition, while the nomenclature overlaps between the articles, it is not exactly the same and some symbols have different meanings in each chapter. A table of the terminology used in each article is provided near the beginning of the chapter and should be referred to accordingly.

Chapter 2

Modeling the Variable Amplitude Fatigue of Composite Materials: a Review and Evaluation of the State of the Art for Spectrum Loading

Modeling the Variable Amplitude Fatigue of Composite Materials: a Review and Evaluation of the State of the Art for Spectrum Loading

N.L. Post, S.W. Case, J.J. Lesko
MC 219, Virginia Polytechnic Institute and State University, Blacksburg, VA 24061, USA

ABSTRACT

In this article, we review the experimental research and modeling of fiber reinforced polymer composite materials subjected to variable amplitude fatigue. In general, these models are empirical or phenomenological and contain parameters that must be determined using constant, and in some cases variable, amplitude fatigue data for the material system in question. In many cases, the authors who proposed these models simply fit them to their experimental variable amplitude results and thus their predictive ability has remained uncertain. The predictive accuracy of the fatigue models examined in this article was compared by applying them to four material systems for which extensive fatigue data was available. Several approaches are rejected because the data required to fit them are not available or their formulation prevents straightforward application to a spectrum loading with blocks of one cycle in length. Four damage accumulation rules and eight residual strength approaches are fit to the static, constant amplitude fatigue, residual strength, and two block repeated fatigue loading for each data set. Then the models are used to predict the fatigue life under variations of WISPER, WISPERX, and Rayleigh distributed spectrum fatigue loads that were applied experimentally. Results show that the Palmgren-Miner rule is non-conservative in every case and gains in accuracy are possible by using a simple residual strength law such as the one proposed by Broutman and Sahu. More complex residual strength approaches gave more accurate results in some cases, but overall did not provide a significant improvement relative to Broutman and Sahu's model.

This paper will be prepared for submission to the International Journal of Fatigue.

2.1 Introduction

Understanding the fatigue degredation of materials is critical in many applications to ensuring the long term reliability of a component or structure. As fiber reinforced polymer (FRP) composite materials become more common in high cycle fatigue applications including ship hull, aircraft, and wind turbine blade structures, the ability to make accurate predictions of fatigue durability is critical to the design optimization process. Characterization of the statistical distribution and ordering of applied loads on a structure can be made using experimental measurements and structural simulations. Although a material can be tested under a variable amplitude spectrum, that data is only applicable to a specific loading scenario. Traditionally, fatigue characterization of a material is performed under constant amplitude sinusoidal loading. Thus, it is desirable to make variable amplitude predictions for an expected loading sequence (spectrum) using readily collected constant amplitude experimental fatigue data for the material system of interest.

Numerous empirical and phenomenological models have been introduced over the past 40 years of fatigue studies for composite materials. In most cases, authors had limited experimental data available and often any empirically determined model parameters are fit to the variable amplitude data they are modeling. Thus the relative accuracy remains uncertain between the approaches in the literature. Unfortunately, due to the wide variety of component materials, manufacturing methods, and laminate design, developing a universal understanding of the performance of spectrum fatigue models for fiber reinforced polymer composites is very difficult. As a result, many models are developed with a specific material and loading configuration in mind and their generalization to other loading cases also remains uncertain.

Many of the *damage accumulation* based approaches to model the variable amplitude fatigue response of composites have been based on theories developed for homogeneous metallic materials that have been reviewed extensively by Fatemi and Yang [6]. The other two categories of models for variable amplitude loading are *residual strength* and *residual stiffness* approaches based on the distributed damage observed in FRP composites under fatigue loading. In the FRP composite material literature, comparisons of variable amplitude fatigue prediction models have been limited in scope both in terms of the number of models considered and the data sets used to fit them and compare results. Found and Quaresimin [7] compared the Palmgren-Miner (PM) [8], Broutman-Sahu (BM) [9], Marco-Starkey (MS) [10], and Hashin and Rotem (HR) [11] methods for two stage (high amplitude followed by low and low amplitude followed by high) block loading of a woven carbon fiber composite. Epaarachchi and Clausen [12] compared their model [13] to the PM, BM and HR approaches under block loading. Sarkani et al. [14] compared several cumulative damage, residual strength, and residual stiffness models for predicting the fatigue life of a notched composite laminate subjected to a narrow band Gaussian loading sequence. However, they lacked residual strength data to fit non-linear model parameters and simply chose to calculate the predicted life over a range of parameter values. Overall, Sarkani et al. concluded based on a very small data set that the models gave similar results to PM and were generally

conservative for this case [14]. Various "classical fatigue analysis" topics that are relevant to spectrum fatigue loading have been discussed by Filis et al. [15] including rainflow analysis and cycle "mix" event counting in the context of composite laminates under spectrum loading. Recently, a review and comparison of methods for modeling the residual strength distribution of composite materials under constant amplitude fatigue in composites was published by Philippidis and Passipoularidis [16]. In the present research, we provide a broad comparison of the methods that have been employed in variable amplitude fatigue modeling in composite materials under axial loading and compare the predictive ability of a subset of these models for spectrum loading using extensive sets of experimental fatigue data on four different laminates.

2.2 Background to the Exercise

2.2.1 Experimental approaches to variable amplitude fatigue

Most experimental studies of variable amplitude loading in composite materials have focused on loading that consists of two or more constant amplitude blocks with two to four stress levels and R-ratios [7, 9, 13, 17, 18, 19, 20, 21, 22, 23, 24, 25, 26, 27, 28, 29, 30]. While simpler to apply in the laboratory, and perhaps offering a stepping stone between constant amplitude loading and spectrum loading, these block loading tests are not representative of realistic loading situations and may not even generate the same type damage state in the material. Experimental studies of stochastic fatigue spectra in homogeneous materials (metals) include those by Sarkani and Lutes [31], Kihl, Sarkani and Beach [32], Svensson [33], and Sunder [34]. In these studies, a random loading spectrum was generated based on a prescribed distribution of fatigue loads. There are only a handful of experimental studies of composites under this type of generalized loading including those by Sarkani, Kihl and colleagues [35, 14, 36], Aboussaleh and Boukhili [37], Himmel [38], Philippidis and Vassilopoulos [39], Sonsino and Moosbrugger [40] and the recent work we have undertaken [2]. The majority of available experimental data on spectrum loading of composites [41, 39, 42, 43, 44, 45, 46, 47, 48, 49, 15, 50, 51] have been performed using standard loading spectra including FALSTAFF created for fighter aircraft, and WISPER and WISPERX generated to represent the flap direction loading of a mid-sized wind turbine blade [52, 53]. These fixed sequence standard spectra are generated by compiling fatigue loading data for a number of typical structures and are intended as a method for comparison of materials and models under a representative realistic fatigue loading.

2.2.2 Nomenclature

In order to make comparisons between different modeling approaches easier, equations have been translated from their original nomenclature to a set of standard nomenclature listed in Table 5.1.

Table 2.1: Fatigue Nomenclature

Symbol	Description
T-T	tension-tension loading ($0 < R < 1$)
C-C	compression-compression loading ($R > 1$)
T-C	tension-compression loading ($R < 0$). Fully reversed: $R = -1$
f	fatigue frequency
t	time
σ	stress (general)
σ_p	maximum (peak) applied stress during a fatigue cycle
σ_v	minimum (valley) applied stress during a fatigue cycle
$\sigma_m = \frac{1}{2}(\sigma_p + \sigma_v)$	mean applied stress during a fatigue cycle
$\sigma_a = \frac{1}{2}(\sigma_p - \sigma_v)$	stress amplitude during fatigue cycle
$\sigma_{range} = \sigma_p - \sigma_v = 2\sigma_a$	applied stress range during a fatigue cycle
$R = \sigma_v/\sigma_p$	R-ratio (definition)
n	cycles applied
N	cycles to failure under a given loading condition
D	damage parameter
subscript i	indicates quantity for the i^{th} loading step
d_i	damage increment for step i
S_u	initial ultimate strength (prior to fatigue)
S_{uts}	initial ultimate tensile strength
S_{ucs}	initial ultimate compression strength
S_r	residual strength
$Fa = \sigma_p/S_u$	normalized applied stress
$Fr = S_r/S_u$	normalized residual strength
E	Young's modulus
E_t	initial tensile modulus
E_c	initial compression modulus
E_0	initial modulus
E_f	fatigue modulus
α	Weibull distribution shape parameter
S_0, N_0	Weibull scale parameters for strength, life
F(x)	cumulative distribution function of x

continued on next page

continued from previous page

Symbol	Description
f(x)	probability distribution of x
G(x), H(x), ...	functions of x
a	Power law S-N curve slope
b	Power law S-N curve intercept
M_e	Model prediction error relative to experiment

2.2.3 Fatigue terminology

Fatigue in materials is caused by repeated loading and unloading cycles to maximum stresses below the ultimate strength of a material. This cyclic loading causes a progressive degradation of the material properties and eventual failure. In many constant amplitude load controlled fatigue experiments, a specimen is loaded sinusoidally in time with the stress, $\sigma(t) = \sigma_m + \sigma_a \sin(2\pi t/f)$. Common parameters for describing cycling loading are shown in Figure 2.1. Different loading regimes characterized by R-ratio are shown graphically in Figure 2.2. Failure is typically defined by the complete rupture of the material so that it can no longer support any stress ($E = 0$). Some researchers choose to perform displacement controlled tests where the maximum and minimum strain is the independent control variable and the stress is dependent on the material stiffness. Often failure is defined when the stiffness decreases below a certain threshold because in many cases a dramatic failure does not occur under displacement controlled fatigue tests.

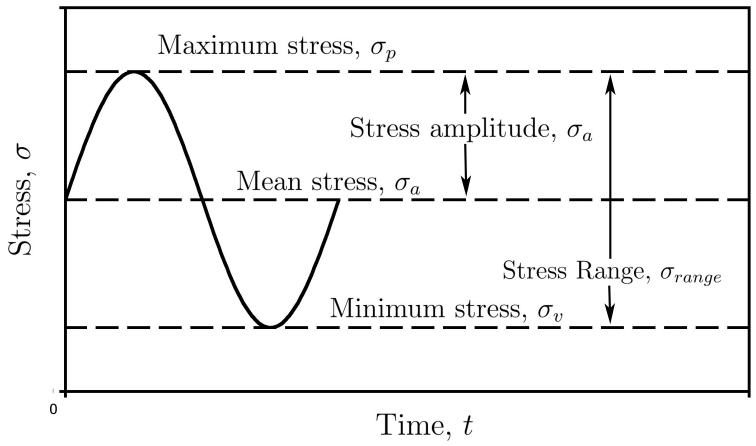

Figure 2.1: Illustration of sinusoidal loading and the relevant terminology to describe it

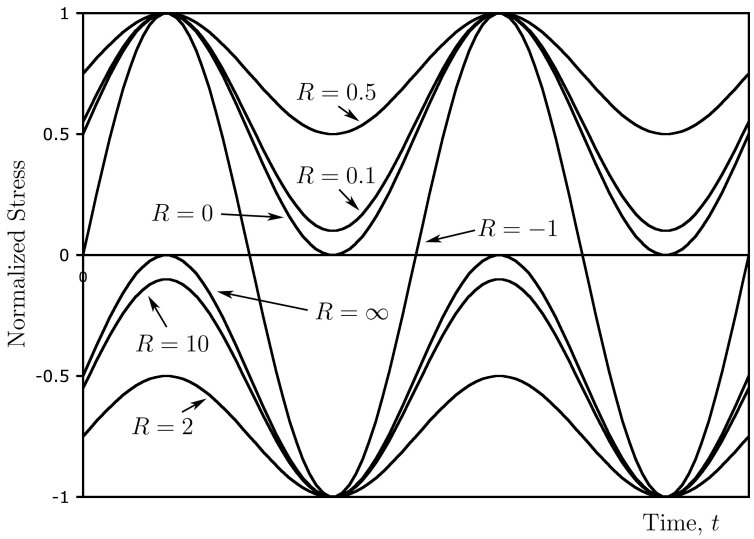

Figure 2.2: Illustration of different loading R-ratios normalized to a maximum absolute value stress of 1.0

Most fatigue models require experimental knowledge of the fatigue life under constant amplitude loading equivalent to the current applied cycle. Although fatigue tests are performed under constant amplitude stress (independent variable) and the resulting fatigue lifetime to failure, N, is recorded (dependent variable), fatigue data is traditionally plotted with the maximum stress or stress amplitude on the vertical axis and cycles to failure on the horizontal axis (for example, see Figure 2.3). A variety of approaches for empirically fitting this "S-N" data are used in the literature including exponential or power law relationships and sometimes more complex formulations that attempt to include frequency, fiber orientation and other parameters. The fatigue life curves can then be represented for various R-ratios on a constant life plot with σ_m on the horizontal axis, σ_a on the vertical axis and lines indicating constant fatigue life (see Figure 2.7). The desired fatigue life at a given R and σ_p can then be determined by linear interpolation or more complex equations fit to the entire constant life plot.

A new and noteworthy alternative for representing constant amplitude fatigue data was presented by Vassilopoulos et al. [54]. These authors used an Artificial Neural Network (ANN) to come up with an algorithm for the fatigue life at an arbitrary loading and stress level. Using an ANN trained with a random sampling of 50% of their experimental constant amplitude fatigue data at various R-ratios and angle ply fiber orientations, the neural network was able to accurately construct constant life diagrams for each fiber orientation as when compared to traditional S-N curve based plots fit to the entire data set [54].

2.3 Damage Accumulation

This category of fatigue models includes those formulations based exclusively on the calculation of a non-dimensional damage parameter, D, related to the amount of life a composite has used up. In most cases, D is initially 0 and increases over the fatigue life until failure is predicted to occur when $D = 1.0$.

2.3.1 Palmgren-Miner

The earliest method still in wide use for analyzing variable amplitude fatigue of materials is the Palmgren-Miner [8] linear damage accumulation rule (hereafter PM). In this approach, also referred to as "Miner's rule," the accumulated damage, d_i, in a given loading block of length n_i cycles, is a linear fraction of the number of cycles to failure, N_i, at the i stress level:

$$D = \sum_i d_i = \sum_i \frac{n_i}{N_i} \tag{2.1}$$

Failure is predicted when the cumulative damage, $D = 1.0$. This model is simple in that in only requires an S-N curve for a given R-ratio or more generally a constant life diagram to make variable amplitude fatigue life predictions. The PM rule is load order independent and thus produces the same damage sum and failure prediction for a given set of loads regardless of their sequence.

Numerous experimental studies including [55] and [9] have shown the PM approach can be highly inaccurate for block loading in both homogeneous materials and composites (conservative in some cases, non-conservative in others). Experiments performed under spectrum loading has shown Miner's rule to be highly not conservative, sometimes by more than an order of magnitude [56, 14]. Yet, over 60 years since its first publication by Miner in 1945 [8], the Palmgren-Miner rule is still the most extensively used method used by engineers for fatigue prediction in reliability based design analysis [57, 58, 59, 60, 61, 62, 63, 39]. Structural fatigue damage analysis using finite element models also often employs PM to evaluate failure [64, 65, 66]. In addition, PM also remains the standard by which research on all other approaches for variable amplitude loading are compared.

Many variations on linear damage accumulation have been proposed for homogeneous materials [6]. Hwang and Han [67] provide a review of some of these approaches applied to fatigue in composites. However the orthotropic properties of each lamina and tendency for distributed damage rather than dominate flaw crack growth make the assumptions in more sophisticated damage mechanics approaches for homogenous materials invalid for most FRP composites.

2.3.2 Marco-Starkey

The Marco-Starkey [10] rule (MS) is a variation of PM:

$$D = \left(\frac{n}{N}\right)^C \tag{2.2}$$

where the parameter C is a function of stress level and R applied. In applying a non-linear damage law like MS, the equivalent number of cycles applied at the new load level must be calculated after each loading step so that in general:

$$D_i = \left(\frac{n_i + n_{eqv,i-1}}{N_i}\right)^{C_i} \tag{2.3}$$

where

$$n_{eqv,i-1} = N_i \left(D_{i-1}\right)^{1/C_i} \tag{2.4}$$

Following this iterative procedure, the level of damage, D, remains constant when transitioning between one cycle or step and the next. For the general case where $C_i \neq 1$ and is a function of stress, the model results will depend on load order and thus it is a non-linear damage accumulation rule. Adam, Gathercole, Reiter and Harris [21][22] extensively explored the application of MS to block loading of graphite/epoxy laminates including a unique approach where they attempted to predict the $R = -1$ T-C fatigue life of the composite using $R = 0.1$ T-T and $R = 10$ C-C constant amplitude and 2 block fatigue data. While PM over-predicted fully reversed lifetimes, the MS approach, fit to two block loading data, was slightly conservative. In the Adam et al. approach, C_i was considered to be a function of R only and constant with respect to the stress level in a given R. The MS damage accumulation law improved the fatigue life predictions over PM, but also required additional block loading cases to fit the non-linear parameters for each case of interest. It should also be noted that it is impossible to determine the actual value of C_i experimentally because D has no physical correlation other than at failure. Instead, based on best fit to block loading fatigue to failure, the ratio's of C_1/C_2 and so on can be found. Adam chose $C = 1$ for tension and then found the value for compression loading from T-T followed by C-C block loading results. Jen and colleagues [20, 68], and Gamstedt and Sjögren [30] have also applied a the MS model to two block loading of graphite composites.

2.3.3 Owen and Howe

Owen and Howe [69] (OH) introduced a damage accumulation model based on their observations of crack development glass reinforced polymer composites:

$$D = \sum_i \left[A\left(\frac{n_i}{N_i}\right) + B\left(\frac{n_i}{N_i}\right)^2\right] \tag{2.5}$$

where A and B are curve fit parameters. In order for $D = 1$ at $n = N$ for constant amplitude fatigue, $A + B = 1$ and thus:

$$D = \sum_i \left[A \left(\frac{n_i}{N_i} \right) + (1 - A) \left(\frac{n_i}{N_i} \right)^2 \right] \tag{2.6}$$

Because the power remains constant, OH is a linear model and the damage can be summed as shown for all the cycles applied. A can be determined using crack damage or perhaps more easily by fitting the model to some type of variable amplitude fatigue loading.

2.3.4 Bond and Farrow

Bond and Farrow [44] considered angle ply and quasi-isotropic graphite composite plates incorporating a metallic fastener under FALSTAFF spectrum fatigue loading. They generalized the Owen and Howe model as:

$$D = \sum_i \left[A \left(\frac{n_i}{N_i} \right) + B \left(\frac{n_i}{N_i} \right)^C \right] \tag{2.7}$$

The parameters A, B, and C, were found that gave the best prediction for experimental results from FALSTAFF based spectra scaled for tensile and compression loading. Bond and Farrow proposed a metric for calculating the parameters based on initial strength and stiffness properties and proposed that for primarily tensile loading:

$$A = B = \|S_{uts}/S_{ucs}\| \tag{2.8}$$

$$C = (S_{uts}(\|S_{uts}/S_{ucs}\| + 1) - S_{uts})/S_{uts} \tag{2.9}$$

and for primarily compression loading:

$$A = B = \|S_{ucs}/E_c\| \tag{2.10}$$

$$C = (S_{uts}(\|S_{uts}/S_{ucs}\| + 1) - \|S_{ucs}\|)/S_{uts} \tag{2.11}$$

Unlike Miner's rule, this approach resulted in conservative lifetime predictions for the repeated spectrum load. Bond and Farrow's approach worked vary well for matrix dominated angle ply laminates, however they found it to be overly conservative for fiber dominated quasi-isotropic laminates, especially under compression fatigue loading [44].

2.3.5 Hashin and Rotem

Hashin and Rotem [11] (HR) developed a set of damage equations based on a concept of equivalent damage lines of the same form as the S-N curve extending from the ultimate stress

or from the fatigue limit points of the curve. When transitioning between stress levels, the constant damage line would be followed to the new stress level and then damage accumulation would proceed from there. Although this model was developed for homogeneous materials, it is general and can be considered for composites. Since the existence of a fatigue limit in composites is uncertain, the approach based on initial strength is more applicable. Based on a power law S-N curve, the HR model can be described generally as:

$$D_i = D_{i-1}^{\frac{\log \sigma_{p,i}}{\log \sigma_{p,i-1}}} + \frac{n_i}{N_i} \tag{2.12}$$

where

$$D_1 = \frac{n_1}{N_1} \tag{2.13}$$

and $\sigma_{p,i}$ is the max stress applied for block i.

2.4 Residual Strength

Residual strength models have a significant philosophical advantage over damage accumulation laws for variable amplitude loading cases because the failure criterion is described in terms of the residual strength S_r and the applied maximum stress σ_p:

$$S_r(n) \leq \sigma_p(n) \rightarrow \text{Failure} \tag{2.14}$$

Thus, life predictions are dependent on the current load as well as damage and improved predictions over damage accumulation models are generally found for large block fatigue loading and cases where a spectrum only has very occasional high loads. Additionally, because the damage is evaluated in terms of a physical quantity, the strength of the specimen, the models can be fit or verified experimentally at intermediate points during the fatigue life.

All residual strength models are based on the assumption that the residual strength is a monotonically decreasing function of the cycles applied and they also make use of the boundary conditions that the initial residual strength equals the static strength, S_u:

$$S_r(0) = S_u \tag{2.15}$$

and that under constant amplitude fatigue, the residual strength at fatigue failure ($n = N$) equals the applied load under constant amplitude fatigue:

$$S_r(N) = \sigma_p \tag{2.16}$$

2.4.1 Strength Life Equal Rank Assumption

Many residual strength approaches have been developed with the objective of modeling the distribution of residual strength or fatigue life. These typically are derived by integrating some form of the generalized rate equation (Equation 4.1) into the statistical distributions of initial strength and life. Inherent in probabilistic fatigue models using residual strength approaches is the assumption that there is a one-to-one relationship between the probability rank of the initial strength and the rank of fatigue life of a given specimen. This relationship was termed the Strength Life Equal Rank Assumption (SLERA) by Chou and Croman [70], although, as they point out, the concept was originally described in a paper by Hahn and Kim [71]. Explicitly, the SLERA means that

$$F_{S_u}(S_k) = F_N(n_k) \tag{2.17}$$

where F_{S_u} and F_N are the cumulative distributions of initial strength and life, and the k^{th} percentile specimen has strength S_k and life n_k [70].

Unfortunately, the SLERA can not be be proved conclusively in experimental testing because it is impossible to measure the initial strength and fatigue life of the same specimen as both tests are destructive. Only the relative success of residual strength models incorporating SLERA can point to its applicability to the fatigue of FRP composites. In its essence, SLERA enables a model to choose an initial specimen with a given k percentile strength, $S_{u,k}$, and also know the lifetime of that specimen at a constant amplitude load $N_{i,k}$ based on the distribution of lifetimes at that load level.

As all residual strength models require knowledge of S_u and N, the SLERA is the primary approach used for predicting residual strength distributions. Philippidis and Passipoularidis made detailed use of SLERA in their comparison of the residual strength distributions predicted by different models for constant amplitude loading [16] based on the approach described by Whitney [72]. As a side note, SLERA can also be used in the context of damage rules such as PM where N is treated as a function of the initial strength distribution [18].

2.4.2 General residual strength models

Sarkani et al. [14] noted that many of residual strength models proposed in the literature are simplified versions of a generalized rate equation where the residual strength S_r is assumed to be a monotonically decreasing function of the cycles applied:

$$\frac{dS_r(n)}{dn} = -B\frac{An^{A-1}}{CS_r(n)^{C-1}} \tag{2.18}$$

where A, B, and C are positive value parameters and $S_r(n)$ is the residual strength. Integration for constant amplitude fatigue and accounting for the initial and final conditions

yields:

$$S_r(n,\sigma_p)^C = S_u^C - \left(S_u^C - \sigma_p^C\right)\left(\frac{n}{N}\right)^A \tag{2.19}$$

where S_u is the initial strength of the material. In this generalized form, we should note that in addition to the fatigue life, N, at each applied load, A and C are material parameters that may be functions of σ_p and R. For the most general case when applied to a spectrum load, the residual strength after the i^{th} load step must be computed iteratively as:

$$S_{r,i} = \left[S_u^{C_i} - \left(S_u^{C_i} - \sigma_{p,i}^{C_i}\right)\left(\frac{n_i + n_{eqv,i-1}}{N_i}\right)^{A_i}\right]^{1/C_i} \tag{2.20}$$

where by assuming that S_r remains constant during the transition from one load step to the to the next:

$$n_{eqv,i-1} = N_i\left[\frac{S_u^{C_i} - S_{r,i-1}^{C_i}}{S_u^{C_i} - \sigma_{p,i}^{C_i}}\right]^{1/A_i} \tag{2.21}$$

Broutman and Sahu

The earliest research on composite fatigue incorporating a residual strength model was performed by Broutman and Sahu [9] (BS). These authors proposed a linear reduction in residual strength ($A = C = 1$ in Equation 2.20):

$$S_r = S_u - \sum_i (S_u - \sigma_{p,i})\frac{n_i}{N_i} \tag{2.22}$$

Broutman and Sahu found that this linear residual strength approach gave much better fatigue failure predictions under two block loading of an E-glass/Epoxy laminate than Miner's rule [9]. The BS model has the advantage that it requires no estimation of additional parameters beyond those required for PM (fatigue life N_i for each applied stress level).

Reifsnider

Reifsnider and Stinchcomb introduced a critical element approach for modeling the fatigue of composite laminates [73, 74]. This model separates the composite into a critical element that controls ultimate failure (typically the 0° fibers in an axially loaded quasi-isotropic laminate) and non-critical elements whose failure leads to increased load on the critical element. The model used for the residual strength of the critical element was:

$$Fr(n) = 1 - \int_0^n (1 - Fa(i))\, A\left(\frac{i}{N_i}\right)^{A-1} d\left(\frac{i}{N_i}\right) \tag{2.23}$$

where $F_r = S_r/S_u$ and $Fa = \sigma_p/S_u$, both evaluated for critical element and A is considered a constant for a given R. Case and Reifsnider [75] gave a derivation of Equation 2.23 from thermodynamic principles. Even under constant amplitude global loading, the load on the critical element will vary as a function of the damage in the non-critical elements and the integration yields:

$$Fr = 1 - \left[\sum_i (1 - Fa(i))^{1/A} \left(\frac{n_i}{N_i}\right)\right]^A \tag{2.24}$$

Post et al. [76] applied this approach and used the SLERA and a Monte-Carlo simulation to predict residual strength distributions. In this work, Post et al. used the change in elastic modulus recorded during the fatigue life to estimate the stress on the critical element [76].

Equation 2.24 is identical to Equation 2.20 with $C = 1$ and A as a constant if we consider the entire composite as a unit. This approach simplifies the analysis as the determination of the stress and fatigue life of the critical element inside the composite is not required. Wahl et al. [47][48, 49], and Post et al. [77] applied Equation 2.24 to constant R-ratio spectrum fatigue loading with varying degrees of success.

Schaff and Davidson

Schaff and Davidson published two papers on variable amplitude loading of composites [78, 79] describing and applying a phenomenological residual strength model:

$$S_r(n) = S_u - (S_u - \sigma_{p,i}) \left(\frac{n}{N}\right)^{A_i} \tag{2.25}$$

where A is treated as a function of σ_p and R. To account for statistical spreading of the residual strength data, Schaff and Davidson applied a linear reduction to the Weibull shape parameter fit for each applied stress level to give the initial strength distribution shape parameter at $n = 0$ to provide a reasonable prediction of the fatigue life distribution. This method essentially forms a complex curve fit for the statistical distribution rather than relying on a mathematically consistent model as proposed by Yang and Liu [80] for example.

In the first paper, Schaff and Davidson [78] applied the model to two stress level repeat block loading fatigue. They observed that in some cases, repeatedly changing the stress level seems to cause more fatigue damage than applying the same loads in larger blocks. To account for this effect, which Schaff and Davidson called the "cycle mix effect", they introduced a cycle mix factor, CM, to reduce the residual strength whenever the magnitude of the mean stress increased [78]:

$$S_r(n^{(+)}) \rightarrow S_r(n^{(-)}) - CM \tag{2.26}$$

where

$$CM = C_m S_u \left[\frac{\Delta\sigma_m}{S_r(n^{(-)})}\right]^{(\Delta\sigma_p/\Delta\sigma_m)^2} \tag{2.27}$$

The constant C_m must be determined from experimental data on repeat block fatigue loading with different numbers of cycle mix events. It is not clear how Schaff and Davidson selected the above form for calculating the cycle mix reduction in residual strength. Adam et al. [21, 22] also found that large changes in the stress range in repeat block loading result in increased damage, corresponding to the type of "cycle mix" events highlighted by Schaff and Davidson [78, 79] and Filis et al. [15]. For the limited two stress level case that Schaff and Davidson tried [78] the model appeared to fit the experimental results reasonably well.

In a second paper [79], Schaff and Davidson applied their model to spectrum loading cases using two sets of data. In both cases, they performed curve fitting of the constant life diagram and a linear interpolation of a "constant-A" diagram to determine the value of A for each loading cycle. As there was no appropriate data to evaluate C_m in these materials, Schaff and Davidson assumed that it was not significant [79]. Thus, the effectiveness of the cycle mix factor approach in spectrum loading remains unknown.

Nijssen et al. [81] evaluated whether it made sense to treat A as a function of applied stress and found that a large data set is required to generally develop an empirical functional form for the variable. So far doing so has only been possible for individual materials and as only a few stress levels are usually evaluated, the overall form of the parameter is still uncertain. Nijssen et al. did show that improved predictions were possible for two stress level block loading when the respective values of A found from constant amplitude residual strength tests for each stress level were used, compared to using a single value of the parameter regardless of the applied stress [81].

Hahn and Kim

Others, including Hahn and Kim [71, 82], Hashin [17], and Whitney [72], have used residual strength equations equivalent to Equation 2.20 where $A = 1$ and C is an unknown parameter fit to experimental data and potentially a function of stress level:

$$S_r^C = S_u^C - (S_u^C - \sigma_p^C)\left(\frac{n}{N}\right) \tag{2.28}$$

2.4.3 Other residual strength approaches

Probability distribution based approaches

Yang and Liu [80] developed a residual strength model starting with the generalized rate equation:

$$\frac{dS_r(n)}{dn} = \frac{-H(\sigma_p, f, R)}{CS_r(n)^{C-1}} \tag{2.29}$$

where $H(\sigma_p, f, R)$ is left as a general function of the applied stress, frequency and stress ratio. Integration, applying boundary conditions, and taking $H = H(\sigma_p)$ for constant frequency

and R leads to:

$$S_r(n)^C = S_u^C - H(\sigma_p)n \tag{2.30}$$

Then, Yang and Liu assumed that the initial strength follows a two parameter Weibull [83] distribution with location parameter S_0 and shape parameter α:

$$F_{S_u}(x) = P[S_u \leq x] = 1 - \exp\left[-\left(\frac{x}{S_0}\right)^{\alpha}\right] \tag{2.31}$$

By substituting Equation 2.30 into Equation 2.31 and taking the fatigue failure boundary condition described by $S_r(N) = \sigma_p$ at $n = N$ yields the predicted distribution of fatigue life:

$$F_N(n) = 1 - \exp\left[-\left(\frac{n + \sigma_p^C/H(\sigma_p)}{S_0^C/H(\sigma_p)}\right)^{\alpha/C}\right] \tag{2.32}$$

which has the form of a three parameter Weibull distribution where the characteristic fatigue life is given by $N_0 = S_0^C/H(\sigma_p)$. Assuming that the characteristic fatigue life follows a power law relationship $K\sigma_p^B N_0 = 1$ where K and b are constants yields the final form of Yang and Liu's [80] residual strength model:

$$S_r(n)^C = S_u^C - S_0^C K \sigma_p^B n \tag{2.33}$$

where S_0 is determined from the statistical distribution of initial strength data. Rather than attempt to fit B and K to S-N fatigue data which would require extensive fatigue data at multiple stress levels to determine the scale factor N_0 as a function of stress, Yang and Liu suggest fitting the parameters, B, K, and C simultaneously using a combination of fatigue and residual strength data points and the SLERA implicit in their model. The idea that they present is to calculate the initial strength of each specimen tested by solving Equation 2.33 for S_u and then minimize the least square error in the first three moments of the predicted initial strength distribution relative to the actual distribution that was measured. In principle, Yang and Liu believe that this will enable calculation of the parameters with a relatively small data set of 12-15 initial strength tests and about 30 fatigue tests [80].

The Yang and Liu model gives the residual strength distribution in the form of a three parameter Weibull distribution:

$$F_{S_r(n)}(x) = 1 - \exp\left[-\left(\frac{x^C + KS_0^C\sigma_p^B n}{S_0^C}\right)^{\alpha/C}\right] \tag{2.34}$$

thus accounting for the specimens that fail prior to n by cutting off the lower end of the distribution at the applied fatigue stress level. Similar approaches to that of Yang and Liu were taken by Hahn [82] and by Chou and Croman [84] resulting in equivalent expressions for the residual strength as three parameter Weibull distributions.

Yang and colleagues applied their model (Equation 2.33) to constant amplitude reversed fatigue loading ($R = -1$) [85] and to two block loading high-low and low-high fatigue loading [86] and repeat block loading [87] of composites. In these latter cases, the residual strength can be found by summation over the applied stresses and cycles if we assume that C is independent of the applied stress:

$$S_r = \left[S_u^C - \sum_i S_0^C K \sigma_{p,i}^B n_i \right]^{1/C} \tag{2.35}$$

Yang and Du [88] applied another residual strength model to spectrum loading. The general form of this model included two more parameters, w and A:

$$S_r^w = S_u^w - \frac{S_u^w - \sigma_p^w}{\left(S_u^C - \sigma_p^C\right)^A} S_0^{CA} (K \sigma_p^B n)^A \tag{2.36}$$

However, as noted by Philippidis and Passipoularidis [16] having 5 unknown parameters makes fitting the equation very difficult and in all of their examples Yang et al. simplified the model by assuming that either $w = 1$ or $A = 1$.

For the spectrum loading case, Yang and Du [88] used the aircraft duty cycle based data collected by Schultz and Gerharz [42]. The model was simplified by taking $w = 1$ and assuming that A was a constant for all loading conditions. The parameters C, B, and K were fit as a function of R to constant amplitude fatigue failure data. B and K were estimated for each applied load in the spectrum block using a constant life diagram approach and C was evaluated by linear interpolation on a similar "constant C" plot. Lacking any residual strength data to evaluate A, Yang and Du tried $A = 1$ and $A = 0.95$. In their evaluation of the model for spectrum loading, Yang and Du summed the third term for all of the loading blocks:

$$S_r = S_u - \sum_i \frac{S_u - \sigma_{p,i}}{\left(S_u^{C_i} - \sigma_{p,i}^{C_i}\right)^A} S_0^{C_i A} (K_i \sigma_{p,i}^{B_i} n_i)^A \tag{2.37}$$

While this will work for $A = 1$ when the accumulation is linear with applied cycles, it is incorrect for any other value of A. Instead either the equivalent number of cycles must be calculated and added to the new cycles applied at each stress level, or with A taken as constant, the summation can take place prior to raising the third term to the power as:

$$S_r = S_u - \left[\sum_i \frac{(S_u - \sigma_{p,i})^{1/A}}{\left(S_u^{C_i} - \sigma_{p,i}^{C_i}\right)} S_0^{C_i} K_i \sigma_{p,i}^{B_i} n_i \right]^A \tag{2.38}$$

Rotem

Rotem [89] extended the previous damage law concept by Hashin and Rotem (Equation 2.12) to a residual strength model with the form (for power law S-N curves):

$$\frac{S_r}{B} = \left[\frac{\sigma_p}{B}\right]^{\log\left(\left(\frac{\sigma_p}{B}\right)^{1/K}-1\right)/\log(n)} \tag{2.39}$$

where K is the slope and B is the intercept of a power law S-N curve fit as $\sigma_p = BN^K$ with the limit that $S_r \leq S_u$ for the case where $B < S_u$. This residual strength model does not have any fitting parameters outside those of the S-N curve and as noted by Rotem and Nelson [90] gives a nearly "sudden-death" representation where the residual strength remains nearly constant for most of the fatigue life and then drops rapidly close to fatigue failure. The extension of this model to variable amplitude loading was not considered by the authors.

Interaction model

Adam et al. [91] developed an interaction (INT) residual strength model by defining a residual strength ratio, r as

$$r = \frac{S_r - \sigma_p}{S_u - \sigma_p} \tag{2.40}$$

and a normalized time (cycle) ratio including the fact that an initial strength measurement actually occurs at 1/2 cycle or n=0.5 [91]

$$t = \frac{\log n - \log 0.5}{\log N - \log 0.5} \tag{2.41}$$

Adam found that all of the constant amplitude residual strength data for $R = 0.1$ at different maximum stress levels collapsed to a single curve on an r vs. t plot (see Figure 2.14) [91]. A model for the $r - t$ relationship is then proposed:

$$t^x + r^y = 1 \tag{2.42}$$

which can vary in shape from linear to circular arc to extremely angular depending on the x and y parameters. Thus, this normalized model can accommodate both gradual wear-out and sudden death type behavior. Adam et al. describe several methods of calculating the error between experimental data and this curve in order to optimize the fit of x and y [91]. Having determined x and y from a master curve, the residual strength is evaluated as

$$S_r = (S_u - \sigma_p)\left[1 - \left(\frac{\log n - \log 0.5}{\log N_i - \log 0.5}\right)^x\right]^{1/y} + \sigma_p \tag{2.43}$$

This empirical model that appears to work well to collapse residual strength curves at different stress levels. Although Adam et al. did not apply their model to spectrum loading,

the extension is obvious if we assume that residual strength must be a continuous function of cycles:

$$S_r(i) = (S_u - \sigma_{p,i}) \left[1 - \left(\frac{\log(n_i + n_{eqv,i-1}) - \log 0.5}{\log N_i - \log 0.5} \right)^x \right]^{1/y} + \sigma_{p,i} \tag{2.44}$$

where

$$\log n_{eqv,i-1} = (\log N_i - \log 0.5) \left(1 - \left(\frac{S_{r,i-1} - \sigma_{p,i}}{S_u - \sigma_{p,i}} \right)^y \right)^{1/x} + \log 0.5 \tag{2.45}$$

Epaarachchi and Clausen model

Epaarachchi and Clausen proposed an empirical model for predicting the fatigue life of composite laminates as a function of fatigue R-ratio, frequency and fiber orientation [92]. The form of this model is represented as a power law relationship, but the stress side of the equation is modified to include the additional testing parameters:

$$D = \left(\frac{S_u}{\sigma_{max}} - 1 \right) \left(\frac{S_u}{\sigma_{max}} \right)^{0.6 - \psi |\sin\theta|} \frac{1}{(1-\psi)^{1.6 - \psi|\sin\theta|}} f^A = B(N^A - 1) \tag{2.46}$$

where θ is the smallest angle between the fibers in any ply and the loading direction, f is the fatigue frequency in cycles per second, $\psi = R$ for $R < 1$ and $\psi = 1/R$ for $R > 1$, and A and B are material parameters fit to data. The constants of 1.6 and 0.6 were selected based on previous work by Herzberg and Manson [93]. Fitting can take place using the S-N curve for one fiber orientation, frequency and R-ratio because, if this equation holds, all tests regardless of the parameter will collapse to one $\log D$ vs. $\log N$ line. Epaarachchi and Clausen showed generally good calculated predictions for S-N curves over a wide range of laminates stacking sequences, R-ratios, and frequencies using this model [92]. This approach has the advantage of explicitly describing the R-ratio, frequency, and fiber orientation effects on the S-N curve parameters and thus describing the entire constant life plot for a class of materials and applied testing frequency. Qiao and Yang [94]also proposed an empirical generalized S-N model similar to Epaarachchi and Clausen's.

Epaarachchi and Clausen [12, 13] extended their general fatigue model to variable amplitude loading by adding a term, ϕ_n, to account for the amount of life previous used:

$$S_r = S_{r,n-1} - B \left(\frac{\sigma_{p,n}}{S_{r,n-1}} \right)^{0.6 - \psi |\sin\theta|} \frac{1}{(1-\psi)^{1.6 - \psi|\sin\theta|}} \frac{1}{f^A} (n^A - 1)\phi_n \tag{2.47}$$

where

$$\phi_n = 1 - \left[1 - \left(\frac{n}{N_{\sigma n}} \right)^A \right]^A \tag{2.48}$$

and $N_{\sigma n}$ is the residual life at $\sigma_{p,n}$ stress after the $n-1$ step. Generally this approach provided much better results for life prediction than previous models for the block loading cases these authors studied [13, 12]. Epaarachchi and Clausen indicate that the change in residual strength under variable amplitude loading can simply be taken as the sum of the right hand term in equation 2.47 over the applied loading blocks [13]. However it would appear that a method using equivalent cycles would be more appropriate given the non-linear relationship between the residual strength and n.

Three stages of residual strength degradation

In their discussion of constant amplitude fatigue experiments on composite materials, Reifsnider and Jamison [95] identified three main stages of fatigue damage: (1) initial rapid degradation due to matrix cracking, followed by (2) a slow decline due to random fiber breaks and delamination and (3) a sharp decline in properties near the end of life when failure was imminent. Reifsnider and Jamison thought that the residual strength followed a similar trend [95]. The residual strength models discussed so far are capable of modeling either the first two or last two stages, but not all three. The only exceptions are Equation 2.20 and the interaction model Equation 2.42 when applied with one parameter greater than 1 and the other is less than 1. For Equation 2.42, Adam et al. found both x and y to be greater than one for the case they looked at. More recently Philippidis and Passipoularidis [16] found either x or y to be less than 1 in two quasi-isotropic graphite laminates but both were greater than 1 in glass laminates that were primarily unidirectional/CSM or ± 45. To date there have been no attempts to fit Equation 2.20 with both A and C as parameters.

Recently, several authors have considered other models capable of fitting this entire range of trends. Yao and Himmel [96] proposed a model with that takes the form:

$$S_r(n) = S_u - (S_u - \sigma_p)\frac{\sin\left(A\frac{n}{N}\right)\cos\left(B-A\right)}{\sin\left(B\right)\cos\left(B\frac{n}{N}-A\right)} \tag{2.49}$$

Yao and Himmel applied their model to two block variable amplitude loading [96]. This was presumably done by finding the equivalent number of cycles required to give the same residual strength at the second stress level after the first loading step was completed and proceeding from there, however Yao and Himmel did not show this process explicitly.

In their comparison of models for residual strength distribution under constant amplitude load, Philippidis and Passipoularidis [16] introduced a new variation to the general residual strength model (Equation 2.20) where the exponent depends on the life fraction rather than the applied stress:

$$S_r = S_u - (S_u - \sigma_p)\left(\frac{n}{N}\right)^{A_1 \exp\left(A_2 \frac{n}{N}\right)} \tag{2.50}$$

Like the Yao and Himmel model, Philippidis and Passipoularidis comment that their form has the advantage of modeling a residual strength curve that drops initially, reduces slower

during most of the fatigue life and then decreases rapidly near the end of life [16]. This behavior has been observed experimentally in composites, especially under tensile fatigue loading. Although based on Equation 2.20, Equation 2.50 really represents a new form because it could not be derived from the same rate equation.

2.5 Micro-mechanics and modulus based approaches to fatigue in composite laminates

Micro-mechanics approaches to fatigue seek to characterize the damage created by fatigue in the laminate at a local level and thereby determine the global strength, stiffness, and life properties. In the ideal case, these approaches would take component properties and geometry of the composite and be able to determine static and fatigue behavior without any measurements on the bulk composite material. However, in reality micro-mechanics based fatigue models typically have unknown parameters that are fit using the global material behavior.

In metallic materials where fatigue life is often dominated by the development and propagation of a single large flaw, the focus for predicting fatigue life has been on crack initiation and growth using fracture mechanics [34]. However, in continuous fiber composites, fatigue damage is typically highly distributed and failure occurs when the damage state reaches a critical level. The development of a micro-mechanics approach to fatigue of composites is further complicated by the interaction of different lamina within the laminate that have different fatigue failure modes and result in stress redistribution throughout the life of the composite. The critical element approach developed by Reifsnider and colleagues [73, 73, 97] is a classic example of this phonological approach to composite fatigue. Lamination theory and various static failure theories are often employed in micromechanics fatigue models.

2.5.1 Fatigue life based on static properties

Huang [98] presented several fatigue prediction models for composites fit using static properties only. He also extended the model to woven textile based laminates [99] using a bridging model [100]. Huang believes that the benefit of woven composites in design can only be truly achieved if fatigue S-N response can be estimated without any fatigue testing at all. His work based on the micromechanics within a unit cell geometry attempts to do this using fitting based on the stress-strain curve for the composite in bi-axial loading [99]. While this type of approach could be very useful if it works, it has not been shown to be robust for constant amplitude fatigue and the application to variable amplitude loads has not been considered.

2.5.2 Methods using physical damage measurements

Dzenis, whose previous research studied random monotonic loading of composites [101, 102, 103], published a study of composite behavior under low cycle (high stress) fatigue [104]. In this study, Dzenis used acoustic emission monitoring under triangle wave loading found that most of the damage was occurring under the loading part of the cycle and that even low applied stresses caused damage [104]. In a second paper the author proposed a "stochastic mesomechanics" model for the damage accumulation under low cycle fatigue [105]. This approach shows promise in its ability to handle cycle by cycle damage events directly, however, since Dzenis focused on low cycle fatigue (less than 20 cycles to failure) it is unclear how applicable the findings are to the high cycle fatigue regime.

Bartley-Cho et al. [27] undertook a study of the impact of block loading on the lamina level properties of a quasi-isotropic graphite/epoxy laminate. They used edge replication to count crack densities in the 90 and ±45 plies under T-T (R=0.1) and T-C (R=-1) fatigue. By using classical lamination theory and a stiffness discount method for cracked plies, the ply level stresses were calculated. By considering the equivalent RMS power applied (load times displacement), the T-T fatigue results were used to predict T-C damage at equivalent loading with reasonable sucess. A damage accumulation law based on the off-axis ply cracks was less successful at predicting the resulting damage under two block variable amplitude fatigue. The authors noted that there was an experimentally measured difference in ply crack density between high-low and low-high two block sequences with the later resulting in more cracks [27]. This observation reinforces that there are sequence effects in composite fatigue damage.

Akshantala and Talreja [106] proposed a micromechanics based model where a progressive damage model was used to predict fatigue lives in a carbon/epoxy cross-ply laminate. In addition to predicting the fatigue life, the damage state in terms of crack density and delaminations was defined. Although some empirical data is still required to fit the model, the authors claim that this is kept to a minimum. However, since crack density data is required, this may be more effort to measure than bulk strength and failure time properties. Akshantala and Talreja developed and tested this modeling approach in the context of a constant amplitude strain controlled test environment [106].

Pantelakis et al. developed an approach to variable amplitude life prediction based on non-destructive evaluation of constant amplitude tests to fit a damage accumulation model [107]. Papanikos et al. [108] created a progressive failure model including de-laminations in which they fit the degradation of stiffness in each ply under fatigue and also considered delamination area (predicted based on 3-D edge effects in the laminate). While these authors showed marked improvement in the variable amplitude loading predictions over Miner's rule (which was non-conservative in this case), considerable effort in experimentally measuring the damage state of the composites during the CA fatigue was required to fit the model.

The modeling of fatigue damage based on crack density distribution was also studied in detail

by Sun et al. [109]. Using a Monte Carlo simulation, Sun was able to predict crack densities in transverse plies using fatigue life curves and change in stiffness [109]. Micromechanics for woven carbon/epoxy laminates under tension fatigue was evaluated experimentally through destructive and nondestructive evaluation by Yoshioka and Seferis [110]. These authors showed that in some cases, the residual strength increases under the first part of fatigue loading and postulated that this is due to load redistribution and straightening of the 0 direction tows in the laminate.

2.5.3 Fatigue of laminates with different ply orientations

Hashin and Rotem approached the problem of predicting off axis fatigue failure in composite lamina [111]. In their model, they considered the stresses in the principle orthotropic directions of the lamina and defined failure criteria for fiber and transverse/shear failure similar to those used by Tsai and Wu [112]. However, fatigue strengths in the fiber and transverse directions are used instead of ultimate strength. The model predicted S-N curves well for arbitrary angle ply laminates. Diao et al. [113] extended Hashin and Rotem's model to include statistical prediction of fatigue durability. They developed the analysis using Weibull statistics to represent the fatigue strength variables. Again predictions were compared to data collected on angle ply laminates, this time in terms of their statistical distribution [113].

Aboudi [114] described the extension of a micro-mechanics failure analysis for static loading to fatigue loading. In this model, it was assumed that the fatigue strength of the fiber and matrix was known. Then the fatigue failure criterion was defined as:

$$\|S_{11}^{(11)}\| = X_f^{(F)} \tag{2.51}$$

and

$$\left[\frac{S_{22}^{(\beta\gamma)}}{X_m^{(F)}}\right]^2 + \left[\frac{S_{12}^{(\beta\gamma)}}{S_m^{(F)}}\right]^2 = 1 \tag{2.52}$$

where $(\beta\gamma) = (12), (21), (22)$ and $X_f^{(F)}$,$X_m^{(F)}$, and $X_m^{(F)}$ denote the fatigue failure functions of the fiber and matrix materials, and are dependent on the R ratio, applied stress, frequency, etc. This method relies on the knowledge of the appropriate fatigue failure curves (S-N diagrams) of the fiber and matrix. However, they can also be fit using the axial and transverse fatigue loading curves on the composite. Having performed this fitting, Aboudi then was able to predict the fatigue life curves for unidirectional laminates under off axis fatigue and for [+/-30], [+/-45], [+/-60] laminates. Predictions were good for the unidirectional composite except at a small off-axis angle of 5 degrees and worked fairly well for the 30 and 60 degree angle ply laminates while over-predicting the performance of the 45 degree angle laminate. The author claims that this could be extended to general laminates using classical lamination theory [114]. However, this would produce additional challenges because failure would first occur in off axis plies and if a discount theory was incorporated, it would

lead to varying applied fatigue load on the remaining lamina. No mention is included in this modeling approach for how to handle variable amplitude loading. Because of the requirement for fatigue life curves of matrix and fiber properties (including the interface), this model requires a lot of experimental data.

Fawaz [115] used PM with a critical element type approach and considered progressive lamina failure under fatigue to determine the fatigue life of the laminate. In this approach, the fatigue life of individual lamina with different orientations is obtained and the stress on the remaining elements is calculated using classical lamination theory and discounting the stiffness of failed plies [115]. This approach in theory has the benefit of being a generalized fatigue model for any laminate created with lamina components that have known fatigue behavior. However, typically those lamina fatigue curves are not known and even when they are, knowing how to apply the discounting of properties a priori is a challenge.

2.5.4 Fatigue and creep

Recent efforts by Miyano, Christensen and colleagues [116, 117, 118] have worked to develop cumulative damage theories for FRP composites using continuum concepts based on the viscoelastic creep response of the matrix material. In [116], Miyano and Nakada considered the problem of accelerated testing for FRP laminates under elevated temperature and developed predictions for the flexural fatigue strength at different temperatures based on the creep response master curve data. Christensen and Miyano [117] discussed stress intensity influence on crack growth in creep rupture of polymers and combined these concepts to develop a cumulative damage approach based on physical principles [118]. This crack growth based formulation uses constant stress creep-rupture data and fatigue at constant amplitude to the predict creep-rupture behavior under variable stress or fatigue under variable amplitude loading by accounting for the time history of the stress. Christensen and Miyano applied their final model only in a theoretical context without comparing the results to real experimental data [118], so the effectiveness of this approach remains uncertain, even for matrix dominated failures such as the flexural fatigue tests noted earlier [116].

2.5.5 Finite element analysis of fatigue damage in laminates

FEA approaches have been used by several authors to model fatigue damage in composites. These models can incorporate stiffness reduction of elements, discount elements that fail, and apply cohesive elements in the neighborhood of crack initiation and propagation in an effort to accurately model the global response of the material. Shokrieh and Lessard [119, 120] presented a study of the fatigue behavior of various bolted composite geometries predicted based on S-N data for in plane axial and shear loading and out of plane shear experiments. This residual strength model was also used to make some predictions under two block loading experiments. Results showed reasonable comparison to experimental data (within 25% error

relative to the actual life) and were much better than the highly non-conservative Miner's rule. Also, the model presented was, at least to an extent, load sequence dependent because it took into account the damage present in the composite when considering the load on each element in the FEA simulation [120]. Gowayed and Fan employed an FEA model to analyze the fatigue of woven textile composites under tension-tension loading [121]. Because FEA models generally require the input of some sort of degradation law for the elements based on the applied stress or strain on that element their real strength lies in being able to apply these damage rules to non-uniform stress states in the neighborhood of a stress concentration feature of a structure.

2.5.6 Fatigue Modulus Approaches

Hwang and Han [67] introduced the "fatigue modulus" as a measure of fatigue damage for life prediction. They defined the fatigue modulus $E_f(n)$ as:

$$E_f(n) = \frac{\sigma_p}{\epsilon_p(n)} \tag{2.53}$$

where σ_p is the peak stress and $\epsilon_p(n)$ is the peak strain of the n^{th} cycle. Thus as the fatigue creates permanent deformation of the material, the fatigue modulus will decrease even if the elastic modulus remains relatively constant. As with most modulus based approaches, a degredation rate law was applied to the fatigue modulus:

$$E_f(n) = E_f(0) - An^C \tag{2.54}$$

where A and C are fitting constants and a strain based failure criterion was used such that the strain to failure is assumed to remain constant over the lifetime. The resulting relationship for fatigue life is equivalent to a power law equation:

$$N = \left[B\left(1 - \frac{\sigma_p}{S_u}\right)\right]^{1/C} \tag{2.55}$$

In a second paper, Hwang and Han [122] explored several damage accumulation laws with constants calculated based on fatigue modulus measurements and compared the results to the Palgren-Miner rule and several other models under two block high-low and low-high fatigue loadings.

A stiffness model developed by Whitworth [123] considered the relationship between strength and stiffness using Yang and Liu's residual strength degradation theory [80] as a starting point. In a second paper, Whitworth [19] considered a cumulative damage model based on change in stiffness. Experimental verification was done with T300 graphite/epoxy laminates under two block loading. The proposed model was shown to work nearly perfectly (to three significant digits) which seems questionable unless it was really simply fit to the experimental

results [19]. Talreja [124] described a continuum damage model for a laminate applied using the measured stiffness change as an input.

Lee et al. [125] used the fatigue modulus based lifetime prediction in a stochastic formulation to predict the distribution of fatigue life at different stress levels. Their model was largely successful for the matrix dominated laminates tested. Kim and Zhang [126] also undertook a fatigue lifetime prediction model based on fatigue modulus using woven E-glass laminates with Durakane 410-400 Vinyl Ester for experimental verification. As defined, the fatigue modulus decreases significantly more than the stiffness under fatigue because of permanent deformation (shifting of the hysteresis loops). Kim and Zhang also used crack density data to inform their model. Their resulting S-N curve prediction was fairly good although conservative over the limited fatigue data they showed [126].

Momenkhani et al. [127] proposed another approach related to using the fatigue modulus, based on the translation of the center of gravity of the hysteresis loop during fatigue loading. The authors felt that this method provided more insight into how the damage parameter related to the state of the material under fatigue [127]. In a second paper, Momenkhani and Sarkani describe how this model can be used instead of a traditional power law S-N curve [128].

Van Paepegem and Degrieck developed a coupled residual stiffness/residual strength empirical model [129, 130]. This approach had the advantage of modeling the stiffness throughout the life and the final failure point of the composite. As is common with the stiffness based damage models, Van Paepegem and Degrieck tested their model using displacement controlled bending fatigue tests. They used a bending fatigue setup and implemented their empirical equations along with a modified Tsai-Wu stress failure criterion in a finite element code to account for the stress variation through the thickness of the laminate. For this simplified case, the model performed well [130]. In a third paper, Van Paepegem and Degrieck reviewed several damage accumulation and residual strength models and discussed the application of their new coupled approach to variable displacement amplitude block loading [28]. However, little variable displacement data was actually collected and most of this paper simply reports the simulated results showing load sequence effects on life, which are identical to those that would be captured by a simple residual strength model. Therefore, although Van Paepegem and Degrieck have explored an important topic, their results appear to be falsely positive in the context of making useful predictions beyond what can be done with simpler models.

Whitworth [123], Yang et al. [131], Rotem and Nelson [90], Wu et al. [132], and Tang et al. [133] have also discussed correlation between stiffness reduction and residual strength in laminates. However, beyond fitting the data, little progress has been made on this front toward actually predicting stiffness degradation. Therefore, fatigue tests must still be run in order to evaluate the stiffness and predict life. Most fatigue modulus models have only been applied successfully in off axis laminates that lack fibers in the loading direction. In E-glass laminates containing a significant proportion of fibers in the loading direction, statistical

correlation of stiffness during fatigue to residual strength or life is usually insignificant as shown by Post et al.[76]. Thus, the development of a strength model based on stiffness for quasi-isotropic laminates is statistically unjustifiable.

2.6 Application of variable amplitude fatigue models to spectrum loading

The present objective is to compare the different cumulative fatigue models for predicting fatigue life under uniaxial spectrum loading. Past studies have primariliy focused on block loading and often model constants have been chosen based on a best fit to the experimental variable amplitude results. Those who have compared models for spectrum loading have only selected a small subset of models [14][12]. In the following application using several extensive composite data sets, we will attempt to be as fair as possible to each approach and will comment on the challenges to the fitting and application of each equation.

2.6.1 Method for comparison of models

Many variable amplitude model comparisons have been done by calculating a normalized damage parameter, D, for each model and then comparing the resulting value relative to 1.0 (or some other predetermined failure criterion) for each experimental failure [9, 81, 48, 12]. Typically the damage index for representations take the form:

$$D(n) = \frac{S_u - S_r(n)}{S_u - \sigma_p(n)} \tag{2.56}$$

for residual strength models, and

$$D(n) = \frac{E_0 - E(n)}{E_0 - E_{fail}} \tag{2.57}$$

for fatigue modulus models where E_0 is the initial modulus and E_{fail} is the final fatigue modulus (often taken to be 0). Damage accumulation models are inherently described in terms of D already. While the damage index approach maintains the same failure criterion ($D = 1$), neither Equation 2.56 or Equation 2.57 will provide an accurate representation of how much a model is in error of the experimental result if the model is non-linear as a function of cycles. Particularly for residual strength models, D defined in Equation 2.56 is dependent on the applied stress and thus will not be a monotonically increasing function of cycles for a spectrum load.

The damage index is an academic quantity that does not have a bearing on the durability properties of a material outside of the model which generated it. Therefore, it is not

appropriate for the comparison of predictions from different modeling methods. From the engineering perspective, we are interested in knowing the life of a material in cycles or the residual strength at a given lifetime. In this study, the predicted cycles to failure under spectrum loading will be compared to the actual mean life measured under those loading conditions using a model error function:

$$\text{Model Error} = M_e = \log\left(\frac{N_{model}}{N_{experiment}}\right) \tag{2.58}$$

where N_{model} is the predicted life for a specimen with average properties and $N_{experiment}$ is the average cycles to failure for the experimental tests under the considered spectrum condition. By using the base 10 logarithm of the ratio of model and experimental results, M_e measures how many orders of magnitude a prediction is off from the experimental results. A negative M_e indicates a conservative error (model under-predicts life) while a positive M_e is a nonconservative error. In evaluating the general use of spectrum fatigue models, we will be particularly interested in how far off the worst case for a model is and what the range of errors are.

Reliability engineering methods require knowledge of the distribution of fatigue life and residual properties under probabilistic loading. Using the SLERA, nearly any variable amplitude fatigue model can be extended to prediction of the distribution of the fatigue life under specified loads. For stochastic loading, a Monte-Carlo simulation approach can be used if the model does not allow analytical inclusion of the load distribution. In order to keep the analysis comparison simpler for the present study, only the first moment (mean) results will be calculated and compared, using the mean initial strength as an input. Before considering the prediction of life distributions, a first step is to evaluate the prediction of the mean value, and thus is the extent of our present efforts.

2.6.2 Data Sets

In general, variable amplitude fatigue models require empirical fitting of parameters for a given material. Therefore, predictions made with that model can only be applied to the laminate for which they were fit. Thus, comparison of the models can take place where the data required for fitting all of the selected models is available and at least one spectrum case that is to be used for verification of the predictions is available on a given material system. Data sets containing fatigue life under stress controlled tests similar to those typically available for structural design applications were selected for this study.

Data on four materials have been selected for this comparison covering a broad range of E-glass/polymer composite laminates for wind turbine blades and naval architecture. These data sets were selected because they each include a statistically significant number of measurements of the initial strength, constant amplitude fatigue to failure under various R-ratios, and residual strength at various percentages of life under constant amplitude loading. Some

of the data sets also have various cases of block loading. Each material data set contains several spectrum distributed loading cases to use for verification of the predictive ability of each model. Selected properties of each data set are highlighted in Table 2.2.

The first material data set, denoted DD16, is part of the DOE/MSU database [41] and the tests performed are detailed in [49]. Various analyses of this data are provided in references [47, 48, 49, 134, 135, 81]. Quasi-static loading was performed in displacement control at 13 mm/min. Fatigue frequencies were varied from 1 to 10 Hz. in an effort to maintain constant temperature under high stress fatigue. Verification spectrum available for DD16 include fatigue to failure under the standard WISPERX spectrum and two modified versions of the WISPERX where the valleys of each cycle were forced to a constant $R = 0.1$. We will use the Wahl et al. notation for these spectra [49]: WISPK includes all WISPERX cycle peaks but forces following valleys to $R = 0.1$, while WISXR01 includes only the T-T WISPERX cycles and forces following valleys to $R = 0.1$ (results in 12687 cycles).

The MD2 (R0400 geometry), UD2 (I1000 geometry) material data sets are part of the Optimat Blades database [51, 136], publicly available online in Excel format. Spectrum predictions for these material will be made for the WISPER and WISPERX standard spectra fatigue to failure experimental results available in the data set. The laminates are are unidirectional (UD2) and multidirectional (MD2) $[[\pm 45/0]_4/\pm 45]$. The data was collected at several different laboratories and for the present study the results from all the laboratories were pooled for each test type. Fatigue frequencies ranged from about 1 to 10 Hz.

The final data set was collected at Virginia Tech and the details and test results are provided in Appendix B. This material consisted of 10 layers of woven roving E-glass in a $[0/+45/90/-45/0]_s$ stacking sequence (donated by the warp direction fibers in each layer) with a rubber toughened vinyl ester matrix (Ashland Chemical Durakane 8084). Unlike the previous data sets geared toward wind turbine blades, the VT8084 material was primarily intended for naval ship hull construction. Variable amplitude fatigue loading includes Rayleigh distributed loading with 95% autocorrelation (degree of load ordering, see [2]) with a nominal $R = -1$ and the same peaks with following valleys forced to $R = 0.1$ called RAY95 and RAY95R01 respectively. Fatigue frequency was held constant for all tests at 5 Hz, while quasi-static loading was performed in load control at 667 N/s.

2.6.3 Selection and programing of models

The choice of models for fatigue is inherently limited by the data available to fit them. Although the DOE/MSU and OPTIMAT project data bases present some of the most extensive fatigue testing on composite materials available, they only include limited information about the strain and modulus (initial properties and sometime residual modulus after a fatigue test). Thus, the fatigue modulus based approaches that require knowledge of elastic behavior over the fatigue life in order to fit the parameter are not an option and will not be included in this comparison. Each of the damage accumulation and residual strength models

Table 2.2: Overview of experimental data sets used for fitting and evaluating cumulative fatigue models

Material ID	Fiber	Matrix	Laminate structure	FVF	Data source	Spectrum loading
DD16	E-glass	Ortho-polyester	$[90/0/\pm 45/0]_s$	0.36	DOE/MSU [41][49]	WISPERX, WISPK, WISXR01
MD2	E-glass	Prime 20 epoxy	$[[\pm 45/0]_4/\pm 45]$	0.52	OPTIDAT [51]	WISPER, WISPERX
UD2	E-glass	Prime 20 epoxy	$[0]_4$	0.52	OPTIDAT [51]	WISPER
VT8084	Woven E-glass	Ashland VE 8084	$[0/+45/90/-45/0]_s$	0.52	Virginia Tech (Appendix)	RAY95 RAY95R01

will be evaluated and if they are appropriate for the data and spectra, required curve fitting parameters will be determined from the experimental data sets.

Fitting model parameters based on the experimental data sets was performed in Microsoft Excel using the Linest (linear least squares) and the Solver (optimization) tools as described in this section. The models were then programed in Java to perform the iterative equations required to apply the models to the spectra for each set of fitting parameters and stress level.

2.6.4 Determining N_i

With the exception of the Yang and Eraapachchi and Clausen models, all of the damage accumulation and residual strength approaches reviewed require a separate empirical model for determining the total cycles to failure, N_i, under a constant amplitude load equivalent to the current applied cycle in the spectrum (defined by σ_p, σ_v) as an input. Wahl et al. [48, 49] compared spectrum fatigue predictions given by the Palmgren-Miner rule and two residual strength models by modifying the empirical representation of the S-N curve. They considered exponential and power law representations, both including and excluding initial strength data in fitting the parameters. There can a significant difference in the resulting spectrum predictions because of differences in the shape of the extrapolated S-N curve to longer lifetimes [48, 49]. While the selection of S-N curve representations is important, particularly because of the need to extrapolate to fatigue lives longer than those measured experimentally, this should be based on the best fit to experimental constant amplitude data rather than as a way to "improve" variable amplitude fatigue models that aren't performing as well as desired. The selection of an S-N curve equation is beyond the scope of the present effort, and in an effort to simplify the analysis and apply it as fairly as possible to the models, only one approach will be used to fit the constant amplitude fatigue life data.

A common approach is to fit constant amplitude fatigue data at each R-ratio with a power law model:

$$N = B\|\sigma_p\|^a \tag{2.59}$$

where B and a are the fitting parameters, N is the cycles to failure and σ_p is maximum stress in the applied cyclic loading. This equation gives a straight line on log-log plot of stress vs. cycles and is often written as:

$$\log N = a \log \|\sigma_p\| + b \tag{2.60}$$

where a and $b = \log B$ are the slope and intercept. This equation can be fit to experimental fatigue data using least squares regression analysis, which Johannesson et al.[137] noted coincides with the maximum likelihood method assuming log-normally distributed errors in fatigue life data. In the present analysis using the Excel Linest tool, $\log \|\sigma_p\|$ is considered the independent variable and $\log N$ is the dependent variable so that the least squares error for finding a and b should be in the experimentally measured $\log N$ direction. This method is preferable because experiments are performed in stress control and measure the resulting (stochastically varying) fatigue life.

The typical approach is to use the $max\{\|\sigma_p\|, \|\sigma_v\|\}$ for σ_p in Equation 5.17 and thus calculate N in terms of the minimum stress, σ_v, for $R < 0$ and $R > 1$. However, we will just use the absolute value of the maximum stress as indicated in Equation 5.17 because it simplifies the mathematics of interpolation on the constant life diagram. Thus, the values of b that we report will be different for these R-ratios than seen elsewhere and the plotted S-N curves for $R > 1$ appear to be at much lower stresses in Figures 2.3-2.6. As long as a consistent approach is applied throughout the analysis, this choice will not impact the outcome of the calculations. The S-N curves with their best fit lines are presented for each data set in Figures 2.3-2.6. The resulting a and b parameters are listed in Table 3.3.

Table 2.3: Average initial strength and least squares fit power law S-N curve parameters for each laminate

Data set	S_{uts} (MPa)	S_{ucs} (MPa)	R	# tests	a	b
DD16	602.9	-401.2	2	15	-11.91	30.95
			10	52	-18.02	29.68
			-2	32	-11.72	29.26
			-1	35	-8.56	23.90
			-0.5	21	-7.89	22.51
			0.1	98	-9.99	28.54
			0.5	66	-10.60	30.95
			0.7	23	-9.44	28.27
			0.8	27	-11.35	33.77
			0.9	24	-22.18	62.93
MD2	555.6	-459.8	2	9	-15.51	40.89
			10	28	-29.19	47.72
			-1	65	-9.35	25.65
			-0.4	28	-7.58	22.29
			0.1	47	-9.27	27.03
			0.5	15	-10.54	30.94
UD2	800.0	-500.9	10	47	-8.19	17.93
			-1	153	-9.23	26.67
			0.1	57	-8.40	26.17
VT8084	346.8	-299.2	10	57	-14.60	22.08
			-1	66	-8.34	20.83
			0.1	61	-6.88	19.03

The next step is to evaluate fatigue life at R-ratios that were not measured experimentally. Several authors [79, 92, 6] have chosen to curve fit an equation to the constant life diagram

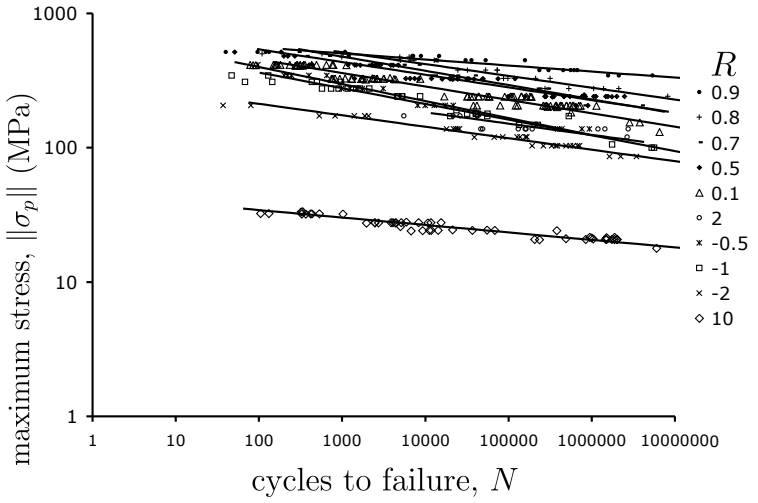

Figure 2.3: S-N curves for the DOE/MSU DD16 material data set on a log-log scale plot

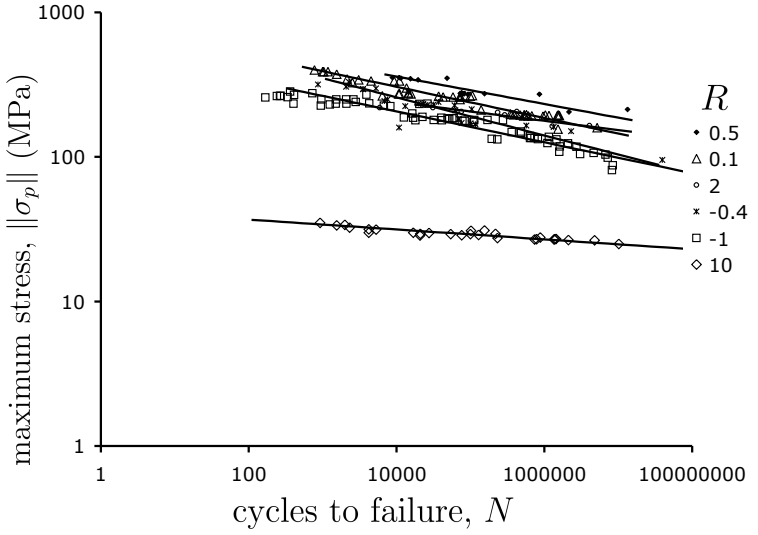

Figure 2.4: S-N curves for the Optimat MD2 material data set on a log-log scale plot

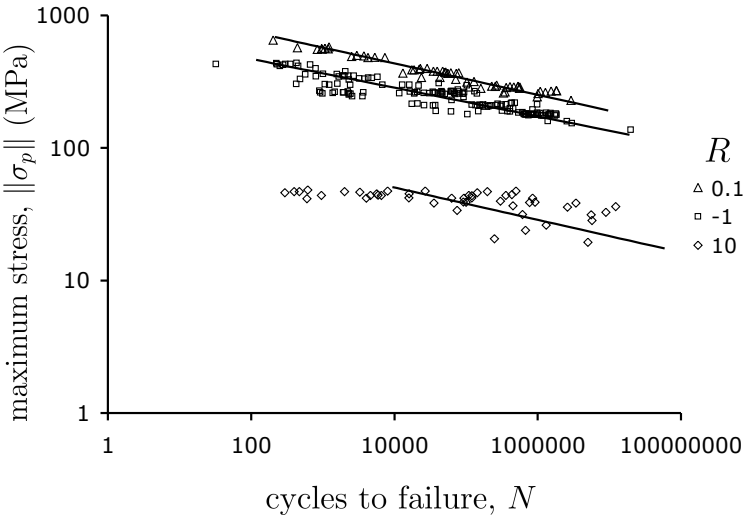

Figure 2.5: S-N curves for the Optimat UD2 material data set on a log-log scale plot

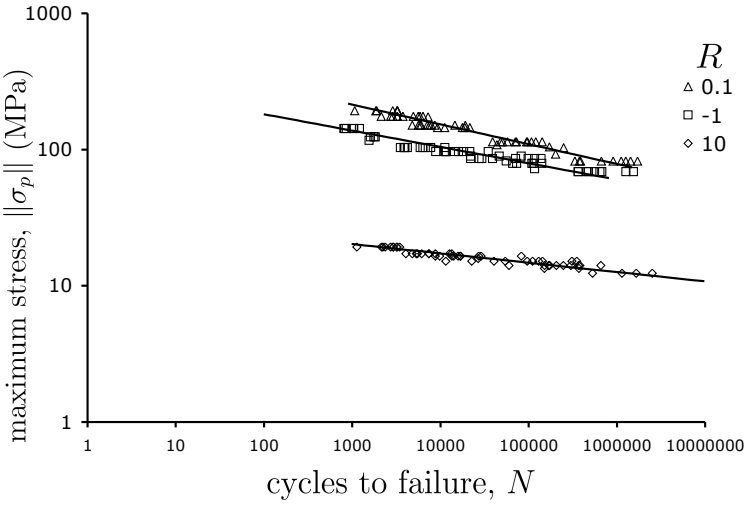

Figure 2.6: S-N curves for the Virginia Tech VT8084 material data set on log-log scale plot

from which N_i can be determined directly for a given σ_p and σ_v. However, it is unlikely that any of these equations will satisfactorily fit all of the data available for all four data sets. The approach by Vassilopoulos et al. [54] to use use artificial neural networks to develop an algorithm for calculating N based on a range of experimental data also has merit but is too complex for the present study. Instead, with a desire to use as much of the available constant amplitude fatigue data as possible, linear interpolation on the constant life plot between the available S-N curves will be used to compute N_i at arbitrary R-ratios. In order to do this, we must find the slope and intercept of a line running through the desired point in $\{\sigma_m, \sigma_a\}$ space and connecting with the two adjacent known S-N curves at equal lifetimes. If the current cycle has an R that is greater than the largest measured $R < 1$, then the S_{uts} on the mean stress axis is used as one end point of these lines and if R is greater than the largest measured $R > 1$ then the S_{ucs} point on the mean axis will be used as the endpoint. Constant life plots showing the linear connection of several decade increments of fatigue life are shown for each data set in Figures 2.7-2.10.

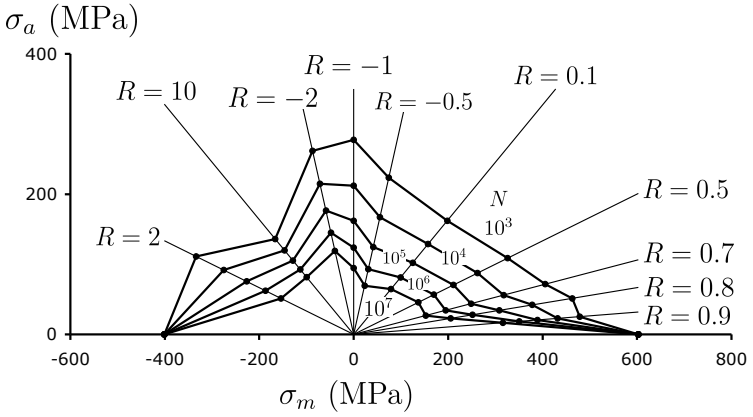

Figure 2.7: Constant life plot for the DOE/MSU DD16 material data set

Equations used in programing the linear interpolation are as follows and the process is shown graphically in Figure 2.11. First, determine the R and σ_m of the current cycle in the spectrum:

$$R_2 = \frac{\sigma_v}{\sigma_p} \tag{2.61}$$

$$\sigma_{m,2} = \frac{\sigma_p + \sigma_v}{2} \tag{2.62}$$

Then, find the R_1 and R_3 values with known S-N curves defined by a_1, b_1 and a_3, b_3 that R_2 lies between on the constant life plot. For a given life N, if $R_k < 1.0$ the corresponding mean and amplitude stress are:

$$\sigma_{m,k} = \frac{(1+R_k)\sigma_{p,k}}{2} = \frac{(1+R_k)}{2} 10^{(\log(N)-b_k)/a_k}, \; k = 1, 3 \tag{2.63}$$

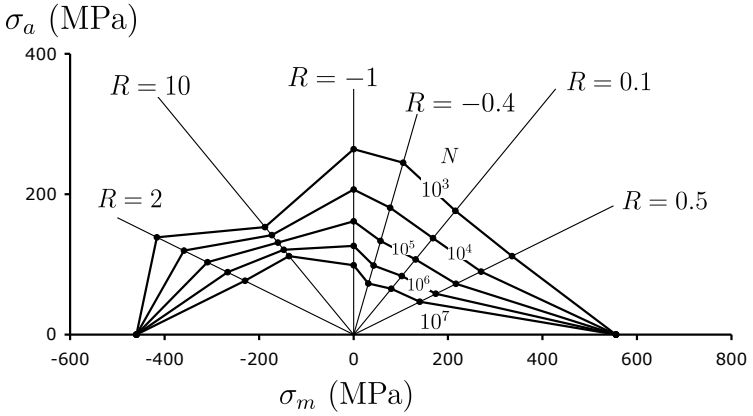

Figure 2.8: Constant life plot for the Optimat MD2 material data set

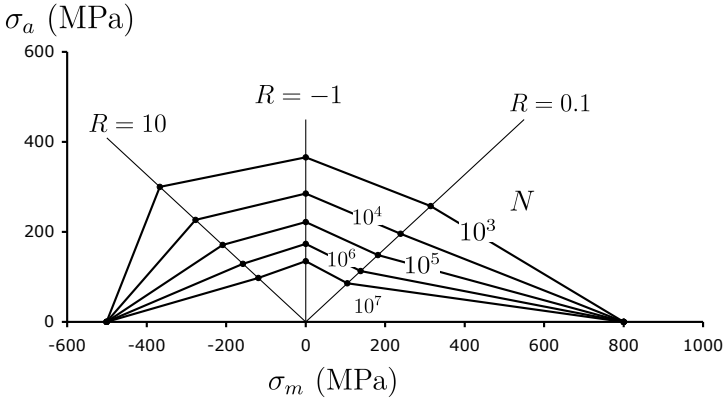

Figure 2.9: Constant life plot for the Optimat UD2 material data set

$$\sigma_{a,k} = \frac{(1-R_k)\sigma_{p,k}}{2} = \frac{(1-R_k)}{2} 10^{(\log(N)-b_k)/a_k},\ k = 1,3 \tag{2.64}$$

and if $R_k > 1.0$ then:

$$\sigma_{m,k} = \frac{(1+R_k)\sigma_{p,k}}{2} = -\frac{(1+R_k)}{2} 10^{(\log(N)-b_k)/a_k},\ k = 1,3 \tag{2.65}$$

$$\sigma_{a,k} = \frac{(1-R_k)\sigma_{p,k}}{2} = -\frac{(1-R_k)}{2} 10^{(\log(N)-b_k)/a_k},\ k = 1,3 \tag{2.66}$$

Then the equation of the line connecting points $\{\sigma_{m,1}, \sigma_{a,1}\}$ and $\{\sigma_{m,3}, \sigma_{a,3}\}$ in the constant life plane (see Figure 2.11) is:

$$\sigma_a = \frac{\sigma_{a,1} - \sigma_{a,3}}{\sigma_{m,1} - \sigma_{m,3}} \sigma_m + \sigma_{a,1} - \frac{\sigma_{a,1} - \sigma_{a,3}}{\sigma_{m,1} - \sigma_{m,3}} \sigma_{m,1} \tag{2.67}$$

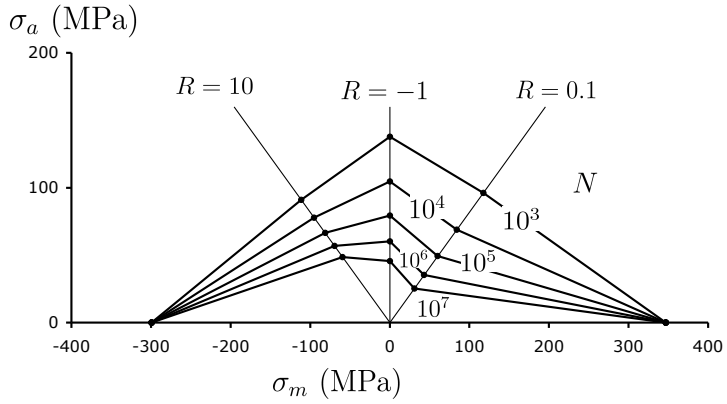

Figure 2.10: Constant life plot for the Virginia Tech VT8084 material data set

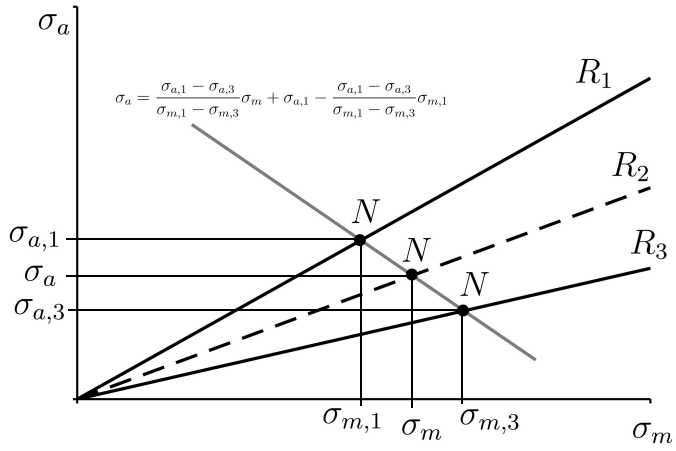

Figure 2.11: Illustration of the linear interpolation method to find constant amplitude fatigue life for any (σ_m, σ_a) cycle

and the equation for the of the desired R_2 line is:

$$\sigma_a = \frac{1 - R_2}{1 + R_2}\sigma_m \tag{2.68}$$

To find the intersection point of these lines in the constant life plane, the σ_a in Equations 2.67 and 2.68 are set equal to each other and the equation is solved for σ_m:

$$\sigma_m = -\frac{\sigma_{a,1}(\sigma_{m,1} - \sigma_{m,3}) - \sigma_{m,1}(\sigma_{a,1} - \sigma_{a,3})}{(\sigma_{a,1} - \sigma_{a,3}) - (\sigma_{m,1} - \sigma_{m,3})\left(\frac{1-R_2}{1+R_2}\right)} \tag{2.69}$$

If the special case that R_2 is greater than the largest measured $R < 1$ is encountered, then $\sigma_{m,3} = S_{uts}$ and $\sigma_{a,3} = 0$. Likewise, if the case that R_2 is greater than the largest measured $R > 1$ is encountered then $\sigma_{m,3} = S_{ucs}$ and $\sigma_{a,3} = 0$. We desire that $\sigma_m = \sigma_{m,2}$, the mean of the current load cycle. Unfortunately, Equation 2.69 can not be solved analytically for N in closed form. Instead, the equation is solved iteratively by selecting a value of N and refining that value until the calculated $\sigma_m = \sigma_{m,2}$ within an acceptable error. The initial value of N is chosen as the N found for R_1 with the desired σ_p and it is subsequently adjusted by:

$$N = N + N\frac{\sigma_m - \sigma_{m,2}}{\sigma_{m,2}} \tag{2.70}$$

until from Equation 2.69:

$$\left\| \frac{\sigma_m - \sigma_{m,2}}{\sigma_{m,2}} \right\| < 0.0001 \tag{2.71}$$

at which point, N is returned as the constant amplitude life of the current cycle. If the R of the current cycles is within $\pm 1\%$ of an R where fatigue life is measured, than the a and b for that R-ratio are used to calculate N directly and thus save computational time. This entire process is performed to find N_i for each cycle in the spectrum prior to running the model since the spectrum is repeated many times in most cases.

2.6.5 Failure modes

Composite materials typically exhibit different damage development and failure modes under tensile vs. compressive loads. While the damage accumulation is smeared through use of the S-N curves under various R-ratios, none of the the fatigue models discussed in this article are capable of handling both tensile and compressive failure modes simultaneously. The damage accumulation models of Section 2.3 do not explicitly consider a failure mode and thus are directly applicable for loading where the dominate stress changes from tension to compressive or vice versa (although in the BF model, the parameters are found differently for spectra that compressive dominated).

All residual strength models, Section 2.4, use the criterion that failure occurs when $S_r < \sigma_p$ for tensile failures. For compressive dominated fatigue failures, the models can be applied to

the absolute value of the compressive stress peaks and residual compression strength instead by applying the models with $\sigma_p = \|\sigma_v\|$ and the initial strength $S_u = \|S_{ucs}\|$. Schaff and Davidson [78] suggested the approach of calculating the residual compression strength based on the fraction of tensile strength whenever the loading switched from tensile to compressive:

$$S_{r,c} = S_{ucs}\frac{S_{r,t}}{S_{uts}} \tag{2.72}$$

and vice versa whenever the loading switched from compression to tension:

$$S_{r,t} = S_{uts}\frac{S_{r,c}}{S_{ucs}} \tag{2.73}$$

where $S_{r,t}$ and $S_{r,c}$ are the tensile and compressive residual strengths after a given loading. However, Schaff and Davidson never tested this rather arbitrary hypotheses and so the validity of this assumption remains uncertain. Because the damage observed under $R = 0.1$ is dominated by matrix cracking while the damage is dominated by delaminations under compressive loading, it seems unlikely that the equal fractional residual strength approach would be accurate, and thus this method is not considered for the present study.

For a general load history, it may be difficult to determine whether the failure will be tensile or compressive. However, for the spectrum loads in the selected data sets, an obvious choice is apparent. In the DD16 data set, the WISPK and WISXR01 spectra contain only tensile fatigue cycles and the failures will obviously be tensile. In the DD16, MD2, and UD2 data sets WISPER and WISPERX experiments, the spectra is primarily tensile dominated with an average $R = 0.4$ and a minimum $R = -0.6$. Although the minimum R in WISPER and WISPERX is on the order of the ratio between the tensile and compressive strengths of these materials, we will assume that the failures are tensile because the vast majority of cycles are purely T-T. Additionally, observed failures were noted to be tensile for all of the tests in the Optimat data base [51]. For the VT8084 material, the RAY95 spectrum is approximately fully reversed and, under $R = -1$ loading, failures were always observed to occur in compression, so the compression residual strength will be calculated to determine failure. For the RAY95R01 spectrum, the loading is forced to an $R = 0.1$ loading and thus failures will be tensile and tensile residual strength will be tracked.

2.6.6 Fitting model parameters

Each damage accumulation and residual strength model discussed in Sections 2.3 and 2.4 are reviewed in the context of determining the required parameters for each data set. In each case, the method used for fitting the parameters and any details required for applying the model to the spectrum loads is discussed. Several methods are deemed inappropriate for either the available fitting data or application to the loading spectra and the reasons are discussed. A summary of the selected models with a list of the required parameters to be found is provided in Table 2.4. The parameter N_i indicates that the model requires the

constant amplitude life of each cycles as calculated in Section 2.6.4. The resulting parameters (excluding N_i) for each model as applied to each data set are given in Table 2.5.

Table 2.4: Summary of fatigue models as applied to spectrum loading

Model	Eqns	Applied to Spectrum Loading	Parameters
PM[8]	2.1	$D = \sum_{i=1}^{n} \frac{1}{N_i}$	N_i
OH[69]	2.6	$D = \sum_{i=1}^{n} \left[A \left(\frac{1}{N_i} \right) + (1 - A) \left(\frac{1}{N_i} \right)^2 \right]$	N_i, A
BF[44]	2.7	$D = \sum_{i=1}^{n} \left[A \left(\frac{1}{N_i} \right) + B \left(\frac{1}{N_i} \right)^C \right]$	N_i, A, B, C
	2.8-2.11	A, B, C determined from static properties	
HR[17]	2.12	$D(i) = D(i-1)^{\frac{\log \sigma(i)}{\log \sigma(i-1)}} + \frac{n_i}{N_i}$ applied iteratively	N_i
BS[9]	2.22	$S_r(n) = S_u - \sum_{i=1}^{n} (S_u - \sigma_i) \frac{1}{N_i}$	N_i
RS1	2.20	$S_r = S_u - \left[\sum_{i=1}^{n} \left(S_u - \sigma_{p,i} \right)^{1/A} \frac{1}{N_i} \right]^A$	N_i, A
RS2	2.20	$S_{r,i} = S_u - (S_u - \sigma_{p,i}) \left(\frac{n_i + n_{eqv,i-1}}{N_i} \right)^{A_i}$ applied iteratively where:	N_i, A_1, A_2, A_3
	2.75	$A_i = A_1 \frac{\sigma_{p,i}}{S_u} + A_2$, if $A_i < A_3$, then $A_i = A_3$	
	2.21	$n_{eqv,i-1} = N_i \left[\frac{S_u - S_{r,i-1}}{S_u - \sigma_{p,i}} \right]^{1/A_i}$	
RS3	2.20	$S_r = \left[S_u^C - \sum_{i=1}^{n} \left(S_u^C - \sigma_{p,i}^C \right) \frac{1}{N_i} \right]^{1/C}$	N_i, C
RS4	2.20	$S_{r,i} = \left[S_u^{C_i} - \left(S_u^{C_i} - \sigma_{p,i}^{C_i} \right) \left(\frac{n_i + n_{eqv,i-1}}{N_i} \right) \right]^{1/C_i}$ applied iteratively where:	N_i, C_1, C_2, C_3
	2.76	$C_i = C_1 \frac{\sigma_{p,i}}{S_u} + C_2$, if $C_i < C_3$, then $C_i = C_3$	
	2.21	$n_{eqv,i-1} = N_i \left[\frac{S_u^{C_i} - S_{r,i-1}^{C_i}}{S_u^{C_i} - \sigma_{p,i}^{C_i}} \right]$	

continued on next page

continued from previous page

Model	Eqns	Applied to Spectrum Loading	Parameters
RS5	2.20	$S_r = \left[S_u^C - \left[\sum_{i=1}^{n} \left(S_u^C - \sigma_{p,i}^C\right)^{1/A} \frac{1}{N_i}\right]^A\right]^{1/C}$	N_i, A, C
Y1 [86]	2.33	$S_r = \left[S_u^C - S_0^C K \sum_{i=1}^{n} \sigma_{p,i}^B\right]^{1/C}$	C, B, K, S_0
INT [91]	2.42	$S_{r,i} = (S_u - \sigma_p)\left[1 - \left(\frac{\log(n_i + n_{eqv,i-1}) - \log(0.5)}{\log(N_i) - \log(0.5)}\right)^x\right]^{1/y} + \sigma_p$ apply iteratively where: $n_{eqv,i-1} = (\log(N_i) - \log(0.5))\left[1 - \left(\frac{S_{r,i-1} - \sigma_{p,i}}{S_u - \sigma_{p,i}}\right)^y\right]^{1/x}$	N_i, x, y

Damage Accumulation Models

For the damage accumulation approaches, the Palgren-Miner rule (PM), Equation 2.1, is the easiest to apply as it only requires knowledge of the constant amplitude fatigue life for each applied cycle as determined in Section 2.6.4. The Marco-Starkey (MS), Equation 2.3, approach has been used by several authors [21, 22] for multi-block variable amplitude fatigue loading in composites. Typically the value of $C_1 = 1$ for one R and σ_p and then the ratios of C_1/C_2 and so on for each of the other loadings are found using data from two block or repeated block fatigue experimental results. However this method is untenable for the spectra considered in the present comparison because they consist of may different cycle amplitudes and R-ratios and only limited block loading data at a few stress levels is available for the DD16 and MD2 data sets. It is impractical for C_i to be determined empirically for any general realistic loading spectrum and thus the MS model is not included in this comparison. Although we could use a modified PM model where the C of MS is constant, determination of C without additional data (cracks, modulus, etc.) is not possible and regardless of the value chosen, the predicted spectrum fatigue life will be identical to the PM result.

The Owen and Howe (OH) model, Equation 2.6, has only one parameter A which is taken as a constant for a given material. Two block or repeat block loading is required to determine the value of A. This data was only available for the DD16 and MD2 data sets so the OH model will only be applied to those cases. In both data sets, all of the repeated two stress level loading under $R = 0.1$ was collected and A was chosen by minimizing the root mean square (RMS) error between the value of D at the specimen failure and 1.0 for each test.

The Bond and Farrow (BF) damage model, Equation 2.7, has three parameters fit to the initial tensile and compressive properties of the composite as shown in Equations 2.8 -

2.11. The Hashin and Rotem (HR) damage model, Equation 2.12, uses the ratio of peak applied stress to determine the power of D_{i-1} and thus does not require any additional fitting parameters.

Residual Strength

The Broutman and Sahu (BS) model, Equation 2.22, is the simplest residual strength approach and requires only the initial strength data in addition to N_i. Five other versions of the generalized residual strength model, Equation 2.20, labeled RS1 through RS5 will also be considered. For this series of models, the parameters A and C, which impact the shape of the residual strength curve, are fit to residual strength data collected by interrupted constant amplitude fatigue tests where the residual strength was measured. While it is possible to fit any residual strength model using the SLERA as described by Yang [80], this approach can be difficult to optimize and a simpler method is desired that will enable easier comparison of the resulting curves to the experimental data. Also, although the SLERA is implicit in any residual strength model that attempts to predict the distribution of residual strength or fatigue life, we do not know for certain that it is a valid assumption and thus it is equally reasonable to attempt to fit the shape of the residual strength curves to match that of the experimental residual strength data available for each data set.

Because of the scatter in fatigue lifetimes, some residual strength tests will fail early (prematurely) at the applied fatigue stress before the desired number of cycles is reached. Exclusion of premature failures from the residual strength would bias the calculated distribution to higher residual strengths. To avoid this bias, a two parameter Weibull distribution of residual strength was fit to the data at each residual strength (RS) point $\{R, \sigma_p, N\}$ using the method described by Yao and Himmel [138]. This method takes premature failures into account in calculating the median rank of the surviving specimens' strength and thus estimates the entire residual strength distribution including the "imaginary" residual strength that is below the applied loading for those specimens that failed prematurely. Then the mean residual strength can be calculated from the Weibull distribution as:

$$S_r = S_{r0}\Gamma\left(1 + \frac{1}{\alpha}\right) \tag{2.74}$$

where Γ is the Gamma function and α and S_{r0} are the shape and location parameters of the residual strength distribution. The calculated mean residual strength values are then used to fit the residual strength model parameters by minimizing the least square error in residual strength between the model and experiment for the relevant mean RS points.

Unfortunately, a small number of replicates (2-5) are typically available for individual residual strength data points in the Optimat and DOE/MSU data bases. In general calculation of mean residual strength was performed and the RS point used in fitting if at least two specimens survived to have their residual strength measured. If only one value is available,

then the RS point is not included. For the DOE/MSU data base, earlier tests performed on the same material system with more replicates at three life fractions under an applied fatigue stress of 240 MPa were used to estimate residual strength model parameters. For the VT8084 data set, about 10 replicates (some of which failed prematurely) were available for two to four residual strength points at three stress levels.

In RS1, $C = 1$, and A =constant for a given loading. For tensile dominated loading, A was found for $R = 0.1$ data only and is considered a constant with respect to R because adequate residual strength data was not available at other tension-dominated R-ratios for any of the data sets. For the DOE/MSU DD16 material, a very different value of $A = 0.938$ (nearly linear) was found by this method using mean residual strength values as compared to the value $A = 0.265$ (early decline) chosen by Wahl et al. [49]. In the VT8084 data, separate values of A were found for the tensile residual strength under $R = 0.1$, and the compression residual strength under $R = -1$ fatigue, to be used in the RAY95R01 and RAY95 loading spectra predictions respectively.

For RS2, $C = 1$ again, but A is considered a function of σ_p although still constant with respect to R for a given spectrum due to the lack of data. Because the number of stress levels is very limited (typically 3), it is not possible to determine the best functional form for A. As the data appears to be approximately a linear function of stress the chosen form was:

$$A = \begin{cases} A_1 \frac{\sigma_p}{S_u} + A_2 & \text{if} \quad A_3 \leqslant A_1 \frac{\sigma_p}{S_u} + A_2 \\ A_3 & \text{if} \quad A_3 \geqslant A_1 \frac{\sigma_p}{S_{uts}} + A_2 \end{cases} \tag{2.75}$$

A_1 and A_2 are found by least squares fitting to the $\{A, \sigma_p\}$ data points and A_3 is chosen as the smallest value of A found for all stress levels under the assumption that A should not approach 0 or become negative. An example of the resulting fit shape is shown in Figure 2.12. The RS2 model has been applied to the MD2 and UD2 data using $R = 0.1$ tensile residual strength points and to the VT8084 data using $R = -1$ compression residual strength points. The DD16 data set did not have enough data at different stress levels to fit RS2. For the VT8084 data under $R = 0.1$, A was approximately constant as a function of stress (or at least no trend was apparent with only three data points available) and thus RS2 reduces to RS1.

For RS3, $A = 1$ and C is a constant. Fitting proceeds in an identical method to RS1. In RS4, C is considered a function of stress and determined using a method identical to that of RS2:

$$C = \begin{cases} C_1 \frac{\sigma_p}{S_u} + C_2 & \text{if} \quad C_3 \leqslant C_1 \frac{\sigma_p}{S_u} + C_2 \\ C_3 & \text{if} \quad C_3 \geqslant C_1 \frac{\sigma_p}{S_u} + C_2 \end{cases} \tag{2.76}$$

where C_1, C_2 are found by linear least squares fitting of the $\{C, \sigma_p\}$ points found from the residual strength data at each stress level and C_3 is the smallest value of C in those points. The same data sets that were applicable for RS2: MD2, UD2 and VT8084 ($R = -1$), apply to RS4.

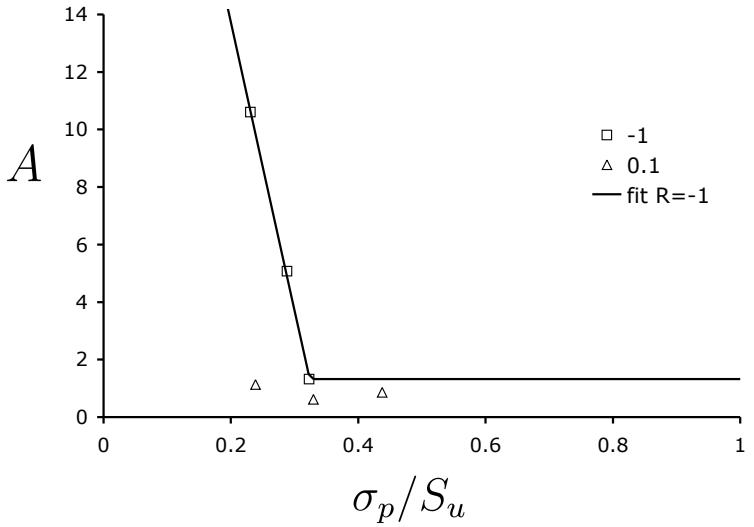

Figure 2.12: Example of A values generated for RS2 model based on the residual strength at different stress levels (VT8084 data set) showing fit line from Equation 2.75

RS5, the final version of the generalized residual strength model tried, is the case where both A and C are treated as fitting constants. Although such a model has not be attempted in the literature, it is an obvious extension of the prior approaches and has the distinct advantage of being able to fit both an initial and final drop in the residual strength as shown in Figure 2.13 if $A < 1$ and $C > 1$ or vice versa are selected. By comparison, RS1-RS4 are capable of modeling either an initial or final decline in the residual strength ($A, C < 1$ or $A, C > 1$ respectively) but not both at the same stress level R. To fit the RS5 model, the same data set was used as in the case of RS1, but now both A and C are adjusted to minimize the error between the model and the real mean residual strength data. While the Excel Solver tool would typically only arrive at one optimum solution with both A and C positive, regardless of the starting point, it is theoretically possible that there could be a second local minimum. Several starting points are selected with either A or C greater than one to determine the best solution (smallest error). A model with A and C both as functions of stress was not attempted because the number of residual strength data points available was too small compared to the number of degrees of freedom for the fitting to be reliable.

Note that the Reifsnider model (Equation 2.24), when applied to a composite as a whole rather than just the critical element, is the same as RS1. Schaff and Davidson's model is the same as RS2 if we exclude cycle mix effects ($C_m = 0$) as they did in most of their examples. Wahl et al. [48, 49] did not find a statistically significant difference in fatigue life under repeated block loading with short or long blocks and Post et al.[2] did not find a detectable difference in fatigue life under Rayleigh distributed loading with various autocorrelations between 0 (completely random) and 1 (ordered). Based on these observations, cycle mixing analysis is not required and thus is not included in this comparison. Schaff and Davidson

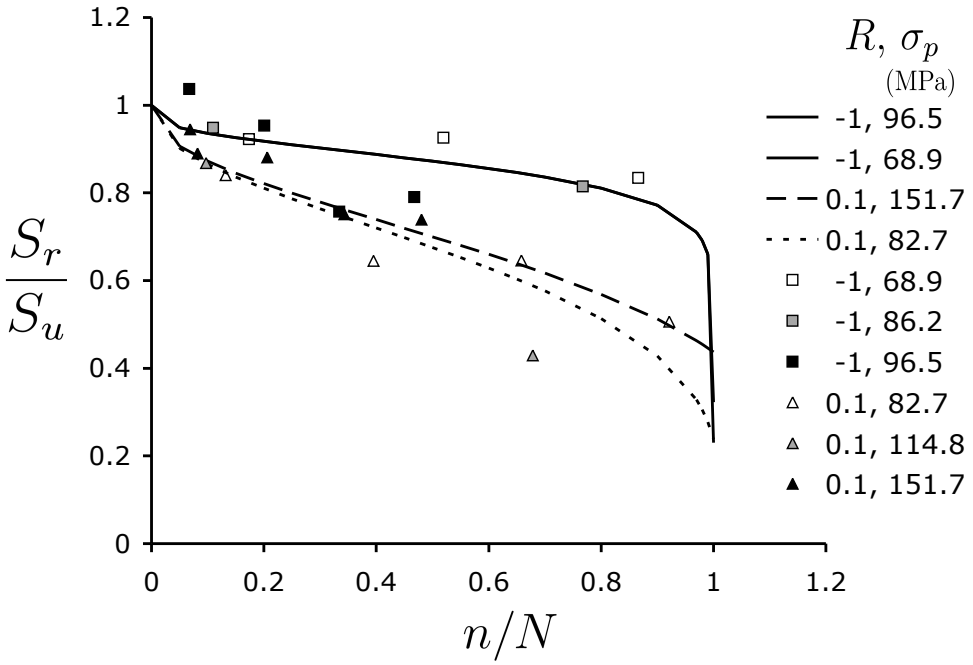

Figure 2.13: Example of resulting constant amplitude residual strength curves for RS5 model fit to VT8084 data showing initial drop, steady decline and final drop in residual strength

fit their model parameters using SLERA and comparing the predicted and experimental life distributions rather than using residual strength data (which they did not have). While this method has some merit, particularly in the absence of residual strength data, Schaff and Davidson did not provide a mathematical means of optimizing the predicted distribution, suggesting that this be done visually instead. Because such a method is subjective, it was not appropriate for the present study. We also note that the Hahn and Kim model is identical to RS3.

The Yang and Liu model (Y1) in Equation 2.33 differs from the general residual strength model of Equation 2.20 in that it bases the degradation rate of residual strength on the Weibull location parameter of the initial strength S_0^C (a constant for all applied loads) rather than on $(S_u - \sigma_p)$ and that n/N is replaced by n/N_0, where N_0 is the location parameter of the constant amplitude life. Therefore, it will be treated as a unique approach here. Fitting for Y1 was performed using the SLERA based method suggested by Yang and Liu [80]. This method fits both the S-N curve parameters, K and B for a given R and the residual strength curve shape parameter C simultaneously using pooled constant amplitude fatigue failures and residual strength data. All of the fatigue and residual strength data for one R was used to fit the model for each data set. The minimization of the error in the moments of the calculated initial strength distribution with respect to all three parameters is relatively unstable and has a tendency to find local minimums. Using various starting places, and

in the case of UD2, excluding the third moment from consideration entirely, was necessary to find stable results. Admittedly, in all cases, a lot more fatigue and residual strength data points were used than Yang suggested and this may have led to some of the difficulty. Because of the challenges faced in arriving at an optimum solution for Y1, neither of the more complex versions of Yang's model (Equations 2.37 and 2.38) were attempted. It is recognized that ideally K, B, and C should be functions of R and C is possibly function of σ_p as well. However, the amount of data available at R other than 10, -1, and 0.1 was limited and some method of interpolation for the values between different R would be needed. This analysis would add a considerable level of complixity to applying the model and was not performed. Instead, Y1 was applied by fitting the parameters to $R = 0.1$ ($R = -1$ for the VT8084 RAY95 case) and then using the σ_p of each cycle regardless of the actual R of that cycle.

The Interaction Model (INT), Equation 2.42, is fit using the method of minimizing the fixed pitch error (using a pitch of 1) as suggested by Adam et al. [91]. r and t are calculated for each mean residual strength point (using the same mean values of the residual strength data as in RS1-RS5) and then the error between the predicted curve and those points in $r - t$ space is minimized to determine x and y. $R = 0.1$ residual strength data is used for all cases except for the VT8084 RAY95 spectrum where $R = -1$ data is used with the compression residual strength being tracked instead. Two example $r - t$ curve fits are shown in Figure 2.14.

The Eraapachchi and Clausen model, Equation 2.47, was applied by the authors to several variable amplitude block load cases in [12] where the blocks of load had lengths $n_i > 1$. However, if we attempt to apply the Eraapachchi and Clausen model to a spectrum loading where in general each block only last 1 cycle, the second term of Equation 2.47 contains a factor $(n^A - 1)$ which for a value of $n = 1$ will be zero and thus the residual strength never changes. This is a problem for Eraapachchi and Clausen's formulation, at least when considering general spectrum loading, and thus it was not possible to use the model to make predictions in the present study.

In order to apply the Yao and Himmel residual strength model, Equation 2.49, to variable amplitude loading, calculation of the the equivalent number of cycles previously applied would be required before proceeding with each new stress level. Unfortunately, the model as presented can not be solved for n explicitly. Thus, in order to apply the model to a general loading, Equation 2.49 would have to be solved numerically for n_{eqv} after each cycle. This process would be too computationally intensive and might result in significant accumulated error through the life of the composite. Thus this model has a significant disadvantage for general spectrum loading and is not included in the present comparison.

Finally, we also consider the model proposed by Philippidis and Passipoularidis, Equation 2.50. Again, it is not possible to solve for n_{eqv} explicitly and thus the model is not ideal for application to variable amplitude spectra. Additionally, we note that the behavior the authors sought in creating the model can also be achieved with RS5 which is considerably

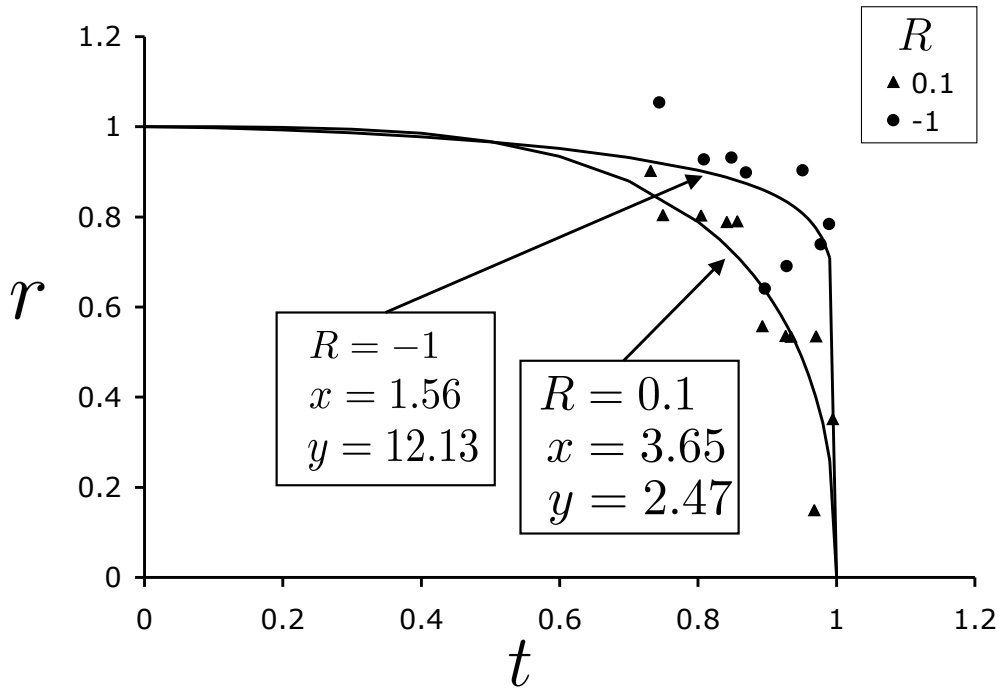

Figure 2.14: Example showing the fit curve for the INT model applied to the VT8084 data set

simpler to apply as the damage can be simply summed over all applied loading cycles.

Calculation of equivalent cycles

Models that involve a non-linear accumulation of damage or reduction of residual strength (caused by variation of the power as a function of the load applied) require the calculation of the equivalent number of cycles at the new stress level, n_{eqv} prior to determining the residual strength under that stress. For example using the RS2 model:

$$S_{r,i} = S_u - (S_u - S_{p,i}) \left(\frac{n_i + n_{eqv,i-1}}{N_i} \right)^{A_i} \tag{2.77}$$

then with $i = i + 1$:

$$n_{eff}(i-1) = N_i \left(\frac{S_u - S_{r,i-1}}{S_u - \sigma_{p,i}} \right)^{1/A_i} \tag{2.78}$$

However, it is possible that in the repeated calculation of the A^{th} root in Equation 2.78 after each cycle, numerical error will accumulate and become significant in the predicted fatigue life result. In order to check for this possibility, the analysis was run using extreme values of

Table 2.5: Summary of the parameter values found for each model and data set

		Data Set				
		DD16	MD2	UD2	VT8084	VT8084
Model	Param	R=0.1	R=0.1	R=0.1	R=-1	R=0.1
OH	A	1.067	1.6326	-	-	-
BF	A	0.6655	0.8275	0.626	0.0133	0.8627
	B	0.6655	0.8275	0.626	0.0133	0.8627
	C	1.5027	1.2085	1.597	1.296	1.1591
RS1	A	0.9376	1.95	1.446	8.000	0.899
RS2	A_1	-	-32.72	10.1226	-100.2	-
	A_2	-	16.42	-2.843	33.77	-
	A_3	-	0.993	0.75	1.322	-
RS3	C	0.7583	5.444	1.058	6.68	1.0956
RS4	C_1	-	7.305	61.03	-94.26	-
	C_2	-	2.864	-22.45	33.02	-
	C_3	-	3.53	0.699	2.016	-
RS5	A	1.206	0.1908	0.9708	0.2020	0.38247
	C	0.307	10.95	2.305	14.91	3.6726
Y1	S_0	639.81	536.91	819.02	305.28	354.03
	K	9.80×10^{-20}	2.967×10^{-10}	8.174×10^{-28}	8.684×10^{-22}	1.842×10^{-26}
	B	5.8924	1.949	8.601	8.4377	10.19
	C	13.654	53.63	28.13	18.92	21.9
INT	x	9.9144	1.451	10.22	1.556	3.650
	y	1.0231	5.177	1.91	12.128	2.469

constant A. For $A_i = A$ =constant the iterative application of Equations 2.77 and 2.78 will have the same mathematical result as RS1:

$$S_r = S_u - \left[\sum_{i=1}^{n} (S_u - \sigma_{p,i})^{1/A} \left(\frac{1}{N_i}\right)\right]^A \tag{2.79}$$

while avoiding possible numerical error accumulation. Simulations on the DD16 spectra and constant life data were run both ways for two cases: $A = 10.0$ and $A = 0.1$. In both cases calculations were performed with double precision variables in Java. Equations 2.77 and 2.78 provided exactly the same number of cycles to failure as calculations performed with

Equation 2.79 for every spectrum loading case including predicted fatigue lives in excess of 1 million cycles. Thus, numerical error is not a significant concern in this analysis. As the computational time for the n_{eqv} calculation method is considerably greater, the method of Equation 2.79 is preferable whenever A can be considered constant for an entire spectrum.

2.7 Results and Discussion

The prediction results from each model for a selection of spectrum load cases from the data sets are presented in Tables 2.6-2.8. In general, lower stress, longer life experimental cases were selected for modeling because this is the regime closest to actual design use of these materials. Equation 2.58 is used to calculated M_e for each model result based on the average experimental result for that case. A value of $M_e = 0$ indicates that the model matched the experimental result, while $M_e = 1$ indicates a predicted life 10 times the experimental life, and $M_e = -1$ indicates that the predicted life was $1/10^{\text{th}}$ of the experimental life. The number of experimental replicates varied from 4 to 11 for each loading case and in some cases the scatter in the experimental spectrum fatigue failures spanned a decade or more so the confidence in experimental mean values is limited. A $-0.3 < M_e < 0.7$ indicates a good result where the predicted fatigue life was within the span of a decade surrounding the experimental life. The median values of M_e are also calculated for each loading case over all 12 models to give an idea of the general level of bias produced by the models in general.

For the DD16 material (Table 2.6), all of the models except for Y1 gave non-conservative results in every load case. For the damage accumulation models, the OH model provided slightly better predictions than PM while BF was the worst model overall (least conservative). Of the general residual strength models, RS5 gave the best results, but they were only slightly better than the much simpler BS version of the model. The INT model gave the best predictions for this data set with predictions ranging 117-192% of the actual mean fatigue life. The Y1 model was overly conservative predicting only about 26% of the actual fatigue life in some cases. The generally larger error for the WISPERX spectra from all of the models can potentially be attributed to the fact that the parameters were fit using $R = 0.1$ data only even though this spectrum contains a wide range of R and N_i was evaluated for each cycle in WISPERX based on the interpolation of the constant life plot. However, larger errors were found for the WISPERX predictions from both the PM and BS models too, neither of which included any fitting beyond N_i.

In the MD2 material data set (Table 2.7), all of the models performed very well, especially for modeling the full WISPER spectra. This was true even for those models containing fitting parameters based on the $R = 0.1$ data only. However, predictions were not nearly as good for the unidirectional UD2 material with median predicted lifetimes about 3.5 times the experimental result. Again Y1 gave conservative results in every case. Other models were right on or slightly conservative for the WISPER spectrum applied to the MD2 laminate. BS gave more conservative results than PM in all cases. The INT model also gave good

Table 2.6: Comparison of model predictions for mean fatigue life of DOE/MSU DD16 material under spectrum loading

Material	DD16	DD16	DD16	DD16
Spectrum	WISPERX	WISPK	WISXR01	WISXR01
$max(\|\|\sigma\|\|)$ (MPa)	259.5	255.3	237.2	203.5
# replicates	6	8	9	6
average exp. N	915,000	532,000	204,000	1,380,000
# spectrum repeats	71.3	41.5	16.0	109
Model	M_e			
PM	0.40	0.26	0.26	0.10
OH	0.37	0.23	0.24	0.07
BF	0.57	0.44	0.44	0.28
HR	0.39	0.26	0.26	0.10
BS	0.32	0.19	0.24	0.08
RS1	0.40	0.26	0.27	0.10
RS2	-	-	-	-
RS3	0.31	0.18	0.24	0.07
RS4	-	-	-	-
RS5	0.30	0.18	0.24	0.07
Y1	-0.58	-0.31	-0.13	-0.57
INT	0.28	0.16	0.23	0.07

results for the MD2 laminate and was similar to the other residual strength models for the UD2 case. In the UD2 laminate, RS2 and RS4 gave better results than the other generalized residual strength models, indicating that having the A and C parameters as a function of stress is useful for modeling the unidirectional laminate behavior. In the UD2 laminate, the RS2 and RS4 model parameters A and C increased with stress while in the other laminates they decreased or were relatively constant. This may explain why the UD2 laminate is the only case where RS2 and RS4 performed better than other residual strength models. The BF model gave by far the worse results for the UD2 laminate, over predicting the life by 6 times, while the Y1 model under predicting the life by about 50%.

The VT8084 data set RAY95 spectrum was the the only compression dominated spectrum fatigue data available for this study. In this case, shown in Table 2.8, most models performed very well with the exception of BF which demonstrated unacceptable error. The PM, RS3, and RS5 models gave nearly identical results and the HR, BS, RS1 and INT models also performed equally well giving slightly more conservative predictions of fatigue life than the former three. The Y1 model, along with RS2 and RS4 models were overly conservative by

Table 2.7: Comparison of model predictions for mean fatigue life of OPTIMAT database materials under spectrum loading

Data set	MD2	MD2	MD2	UD2	UD2
Spectrum	WISPER	WISPER	WISPERX	WISPER	WISPER
$max(\sigma_p)$ (MPa)	355	284	248	375	350
# replicates	4	4	3	7	5
average exp N	678,073	5,944,292	2,735,290	4,787,267	9,198,844
# of blocks	5.1	44.8	213.2	36.1	69.3
Model			M_e		
PM	0.02	0.07	0.23	0.60	0.59
OH	-0.20	-0.15	0.02	-	-
BF	0.08	0.13	0.29	0.80	0.80
HR	0.01	0.06	0.23	0.60	0.59
BS	-0.09	-0.05	0.15	0.50	0.50
RS1	0.08	0.07	0.23	0.60	0.59
RS2	-0.10	-0.04	0.17	0.46	0.47
RS3	0.00	0.06	0.23	0.50	0.50
RS4	0.00	0.06	0.23	0.47	0.48
RS5	0.02	0.07	0.23	0.55	0.55
Y1	-0.03	-0.78	-0.43	-0.30	-0.33
INT	-0.04	0.02	0.21	0.55	0.55

comparison. Under the tensile version of this loading, RAY95R01, most models produced non-conservative results with the exception of RS1 and Y1. RS1 gave the best overall results in VT8084 material system with $-0.03 < M_e < 0.04$ including both the compression and tension dominated fatigue.

Across all four material systems and the range of spectrum loadings applied (Table 2.9), it is apparent that the BF model is the least reliable at producing acceptable results, generally over predicting fatigue life more than the other models and in the case of compression loading (VT8084 RAY95) fails entirely. This on the whole is not surprising given that Bond and Farrow [44] developed the approach based on matrix dominated composites and all of the materials considered here were fiber dominated. While the concept of being able to determine fatigue model parameters from static properties is attractive, this approach is likely impractical for a general model of fiber dominated materials outside of very special cases.

Considering the poor reputation of PM based on two block fatigue loading the model performs well under the repeated spectrum loading considered here with the worst prediction

Table 2.8: Comparison of model predictions for mean fatigue life under spectrum loading of VT8084 material

Material	VT8084	VT8084	VT8084
Spectrum	RAY95	RAY95	RAY95R01
$max(\|\sigma\|)$ (MPa)	127.2	107.7	183.8
# replicates	10	10	5
average exp. N	265,000	916,000	150,000
# spectrum repeats	53.1	183	30.1
Model		M_e	
PM	0.00	0.06	0.27
OH	-	-	-
BF	1.85	1.92	0.26
HR	-0.01	0.05	0.27
BS	-0.07	0.01	0.17
RS1	-0.03	0.04	-0.01
RS2	-0.22	-0.23	-
RS3	0.00	0.06	0.17
RS4	-0.19	-0.11	-
RS5	0.00	0.06	0.20
Y1	-0.12	-0.05	-0.32
INT	-0.06	0.02	0.17

being about 4 times the experimental fatigue life in the unidirectional UD2 material and otherwise giving predictions within 2.5 times the experimental life. The OH model gave more conservative (and generally better overall) results than PM for the cases where block loading data was available to fit the A parameter. The HR model produced nearly identical results to PM in all cases showing that nothing was gained by applying this more complex damage accumulation law.

The simple residual strength model introduced by Broutman and Sahu [9], BS, gave more conservative prediction of fatigue life than PM in all cases due to failure occurring at the highest stress present in the spectrum. Since PM generally over predicted fatigue life, the BS results were generally better. RS1 performed better than BS in the VT8084 material, particularly for tensile loading, but had a worse showing in the DD16, MD2 and UD2 materials under WISPER type spectra compared to BS. The two residual strength models where parameters varied as a function of peak stress, RS2 and RS4, provided better predictions in the UD2 material than the corresponding model with a constant parameter (RS1 and RS3 respectively), but were considerably less effective in other cases. This may be caused by the restriction of the simple linear model with a cut off value chosen for the stress dependence

Table 2.9: Comparison of model predictions statistics compiled for all data sets and spectrum loads

Model	$max(M_e)$	$min(M_e)$	$mean(M_e)$	$median(M_e)$
PM	0.60	0.00	0.24	0.24
OH[1]	0.37	-0.20	0.08	0.07
BF	1.92	0.08	0.65	0.44
HR	0.60	-0.01	0.23	0.24
BS	0.50	-0.09	0.16	0.16
RS1	0.60	-0.03	0.22	0.17
RS2[2]	0.47	-0.23	0.07	-0.04
RS3	0.50	0.00	0.19	0.17
RS4[2]	0.48	-0.19	0.13	0.06
RS5	0.55	0.00	0.21	0.19
Y1	-0.03	-0.78	-0.33	-0.31
INT	0.55	-0.06	0.18	0.17

[1] excludes UD2 and VA8084 data sets
[2] excludes DD16 data set and VA8084 RAY95R01 case

of the parameters and narrow range of stress values over which residual strength data was available to fit it. The RS2 model provided the best predictions in the UD2 data set and thus, this approach should not be dismissed, especially when considering unidirectional material or for implementation in a critical element theory. The two parameter RS5 model provided better results than the other generalized fatigue equation approaches for the DD16 data set and the overall range of $0.0 < M_e < 0.30$ excluding the UD2 data set where $M_e = 0.55$ is very good.

The interaction model by Adam et al. [91], INT, performed very well with $-0.06 < M_e < 0.28$ in all of the multi-directional laminates while over-predicting the fatigue life in the unidirectional laminate ($M_e = 0.55$). The Yang and Liu [80] modeling approach, which we should note is the only model that did not make use of N_i found from linear interpolation of the constant life diagram and instead based the life parameters on $R = 0.1$ or $R = -1$ only, had consistently conservative results for all spectrum load cases attempted in this study. Results for Y1 ranged from $-0.78 < M_e < -0.02$ with both extremes occurring in the MD2 material under WISPER loading. For the UD2 material under WISPER loading Y1 under predicted the fatigue life by about 50% compared with the other models that all over predicted life by 200% or more.

It is difficult to draw general conclusions about the relative performance of these 12 models across the four material data sets because each model has cases where it performed better

and cases where it was less than ideal. While it is tempting to select the Y1 model due to its conservatism, it is sometimes overly so and generally gave inconsistent results. For example the Y1 model gave a life of only 17% of the experimental result under a low stress application of WISPER in the MD2 material while predicting 83% of the experimental fatigue life at a higher stress level. By comparison, most of the other models had a variation of about 14% of the experimental life between these two cases. Thus, the accuracy of Y1 appears to be a function of stress level. It is possible that improved predictions would be achieved with Y1 if the parameters in the model were considered functions of R and σ_p, however this would require considerably more effort to investigate. The BS model gave some of the best predictions overall, especially considering that only constant life data was required to fit it. The BS model provides a significant improvement over PM predictions in some cases and was generally consistent with the other more complex models. The only case where BS did not perform on par with the more complex versions of the generalized residual strength model was the RAY95R01 spectra in the VT8084 material where RS1 was able to predict the fatigue life much more closely than any of the other models.

2.8 Conclusion

This article provided a comprehensive review of modeling approaches for predicting the fatigue behavior of composite materials under variable amplitude load spectra. There are a wide range of approaches available in the literature ranging from various damage accumulation laws, models for the residual strength or stiffness degradation and models based on the micro-mechanical or lamina level properties of the composite. The focus of this article has been uniaxial fatigue loading of un-notched specimen. This is an important step in characterizing these FRP composites, however, understanding the material behavior under biaxial stresses, in the vicinity of stress concentrations, and for some applications out of plane loads, are also important aspects that need to be understood when using composite materials in structural applications.

The application of fatigue models to real data sets highlights many of the advantages and disadvantages of the different approaches. The majority of the models presented in the literature have only been applied to constant amplitude loading and block loading with a few stress levels. The comparison study presented in this article evaluated these models in terms of their predictive capability under more realistic spectrum loading cases of interest to the wind turbine and naval composites industries. Data on four material systems covering a broad range of E-glass polymer composites was selected. For the data sets selected, fatigue modulus and micro-mechanics data was not available and this limited the applicable models to damage accumulation and residual strength approaches. Additionally, the requirements that the model be applied to blocks of one cycle length and that the equivalent cycles be calculated in closed form eliminated several models from consideration. The remaining four damage accumulation and eight residual strength model predictions were compared to the

experimental fatigue life results for 12 spectrum cases tested selected from material system data set.

Most of the models performed adequately over the range of materials and spectra. The worst case scenario was the unidirectional UD2 laminate where models over predicted the fatigue life by 3-4 times the experimental life. While the conservative results generated by the Y1 model are comforting to the design engineer, the goal of spectrum fatigue life prediction should be accurate predictions. Only by having accurate predictions can an appropriate level of conservatism can be built into the design to ensure acceptable reliability without excessively over designing a part. Excessively conservative models (or those without a known level of conservatism) will lead to over-designed structures with excessive weight and cost. Y1 was severely conservative in some cases, especially for lower stress - longer life cases, but the level of conservatism was not consistent so adjusting the method of fitting parameters would not improve the overall results. This behavior, combined with the difficulty in fitting Y1 using the SLERA method means that this approach is not ideal for this type of modeling.

Overall, the simplicity and relatively good accuracy and consistency of predictions generated by the Broutman and Sahu model suggest that it may be a good candidate to replace PM in design practice. Only small gains were found for the more complex residual strength laws RS1-RS5 and INT, all of which require considerably more experimental fatigue data, and none of these models were consistently better than BS across all of the data sets and spectra. The OH model was consistently more conservative than PM, but did not show an overall improvement in accuracy, and the requirement of repeated two block loading data to fit the model parameter is a significant disadvantage. The necessity of determining the failure mode (tension vs. compression) in advance for BS, or any of the other residual strength models, is a distinct disadvantage over PM and will have to be considered carefully if a residual strength approach is used in a reliability based design formulation. On the other hand, prediction of the residual strength over time has the advantage of enabling comparison to extreme stress events to perhaps more accurately assess the safety of a structure than what is possible by considering fatigue life only.

Until the fatigue mechanisms in FRP composites are fully understood from the microscopic level up to the macroscopic level, the application of these materials to structures where they must endure high cycle variable amplitude will continue to rely on empirical or phenomenological models fit to the experimental data. While the Broutman and Sahu linear damage accumulation model appears to be the optimum balance of accuracy and fitting data requirements in the present analysis, the extension to predicting residual strength distributions, will be required to truly assess the relative performance of these models for spectrum loading. Additionally, the development of a residual strength approach that can handle both tensile and compressive failure modes simultaneously is recommended.

Acknowledgments
The authors acknowledge Jason Cain, Wilson Johnson, Hazen White, Brian Clements, and Adam Vittum who assisted with the collection of fatigue data, and Richard Speckhart and

David Kihl who shared their knowledge of statistical load modeling with us. Financial support was provided by the Office of Naval Research (Award #N00014-06-1-0812). Note: The opinions expressed herein are the views of the authors and should not be interpreted as the views of the Naval Surface Warfare Center or the Department of the Navy.

Chapter 3

Fatigue durability of E-glass composites under variable amplitude loading: the importance of load sequence

Fatigue durability of E-glass composites under variable amplitude loading: the importance of load sequence

N.L. Post, J.J. Lesko, S.W. Case
Virginia Polytechnic Institute and State University, Blacksburg, VA 24061, USA

ABSTRACT

As wind turbine blades rotate, they must withstand variable amplitude fatigue. Past studies have shown that residual composite material properties and life under variable amplitude fatigue can be dependent on the load cycle order. We present the results from a study that experimentally characterizes the fatigue behavior of an E-glass/vinyl ester composite as a function of autocorrelation, a statistical measure of the randomness of the loading. Nominally fully reversed Rayleigh distributed loading histories with different autocorrelations from highly correlated to completely random were applied to coupon specimens. The results show that under these conditions, load order does not significantly impact fatigue life.

This paper was reviewed by the European Wind Energy Association and has been accepted for publication in the Scientific Track proceedings of the European Wind Energy Conference 2008.

3.1 Introduction

Modern wind turbine blades are primarily constructed using glass and carbon fiber reinforced polymer composites. As the blades rotate, they must withstand cyclic bending moments due to their own weight and the aerodynamic forces from the wind driving them. The amplitude and mean of these stress cycles varies with wind speed, turbulence, blade pitch and the desired power output [60]. Over the typical design lifetime, the blades will see many millions of cycles and the resulting fatigue damage in the structure can lead to premature failures at stresses that are much smaller than the original strength. Improved understanding of fatigue durability of composite materials will enable blade designs that are more efficient and less expensive while maintaining acceptable reliability.

In a previous study by the authors [77] it was found that for a quasi-isotropic E-glass/vinyl ester laminate the fatigue behavior was drastically different under an ordered block loading compared to when the same load cycles were randomized. The spectrum used was created from a histogram containing 22 stress levels totaling about 736,000 cycles and was applied with a nominal (valley proportional to previous peak) R-ratio of 0.1 corresponding to tension-tension fatigue. We shall refer to this loading histogram as the Post2007 spectrum. When the spectrum was applied in order from highest stress to lowest, or lowest to highest, the resulting residual tensile strength measured after one pass was statistically identical and had a median value of 86% of the median initial strength. However, when the same loads were applied in a random order sequence, all of the specimens failed half way through the spectrum at much lower residual strengths, approximately half of the initial strength of the material [77]. The residual strength model employed did not account for load order and while it was reasonably accurate for the ordered spectra, it failed to predict the random loading results. This type of behavior where frequent changes in the fatigue loading level lead to a greater reduction in strength than the same cycles applied in a more ordered fashion has been termed the “cycle mix effect” [78].

The research presented in this paper replicates the previous experiments in a similar material system and extends the scope to nominally fully reversed Rayleigh distributed loading. The goal is to consider the autocorrelation of extrema as a generalized measure of the degree of randomness in the loading and to evaluate this as a tool for deciding when cycle mix effects are significant in a spectrum load. By considering the autocorrelation of a spectrum in relation to its impact on fatigue life, we may be able to generalize the material behavior as a function of load randomness.

Table 3.1: Nomenclature

Symbol	Description
T-T	tension-tension loading ($0 < R < 1$)
C-C	compression-compression loading ($R > 1$)
T-C	tension-compression loading ($R < 0$). Fully reversed: $R = -1$
$R = \sigma_v/\sigma_p$	R-ratio (definition)
R_n	nominal R-ratio based on the peaks and following valleys in a spectrum
R_h	the R-ratio based on all half cycles in a spectrum
$\overline{R_h}$	average value of R_h for a spectrum
n	cycles applied
N	cycles to failure under a given loading condition
X	a series of stress events in a load spectrum
$\rho_k(X)$	the k^{th} order autocorrelation of the X sequence
$E[x]$	the expected value of x
Q, W	vectors of random numbers q and w on [0,1]
U, V	vectors of normally distributed random numbers, u and v
Y, Z	vectors of independent autocorrelated normal random numbers, y and z
σ	stress (general)
γ	parameter controlling simulation autocorrelation
G	vector of Rayleigh distributed autocorrelated values, g
$\sigma_{applied}$	maximum (peak) applied stress during a fatigue cycle
X_t	initial ultimate tensile strength
X_c	initial ultimate compression strength
X_r	residual strength
A	Power law S-N curve slope
B	Power law S-N curve intercept
j	non-linear residual strength degradation parameter
Fa	normalized applied load
Fr	normalized residual strength

3.2 Review of load order impact in composite materials

One of the earliest and most widely cited efforts to understand composite material behavior under variable amplitude fatigue was published in 1972 by Broutman and Sahu [9]. In this paper, Broutman and Sahu studied two stress level cumulative fatigue damage in an E-glass/Epoxy laminate. Tests were performed in tension-tension fatigue. They showed that for a high-low test, the Miners sum at failure was typically greater than one and that for a low-high test it was less than one. Based on these results, Broutman and Sahu proposed a

linear residual strength model [9]. Numerous other studies over the years have performed similar block loading experiments and used these results to evaluate the effectiveness of damage laws and residual strength models [69, 86, 27, 29, 68, 50, 30].

Adam et al. [21, 22] considered repeated block loading scenarios in graphite epoxy loading where four blocks, each with a different stress amplitude and length equal to 5% of the time to failure at that stress, were rearranged into different orders and then repeated until fatigue failure. For tension-tension loading, the different block load orderings did not impact the fatigue life very much. When a compression-compression fatigue block was introduced (scaled in the same way) the fatigue life was drastically reduced. A similar trend was noted for compression-compression blocks when one tension-tension block was introduced [21]. These results show that the interaction of tension and compression damage in a composite can be significant in determining failure under mixed R-ratio spectra. However, the sequence of constant amplitude block loads are not representative of typical realistic loading spectra distributions.

Some of the earliest spectrum loading experiments performed on graphite composites is reported by D. Schutz and J. Gerharz [42] in 1977. In this study, a flight based loading spectrum for aircraft that included a range of R-ratios was applied. Miners rule was non-conservative by several orders of magnitude for this spectrum loading case. Much better predictions were achieved by Yang and Shanyi [88] using a residual strength approach that did not account for load order in calculating the residual strength at a given point in the spectrum. The method used for applying the spectrum gave it a high level of autocorrelation and it appears that load order did not have a significant impact in these experiments. Similar repeated ordered spectrum loading for aircraft was performed by Schön on composite bolted joints [50].

Sarkani et al. [35] considered the fatigue damage accumulation on laminates and joints under Rayleigh distributed variable amplitude spectrum loading with a high (95%) autocorrelation. A latter study in 2001 by Sarkani et al. [14] compared various residual strength models for life prediction of composite laminates with holes under nominally fully reversed 95% autocorrelated Rayleigh distributed loading. The residual strength models generally provided good fatigue life prediction under these conditions.

Sutherland [60] showed that the WISPER spectrum is significantly more damaging than its shortened version, WISPERX. This result suggests that the inclusion of the low stress cycles can be important. A study by Nijssen et al. [139] also discusses aspects of the WISPER and WISPERX loading spectra in detail. Wahl et al. performed fatigue testing on E-glass/polyester laminates using a modified WISPERX spectra with constant nominal R-ratio and a simple residual strength model worked well for these cases [47][48].

Wahl [47] also found that in tension-tension fatigue for two stress repeated block loading the cycle order of 10 high stress cycles followed by 1000 low, 1 high followed by 100 low, or random interspersion of 1% high stress cycles made no statistical difference in the fatigue life of a glass/polyester laminate. However, Nijssen et al. [81] concluded that a fully re-

versed repeated variable amplitude two stress block loading was more damaging when short blocks were used than for long blocks which indicated the possible need to account for load transitions.

In 1997, Schaff and Davidson introduced a residual strength fatigue model that incorporated a cycle mix factor [78]. In this approach, a spectrum loading is taken as a series of load blocks each defined by an R-ratio, stress amplitude and mean stress. The cycle mix factor is determined empirically from low-high repeated block loadings and is applied to reduce the residual strength whenever the magnitude of the mean stress increases. Schaff and Davidson showed good prediction results for FALSTAFF (fighter aircraft wing) random spectrum loading of angle ply graphite/epoxy laminates using this approach. However, in quasi-isotropic (fiber dominated) laminates, the residual strength model produced good predictions without accounting for cycle mix events and, unfortunately, they lacked data to determine the cycle mix factor for that case [79].

To the authors' knowledge, Schaff and Davidson's approach is the only one of its kind to explicitly handle increased damage resulting from frequently changing the cyclic fatigue stress in a spectrum. Others like Adam and Gathercole et al. [22, 21] and Gamstedt and Sjögren [30] have implicitly included some order effects by using the Marco-Starkey non-linear damage accumulation rule. In both cases, various repeated block loading experiments or other variable amplitude loading with controlled numbers of cycle mix events is required to fit the parameters in these models. In contrast, the damage quantification of most fatigue models for spectrum loading is load order independent, simply summing the impact of all of the applied cycles and then raising the total to a power to create a "non-linear" effect. The improvement in fatigue life prediction found for residual strength models that do not include a cycle mix factor over damage accumulation rules under block or spectrum loading is primarily due to the failure criterion being defined in terms of the currently applied stress relative to the residual strength.

Most experimental data for realistic load spectra is performed on block loaded histograms, where the stress is increased in steps of decreasing length cycle blocks up to the maximum stress and then decreased again, or on pseudo-random fixed order spectra like WISPER and FALSTAFF. Thus, there is a lack of information on the behavior of the composites under realistic loading spectrum subjected to different stochastic load orders. The question of when load order becomes important in determining fatigue life remains unanswered in the present literature on fatigue of composites. Our goal is to develop a system for evaluating the fatigue behavior dependence of a material on load order under realistic spectrum loading that can be used to assess whether the design problem at hand must take load order into account in the fatigue testing and modeling.

3.3 Mathematical Basis

3.3.1 Autocorrelation

In order to better understand if and when load order plays a role in the fatigue life of a material under spectrum loading, a measure of the degree of ordering in a spectrum is required. We propose using the first order autocorrelation between the magnitude of successive events of the spectrum as a mathematical tool to measure the degree of randomness in a loading sequence.

Autocorrelation is a measure of cross correlation of a signal with itself at different points in time. For a discrete process containing n values, $X = \{x_1, x_2, ..., x_n\}$, the autocorrelation coefficient, ρ_k, is defined as:

$$\rho_k(X) = \frac{E[(x_i - \mu)(x_{i+k} - \mu)]}{\sigma^2} \tag{3.1}$$

where μ and σ^2 are the mean and variance of X respectively, k is the lag period considered, and $E[x]$ is the expected value of x. Since we are interested in a measure of cycle-mix type events, we are primarily concerned with the correlation between successive extrema and take $k = 1$. Then, if the spectrum is very long or applied repeatedly many times we can approximate $x_{n+1} = x_1$ and show that:

$$\begin{aligned} \rho_1(X) &= \frac{E[x_i x_{i+1} - \mu(x_i + x_{i+1}) + \mu^2]}{E[x_i^2] - (E[x])^2} \\ &= \frac{\frac{1}{n}\sum_{i=1}^{n} x_i x_{i+1} - \frac{\mu}{n}\sum_{i=1}^{n}(x_i + x_{i+1}) + \frac{1}{n}\sum_{i=1}^{n}\mu^2}{\frac{1}{n}\sum_{i=1}^{n} x_i^2 - \left(\frac{1}{n}\sum_{i=1}^{n} x_i\right)^2} \end{aligned} \tag{3.2}$$

which can be simplified to

$$\rho_1(X) = \frac{n\sum_{i=1}^{n} x_i x_{i+1} - \left(\sum_{i=1}^{n} x_i\right)^2}{n\sum_{i=1}^{n} x_i^2 - \left(\sum_{i=1}^{n} x_i\right)^2} \tag{3.3}$$

It is not clear from the outset what parameter of the fatigue loading should be used to for X. The autocorrelation between successive peaks, valleys or the absolute value of the difference between successive extrema (half cycle amplitudes) could all be of interest. For loading that is nominally fully reversed and contains a 0 level crossing for each half cycle, the absolute value of successive extrema can be used. This last approach was employed when simulating Rayleigh distributed load histories in this study as described below.

3.3.2 Simulating Load Histories

As noted in the introduction, the present objective is to study the behavior of composites under a realistic loading distribution as a function of load order. Although theoretically any load histogram could be used, systematically modifying the load order in a complex stress history is not straight forward. A Rayleigh load distribution was chosen because of the direct method available for simulating load histories with different degrees of autocorrelation and the variety of structural applications it represents. The response power spectral density of a linear structure to normally distributed random load variations is approximately narrowband Gaussian and the resulting loads are Rayleigh distributed [60]. Narrow-band Gaussian processes are often observed in structural response due to natural loading (wind, waves, earthquakes, etc). Veers and Winterstein commented that for vertical axis wind turbines under a given wind condition, the flap-wise load spectrum peaks tend to be Rayleigh distributed while horizontal axis wind turbines generally see exponential load distributions [140]. While an exponential distribution may be more representative of generalized horizontal wind turbine loads, it has the distinct disadvantage from the experimental fatigue testing perspective of including a large number of very small stress amplitudes that would result in much longer test times. Since the objective of this study was to consider material fatigue behavior, the Rayleigh distribution was a more attractive choice. Other applications where fatigue loads have been shown to be approximately Rayleigh distributed include the hog and sag bending moments of ship hulls due to waves for a given set of operating conditions [62].

Kihl and Sarkani [62, 141] describe a useful method for simulating Rayleigh distributed series of n load reversals with a desired autocorrelation, which we will review here. This method is based on the principle that the magnitude of a vector in two dimensions where each of the components are independent normally distributed random variables will be a random variable following the Rayleigh distribution. First, two independent sequences of uniform [0,1] random numbers $Q = \{q_1, ..., q_n\}$ and $W = \{w_1, ..., w_n\}$ are generated. These are then used to create two independent, normally distributed random variables, $U = \{u_1, ..., u_n\}$ and $V = \{v_1, ..., v_n\}$, with zero mean:

$$u_i = \sqrt{-2\ln(q_i)}\sin(2\pi w_i),\ i = 1, ..., n \tag{3.4}$$

$$v_i = \sqrt{-2\ln(q_i)}\cos(2\pi w_i),\ i = 1, ..., n \tag{3.5}$$

From these, two sequences of independently autocorrelated, normally distributed random variables, $Y = \{y_1, ..., y_n\}$ and $Z = \{z_1, ..., z_n\}$, are generated:

$$y_i = \gamma y_{i-1} + \sqrt{1-\gamma^2}u_i,\ i = 1, ..., n \tag{3.6}$$

$$z_i = \gamma z_{i-1} + \sqrt{1-\gamma^2}v_i,\ i = 1, ..., n \tag{3.7}$$

where $y_0 = z_0 = 1$ and γ is related to the desired autocorrelation of the final sequence. Finally, a series of Rayleigh distributed autocorrelated values, $G = \{g_1, ..., g_n\}$, is generated as:

$$g_i = \sqrt{y_i^2 + z_i^2},\ i = 1, ..., n \tag{3.8}$$

The autocorrelation is not known explicitly and thus Equations 3.6-3.8 must be computed iteratively adjusting γ until the desired autocorrelation $\rho_1(G)$ calculated by Equation 3.3 is achieved. For moderate length simulations under non-zero autocorrelation, the distribution may vary significantly from the desired Rayleigh distribution. In order to be sure that the desired distribution is achieved, the first 10 moments of G are compared to the theoretical Rayleigh distribution moments. Sarkani [141] showed that the 9^{th} moment seemed to be critical and the simulation is run repeatedly until the error in the 9^{th} moment is very small (< 0.01). Finally, to create a nominally fully reversed stress history of load reversal points, every other value of G is multiplied by -1 and the entire spectrum is multiplied by the desired RMS stress. The resulting sequence will generate a sinusoidal time stress history that has a root mean square (RMS) of unity. The RMS of the extrema points will be approximately a factor of $\sqrt{2}$ greater.

3.3.3 Fatigue modeling

The topic of evaluating models for the performance of composite materials under variable amplitude loading is not the primary objective of this article; however, a linear (load order independent) residual strength model presented in [77] was used to scale the variable amplitude loading spectra to achieve approximately the desired lifetimes. In this paper, we will perform the calculations for the median initial strength and we apply the model to tension, fully reversed, and compression fatigue. The residual strength equation for variable amplitude loading simplifies to:

$$Fr = 1 - \left[\sum_{k=1}^{n} (1 - Fa_k)^{\frac{1}{j}} \left(\frac{1}{N(Fa_k)}\right)\right]^{j} \tag{3.9}$$

where Fa_k is the normalized applied stress extreme for the kth cycle

$$Fa = \frac{\sigma_{applied}}{X_{t,c}} \tag{3.10}$$

and Fr is the normalized residual strength

$$Fr = \frac{X_{residual}}{X_{t,c}} \tag{3.11}$$

The median initial tension strength, X_t, is used for tension-tension fatigue where tension is the critical failure mode, while the median initial compression strength, X_c, is used for fully reversed and compression-compression fatigue where the failure mode is observed to be compression. Fatigue failure is predicted to occur when $Fr \leq Fa$. $N(Fa)$ is determined based on constant amplitude fatigue data fit to a linear log-log relationship with two parameters:

$$\log(N) = A \log(Fa) + B \tag{3.12}$$

where A and B are fit to the S-N curve data for the material. Thus, this relatively simple model has 3 experimentally determined parameters for each R-ratio considered, A, B, and j, which must be fit to fatigue data collected at constant amplitude.

Fatigue model parameters are typically dependent on R-ratio, $R = \sigma_{peak}/\sigma_{peak}$, and since the general objective is to use a model fit to constant amplitude fatigue data to predict variable amplitude fatigue performance, a method of evaluating R of a spectrum load is required. It is common in other experimental spectrum loading to maintain a constant *nominal* R-ratio, R_n, by forcing the valley following each peak to a value of $R_n\sigma_{peak}$. For spectrum loading, we will refer to the average R calculated in this way using each peak and following valley as the nominal R-ratio of the spectrum. In contrast, for the half cycle R-ratio, R_h, is calculated for all successive extrema, so both the peak-to-valley and valley-to-peak transitions are included. In a spectrum loading, R_h is not constant even if the R_n is kept constant. However, for a spectrum with a high autocorrelation, the average $R_h = \overline{R_h}$ will be nearly identical to R_n.

3.4 Experimental Procedures

3.4.1 Material

The composite material used was manufactured at Virginia Tech by Vacuum Assisted Resin Transfer Molding (VARTM). The fiber reinforcement was Vetrotex 324 woven roving E-glass which has a 5:4 bias in the warp direction and the layup (denoted by warp direction in each layer) was $[0/+45/90/\text{-}45/0]_s$. The matrix material was Ashland 8084 vinyl ester resin (30% styrene) with the cure package by weight consisting of Norox MEKP-925H peroxide initiator (1.5%), cobalt napthenate catalyst (0.3%) and N, N-dimethyl aniline retarder (0.025%) resulting in a gel time of 50-70 minutes. Following a 24 hour cure period under ambient conditions, the material was post-cured for 4 hours at 82℃. The finished composite had an average fiber volume fraction of 52% as measured by burn off tests. Material was manufactured in a series of batches under identical procedures, each producing a 0.9 m by 0.9 m panel 6.13 mm thick that was then cut into specimens. A diamond tile saw was used for initial cutting of the specimens to nominal 26 mm wide by 152 mm long blanks. These blanks were then surface ground on the long edges to provide parallel sided specimens 25.40 +/- 0.02 mm wide. All specimens were cut so that the loading was in the 0 fiber direction. In subsequent analyses of applied stress, the cross sectional area of all the specimens was taken to be 155.7 mm^2.

3.4.2 Experimental procedure

Testing took place using two 90 kN (20 kip) MTS servo-hydraulic load frames with hydraulic wedge grips. A 4 count/mm stainless steel screen and a 1.5 mm thick aluminum sheet were

used on either side of the specimen to cushion it in the grips. This method provided gauge section failures without requiring tabs attached to the specimens. The load-frame servo-valves were controlled by MTS 407 controllers operated in external input mode. A custom LabView program and National Instruments PCI-6221 M series DAQ card generated the desired load voltage signals and recorded the load and strain response data. The gage length between the grips was maintained at 50 mm to insure that compression failures would occur by crushing rather than global buckling. In addition to monitoring the load a 25.4 mm gauge length extensometer was used to measure strain and the visual damage was monitored using a video camera with backlighting shining through the specimen. This paper focuses on the analysis of strength and fatigue life response of the material as measured by complete rupture of the specimen while future analysis of the data will consider other measures for the damage under variable amplitude loading.

In associated research, extensive strength and constant amplitude fatigue data was collected on this material system and the relevant results will be summarized in this paper. The distribution of initial quasi-static stiffness and strength were determined by breaking 30 specimens each in monotonic tension and compression using load control with a loading rate of 667 N/s. Subsequent constant amplitude fatigue to failure tests were performed with tension-tension, reversed and compression-compression R-ratios of 0.1, -1, and 10 respectively. The frequency was maintained at 5 Hz. for constant and variable amplitude fatigue testing to prevent excessive viscoelastic heating. In all cases, a continuous sinusoidal driving fatigue loading waveform was created by fitting a cosine curve between each peak and valley and then the valley and subsequent peak such that the slope of the curve was zero at each load reversal point. Any series of peaks and valleys can be defined in a text file and used as input to the system.

The LabView program used for driving constant amplitude fatigue tests incorporated a feedback loop that monitored the resulting peaks and valleys and adjusted gain factors to multiply the driving signal peak and valley until the desired maximum and minimum loads were achieved. As the specimen stiffness degraded and the machine response changed, the program continuously updated the gains to maintain the desired loads. The MTS 407 PID gain tuning parameters were adjusted manually until the resulting load waveform was as close to a sinusoidal shape as possible. For variable amplitude loading, it was found that the required gain was a nonlinear function of the load applied. An algorithm was developed that dynamically adjusted gain functions, defined as continuous and piecewise linear on 2.22 kN intervals, based on how close the past cycles were to the desired loads. Using this algorithm, the peak and valley loads were generally maintained within +/- 133 N of the desired loads, a level of error that was considered acceptable as it is on the order of the noise in the load signal.

3.5 Results and discussion

3.5.1 Constant amplitude fatigue data and fitting

The measured quasi-static properties from 30 tension and 30 compression tests are given in Table 3.2. Figure 3.1 shows the results of 184 constant amplitude fatigue tests with the applied stress normalized by the tension (R=0.1) or compression (R=-1, 10) median initial strength. For each R-ratio a power law relationship, Equation 3.12, was fit using least squares linear regression and the resulting parameters are listed in Table 3.3. For the case of fully reversed loading ($R = -1$), a single power law curve did not appear to adequately describe the data and thus a bi-linear curve was defined by fitting the power law separately to higher and lower fatigue life portions and then finding the intersection between these curves.

Table 3.2: Summary of quasi-static strength for VARTM E-glass/vinyl ester material

	Mean	Median	Std Dev
X_t (MPa)	346.8	347.7	15.8
X_c (MPa)	-299.2	-302.5	13.2
Modulus (GPa)	22.6	22.7	1.3

Next, an extensive series of 303 residual strength tests under constant amplitude fatigue were performed by stopping the fatigue process at specified number of cycles and breaking the specimen in the dominant failure mode, tension for $R = 0.1$ and compression for $R = -1$ and $R = 10$. This data was used to estimate j for each R-ratio as described in [77]. For $R = -1$ loading, the best fit value was $j = 1.2$ and for $R = 0.1$: $j = 0.78$. Under $R = 10$, a satisfactory j value could not be fit using this method and the data indicates nearly sudden death behavior, suggesting that a large $2 < j < 5$ is appropriate.

Table 3.3: Constant amplitude fatigue power law cycles vs. normalized stress curve fit parameters for VARTM E-glass/8084 vinyl ester laminate data

R	Fa Range	A	B
0.1	all	-6.88	1.55
-1	Fa >0.358	-5.18	1.31
-1	Fa <0.358	-11.15	-1.36
10	all	-14.6	0.513

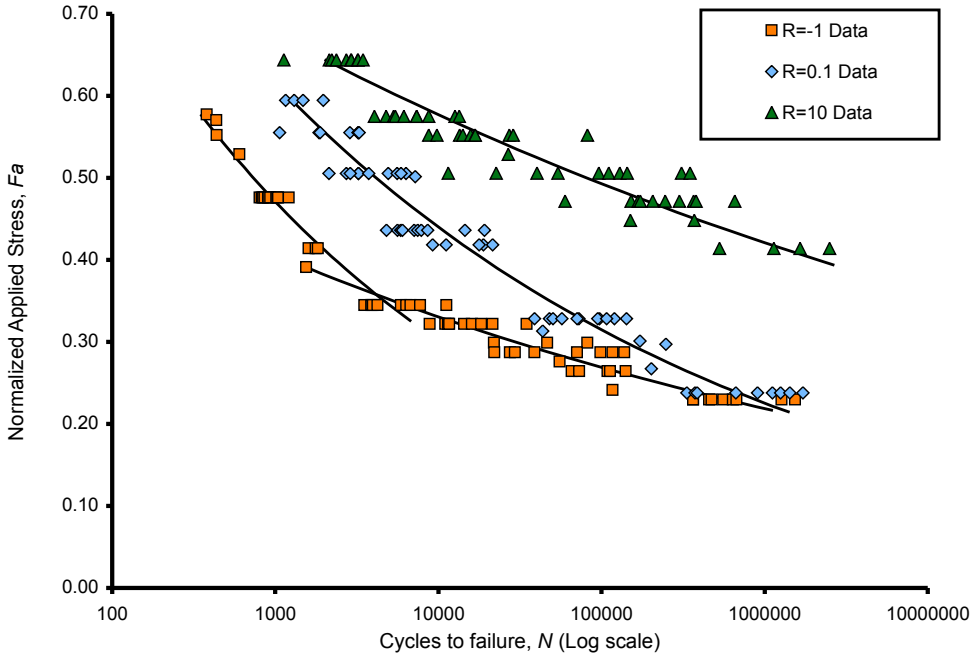

Figure 3.1: Constant amplitude fatigue Fa vs. N curve for VARTM E-glass/8084 vinyl ester laminate

3.5.2 Simulation of loading spectra

Since the objective is to evaluate composite performance under random autocorrelated loading, it would appear at first glance that we should simulate the load history for every cycle applied to every specimen. While this would be the correct approach to experimentally evaluate a reliability model based on the distribution of loads and material behavior, it would not enable direct evaluation of the composite behavior because each specimen would experience a different set of loads in a different order. Thus, it would be difficult to separate the variability of the loads and the material properties when interpreting the results. By simulating one relatively short sequence of loads and repeating it over and over again until failure, every specimen in a batch of replicates will be subjected to the same load sequence to within the length of that short spectrum and the variability in the material is the only cause of variation in fatigue life to that precision. A 5000 cycle (10,000 extrema) simulated load history length was used by Sarkani [35] and this length was selected again because it provides a smooth representation of the distribution while enabling many replicates to be accomplished in a reasonable testing time. An additional advantage of the 5000 cycle simulated history is that it effectively limits the maximum value chosen from the infinite Rayleigh distribution to about four times the RMS of the loading. Alternatively, the distribution could be truncated in order to avoid including excessively large peaks that may exceed the initial strength of

the material, but that was not done in this case.

Three 5000 cycle Rayleigh distributed load histories with target extrema autocorrelations of 0.95, 0.5 and 0 respectively, based on the absolute value of successive extrema, were generated using the method described in Section 3.3.2. The first 20 cycles of each of these spectra are shown in Figure 3.2. A fourth distribution was created by sorting all of the extrema in the 0.95 autocorrelated spectrum from smallest to largest and placing alternating points at the beginning and end of the spectrum to achieve a highly correlated spectrum where the stress amplitude increased monotonically to 2500 cycles and then decreased monotonically in a symmetric way as shown in Figure 3.3. The resulting spectrum has an autocorrelation of 0.99999. These four spectra are refereed to as "Rayleigh0.0," "Rayleigh0.5," "Rayleigh0.95," and "Rayleigh1.0."

3.5.3 Comparison of spectra

In order to make a comparison to the correlation of other loading spectra, the autocorrelation coefficient was calculated for each spectrum based on just the peaks, ρ_1^{peak}, just the valleys, ρ_1^{valley}, and the half cycle amplitudes, $\rho_1^{half\ cycle\ amplitude}$. In addition, the average R-ratio of the half cycles is also presented. These results are given in Table 3.5 for the four Rayleigh distributed loadings and compared to the Post2007 spectrum used in [77], WISPER and WISPERX standard spectra [52], and modified versions of WISPERX run by Wahl et al. [49].

Although each Rayleigh spectrum has the same distribution of peaks and valleys, the average R-ratio changed with the ordering. Also, while the peaks and valleys can be highly uncorrelated, the half cycle amplitudes remain at least partially autocorrelated. This is an obvious result because the same peak, or the same valley must anchor the ends of two adjacent half cycles. The three versions of the Post2007 spectrum correspond to the ordered highest to lowest, lowest to highest and completely randomized versions of the spectrum all of which have a nominal R-ratio of 0.1. The modifications of WISPERX performed by Wahl et al. were done to create a WISPERX-like spectrum with a constant nominal R-ratio of either 0.5 or 0.1. In WISPERXmod1_0.1 and WISPERXmod1_0.5 only the cycles where both load reversals were positive were retained and the valleys were calculated to 0.1 or 0.5 times the preceding peak. In WISPERXmod2_0.1 all of peaks were retained from WISPERX and the valleys were fixed at 0.1 times the preceding peak.

Regardless of which autocorrelation measure is used, it is apparent that the Post2007random spectrum has a very low autocorrelation on par with the Rayleigh0.0 spectrum while the sorted versions of the Post2007 spectra are highly correlated ($\rho_1 \approx 1.0$). WISPER and WISPERX tend to be more comparable to Rayleigh0.95 in terms of the peak and valley autocorrelations, however they have a relatively low half cycle amplitude autocorrelation. The modifications of WISPERX resulted in the same peak and similar valley autocorrelations, but significantly increased the half cycle amplitude autocorrelation.

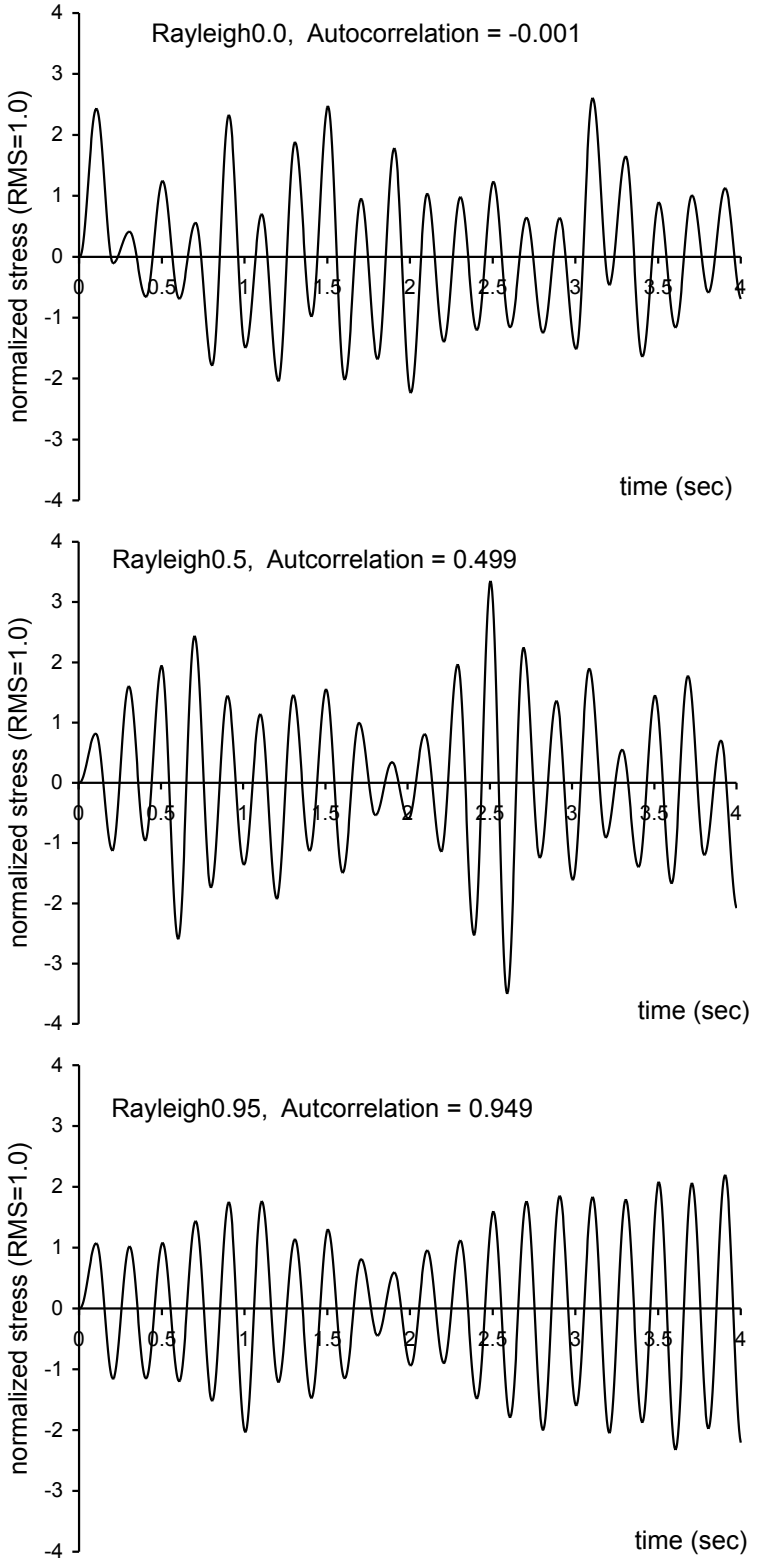

Figure 3.2: Example time history of the first 20 cycles for each simulated Rayleigh distributed loadings

Table 3.4: Comparison of first 10 moments of simulated 5000 cycle Rayleigh distribution extrema to theoretical distribution

Spectrum	extrema			First 10 moments of the distribution of ‖extrema‖									
	RMS	max	min	1	2	3	4	5	6	7	8	9	10
Rayleigh ($\sigma = 1$)	-	∞	0	1.25	2.00	3.76	8.00	18.8	48.0	132	384	1184	3840
Rayleigh0.0	1.415	4.34	-4.30	1.25	2.00	3.77	8.04	18.9	48.3	133	386	1185	3814
Rayleigh0.5	1.426	4.15	-3.88	1.26	2.03	3.85	8.24	19.4	49.6	135	391	1184	3731
Rayleigh0.95	1.426	3.95	-3.88	1.25	2.03	3.92	8.49	20.2	51.5	140	398	1184	3659
Rayleigh1.00	1.426	3.95	-3.88	1.25	2.03	3.92	8.49	20.2	51.5	139	397	1184	3659

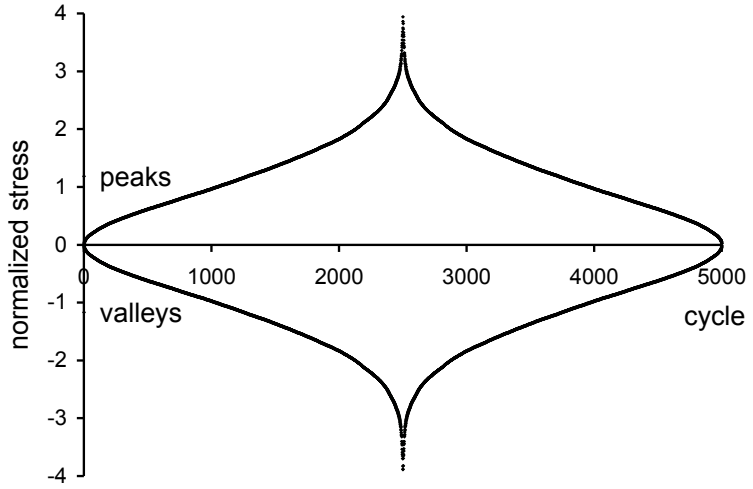

Figure 3.3: Visual representation of sorted peak and valley extrema in Rayleigh1.0 spectrum.

Table 3.5: Average R-ratios and autocorrelation results for various experimental spectrum loadings.

Spectrum	$\overline{R_h}$	ρ_1^{peak}	ρ_1^{valley}	$\rho_1^{half\ cycle\ amplitude}$
Rayleigh0.0	-1.62	0.011	-0.010	0.500
Rayleigh0.5	-1.31	0.249	0.260	0.751
Rayleigh0.95	-1.07	0.902	0.901	0.975
Rayleigh1.0	-1.00	1.000	1.000	1.000
Post2007highlow	0.10	1.000	1.000	1.000
Post2007lowhigh	0.10	1.000	1.000	1.000
Post2007random	0.10	0.002	0.002	0.446
WISPER	0.39	0.843	0.897	0.737
WISPERX	0.25	0.864	0.854	0.587
WISPERXmod1_0.1	0.10	0.870	0.870	0.920
WISPERXmod1_0.5	0.50	0.870	0.870	0.963
WISPERXmod2_0.1	0.10	0.864	0.864	0.916

3.5.4 Spectrum loading results

Because the previous findings in [77] were so drastically different from other experimental spectrum loading results, these tests were replicated to verify the past results. The same three orderings of the Post2007 spectrum were applied in tension-tension fatigue, but this time the E-glass/8084 vinyl ester composite was used rather than the E-glass/510A vinyl ester composite in the previous paper.

The fiber lay-up and FVF in both composites was identical, but the 510A matrix is a brominated vinyl ester and the 8084 matrix incorporates a rubber toughening agent. Despite the similarities in the two materials, the S-N curve for the 8084 under $R = 0.1$ constant amplitude fatigue is significantly steeper with an inverse slope of -6.9 compared to -8.7 for the 510A. In order to achieve comparable results, the Post2007 spectrum was rescaled using the residual strength model from Section 3.3.3 with the 8084 parameters to provide the same predicted median residual strength after one pass through the spectrum as predicted in [77] for the 510A material. The resulting spectrum had a maximum stress of 157 MPa (median $Fa = 0.453$). Six replicates of each load ordering, highest to lowest, lowest to highest, and random, were applied at a constant frequency of 5 Hz. The resulting data are given in the Apendix.

Specimens that made it through the spectrum once were then broken in monotonic tension to determine the residual strength. All of the high-to-low and low-to-high specimens survived the fatigue and the median Fr was 0.90 and 0.89 respectively. For the randomized spectrum, the same random load order was applied as in [77] and in this case half of the specimens failed prematurely in tension between 548,475 and 688,612 cycles. The other three random specimens had widely varying residual strengths with a median value of Fr=0.539. Although not identical to the previous data, these results reinforce that the random spectrum is much more damaging than either version of ordered spectrum under this $R = 0.1$ loading histogram.

The simulated Rayleigh0.95 distribution was scaled to provide predicted median lifetimes of 25000, 200000 and 1000000 cycles to failure based on the residual strength approach of Equation 3.9. The resulting time history RMS stress scale factors of 42.1, 32.8 and 27.8 MPa respectively were also used for scaling the other Rayleigh spectra in this study. Thus all of the Rayleigh distributed spectra had the same statistical distribution of peaks and valley stress extremes at a given RMS level.

The R-ratio varied significantly for the cycles in the spectra with lower autocorrelation. Thus, it is not appropriate to use the simple residual strength law presented in Section 3.3.3 without considering both N and j as functions of R-ratio and this more complex analysis was not attempted. Because the present objective is to consider only the material response to spectrum distributed loading with different autocorrelation, the reliance on a specific damage model to assess equivalence between the spectra is not desirable. Instead, the distribution of peak and valley stress extrema was the best measure of equivalence between the spectra

with varying autocorrelation.

Experimental fatigue data are shown in an RMS vs. cycles plot in Figure 5.7 and mean values are compared in Figure 3.5. At least ten replicates were completed for the Rayleigh0.95 spectrum at each stress level while two to six replicates were performed for the other autocorrelations at most of the stress levels as given in the Appendix. Compression failures were observed in every experimental test of the Rayleigh distributed loading. For the 42.1 MPa stress level application Rayleigh0.95, four of the specimens failed in the 5,000-15,000 cycle range as compared to 40,000-120,000 for the other 11 tests. Because no difference in failure mode or test setup was detected for these specimens, they were included in the final data set despite appearing to be outliers.

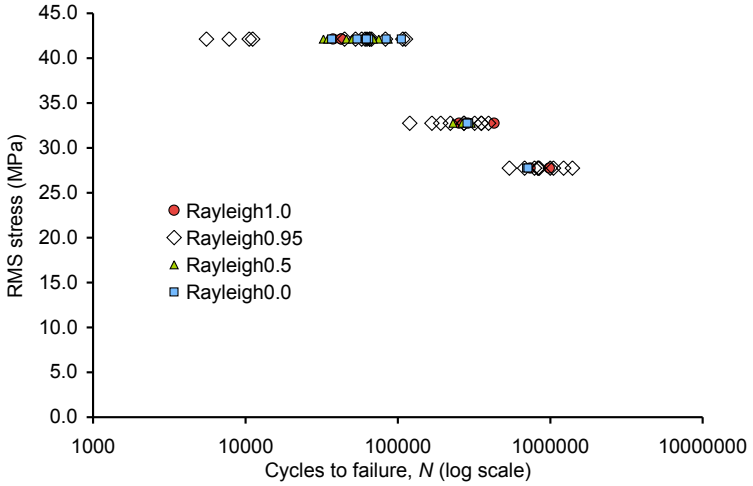

Figure 3.4: Resulting RMS stress vs. fatigue life for four Rayleigh distributed loading spectra with different autocorrelation.

There is no discernible difference in the fatigue lives of the specimens as a function of autocorrelation for the type of loading chosen. This result was unexpected given the previous experience with the Post2007 spectrum under a nominal R-ratio of 0.1. Most likely, the cycle mixing effect impact is different for the different R-ratios and resulting failure modes, tension for Post2007 spectra, compression for the Rayleigh distributed spectra. It is possible that cycle mixing is not significant within the course of a 5000 cycle spectrum that is repeated regardless of how those cycles are ordered, but does make a large difference for a 736,000 cycle spectrum that is only performed once. However, if that was true, we would expect much shorter lives under Rayleigh distributed loading than predicted by the residual strength model and this was not the case.

An unusual feature of the Rayleigh distributed fatigue data is the relatively narrow distribution of fatigue life at lower stress levels. For the Rayleigh0.95 spectrum, the 27.8 MPa RMS level gave an average life of 916,000 cycles with a coefficient of variation (COV) of 0.28 based on 10 replicates. By comparison, R=-1 constant amplitude fatigue with a peak stress

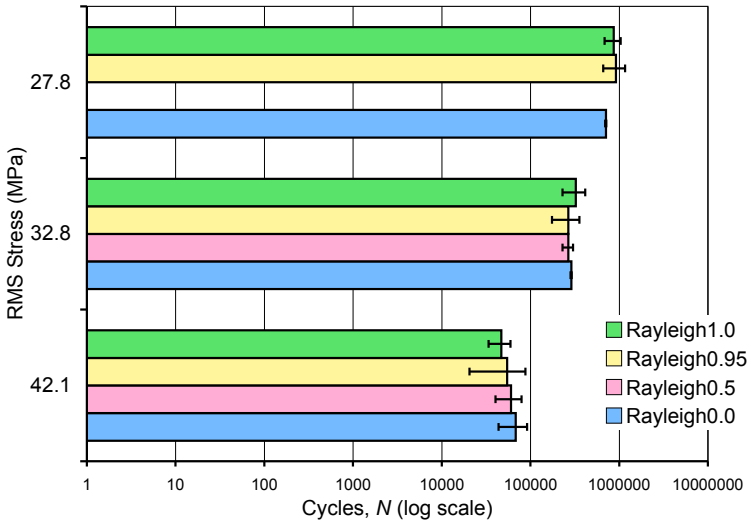

Figure 3.5: Comparison of mean fatigue life for four Rayleigh distributed loading spectra with different autocorrelation under three RMS stress levels. Error bars indicate 1 standard deviation.

of 68.9 MPa gave a mean life of 644,000 cycles from 10 replicates and the COV was 0.67. Likewise, for an R=0.1 constant amplitude fatigue with a peak stress of 82.7 MPa, the mean life was 906,000 cycles from 9 replicates, the COV was 0.55, and R=10 with a valley stress of -141 MPa gave a mean life of 270,000 cycles and COV of 0.62 based on 10 replicates. It is unknown why the Rayleigh distributed fatigue resulted in so much narrower a distribution of fatigue life for a nominal one million cycles to failure.

3.6 Conclusions

We describe a method for evaluating the randomness of the order in a fatigue spectrum by calculating the autocorrelation. By varying the autocorrelation it is possible to assess what impact load order has on the fatigue behavior of a material under a realistic loading spectrum. Previous work demonstrated in a similar material that load order could be very significant in the damage incurred under tension-tension fatigue. Those results were reproduced when the same type of test was performed in the present material system. However, the present research also shows that for this E-glass/Vinyl ester fiber-dominated composite, the fatigue life is not a function of the autocorrelation for a generally fully reversed spectrum where the dominant failure mode is compression. It is apparent that characterizing the fatigue load order dependence of composites is a complex problem dependent on the damage and failure modes of the spectrum applied. Further study and experiments at other R-ratios will be required to determine if autocorrelation provides a good measure of randomness in

relation to the load order cycle mix effects. There is some evidence that autocorrelation will be useful in assessing tension-tension fatigue spectrum loading because residual strength models have been shown to work well for the sorted Post2007 spectrum, and reasonably well for the WISPER and WISPER X type spectra which have autocorrelations of 0.8 to 0.9 depending on the measure used, but failed for the fully random case of Post2007 which had no significant autocorrelation. At present we can conclude that load order as measured by autocorrelation, does not have a significant impact on the fatigue life fiber dominated E-glass/vinyl ester composites under nominally fully reversed Rayleigh distributed loading.

Acknowledgments
The authors acknowledge Jason Cain, Wilson Johnson, Hazen White, Brian Clements, and Adam Vittum who assisted with the collection of fatigue data, and Richard Speckhart and David Kihl who shared their knowledge of statistical load modeling with us. Financial support was provided by National Science Foundation IGERT (Award #DGE-0114346) and the Office of Naval Research (Award #N00014-06-1-0812). Note: The opinions expressed herein are the views of the authors and should not be interpreted as the views of the Naval Surface Warfare Center or the Department of the Navy.

Chapter 4

A new phenomenological model for the tension and compression residual strength of fiber dominated composite materials

A new phenomenological model for the tension and compression residual strength of fiber dominated composite materials

N.L. Post, S.W. Case, J.J. Lesko
MC 219, Virginia Polytechnic Institute and State University, Blacksburg, VA 24061, USA

ABSTRACT

This article considers the problem of fatigue life prediction of fiber reinforced composites under axial (tension and compression) variable amplitude loading. Traditionally this analysis is performed using damage accumulation rules or residual strength models. In the case of damage accumulation rules, failure is defined as the point when a damage parameter reaches a critical value, without consideration of failure mode (tension or compression) or the current applied load. Residual strength models define the failure explicitly in terms of the applied load and current residual strength in either tension or compression. However, current residual strength models can only consider one failure mode, either tension or compression, for a given loading. We propose a new phenomenological residual strength model for fiber dominated composites that simultaneously calculates the tensile and compressive residual strengths as a function of an arbitrary spectrum defined as a series of peak and valley applied stresses. Example applications of the model are demonstrated for two E-glass composite laminates under a variety of loading conditions. The new model can accurately represent the reversed tension-compression constant amplitude fatigue life of these composites in terms of the tension-tension and compression-compression fatigue behavior. Variable amplitude fatigue life predictions were very good for a nominally fully reversed Rayleigh distribution spectra and the WISPER standard spectrum fatigue to failure data.

This paper will be prepared for submission to Composites Science and Technology.

4.1 Introduction

Fiber reinforced polymer composite materials are increasingly being used in structural applications where they are subjected to high cycle variable amplitude fatigue. Examples include wind turbine blades, aircraft, and ship hulls. The ability of the design engineer to predict the fatigue life and residual mechanical properties of composites during the expected lifetime is critical to ensuring an optimized structure with acceptable reliability. Most fatigue models consider the axial loading of composites with failures occurring in either tension or compression (crushing). Although there have been attempts to develop fatigue models for FRP composites based on micro-mechanics principles [27, 73, 97, 104, 105, 106] or without empirical parameters at all [98], the majority of papers on variable amplitude fatigue of FRP materials explore empirical or phenomenological models that contain parameters fit to constant and in some cases variable amplitude loading. These models include damage accumulation rules, residual strength models, and residual stiffness models.

Damage accumulation methods include the well known Palmgren-Miner [8] linear damage rule, and non-linear variations on the Palmgren-Miner rule such as those by Marco and Starkey [10], Owen and Howe [69], Bond and Farrow [44] and Hashin and Rotem [11]. In general, all damage accumulation rules calculate a damage parameter, D, in terms of the fraction of cycles to failure applied at the current stress level. Failure is typically predicted to occur at $D = 1$. The primary failing of damage accumulation rules is that they do not explicitly consider the failure mode in terms of the applied loading and thus often produce poor results for large block loading, especially where tension-tension loading is mixed with reversed or compression-compresion loading [21, 22]. At present, residual strength approaches calculate either the tensile or compressive residual strength as a function of the applied loads and the failure criteria is defined in terms of either the maximum or minimum stress respectively [9, 12, 13, 14, 16, 70, 71, 72, 76, 78, 79, 80, 82, 86, 87, 88, 89, 91, 92, 96]. The choice to model tension or compression residual strength depends on whether the loading is assumed to be tension or compression dominated. Residual stiffness models are primarily used in conjunction with displacement controlled fatigue tests and failure criterion are typically defined by the stiffness decreasing below a predetermined value [19, 67, 122, 125, 126, 127, 129, 130]. Although residual stiffness models have been successful in matrix dominated composites, Post et al.[76] showed that residual stiffness and residual strength are relatively uncorrelated in fiber dominated composite laminates, and thus residual stiffness is not a good indicator for fatigue failure.

If we consider the case of a generalized spectrum fatigue load consisting of a series of random (or semi-random) peaks and valleys, we may not know *a priori* if the failure will occur in tension or compression. Alternatively, we might consider a situation where a fatigue spectrum load on a component is primarily tension dominated, but the component must be designed to withstand an extreme compression load (or visa versa). Therefore, it is desirable to have a fatigue model that can simultaneously predict the tension and compression residual strength after an arbitrary loading sequence. Schaff and Davidson [78, 79] suggested that the

residual tensile and compressive strengths would undergo proportional reduction and thus the failure criteria could be switched for changes in the primary loading direction. However, Schaff and Davidson never evaluated the effectiveness of this approach and we shall show that the available data do not support their assumption. This paper presents the development and preliminary testing of a new phenomenological residual strength model that calculates the tensile and compressive residual strengths simultaneously based on a set of coupled rate equations.

Table 4.1: Nomenclature

Symbol	Description
T-T	tension-tension loading ($0 < R < 1$)
C-C	compression-compression loading ($R > 1$)
T-C	tension-compression loading ($R < 0$). Fully reversed: $R = -1$
D	damage parameter
$R = \sigma_v/\sigma_p$	R-ratio (definition)
$V = 1/R = \sigma_p/\sigma_v$	reciprocal of the $R - ratio$
n	cycles applied
N	cycles to failure under a given loading condition
N_t	cycles to failure considering only increasing tensile stress
N_c	cycles to failure considering only decreasing compressive stress
σ	stress (general)
σ_p	maximum (peak) applied stress during a fatigue cycle
σ_v	minimum (valley) applied stress during a fatigue cycle
$\sigma_m = \frac{1}{2}(\sigma_p + \sigma_v)$	mean applied stress during a fatigue cycle
$\sigma_a = \frac{1}{2}(\sigma_p - \sigma_v)$	stress amplitude during fatigue cycle
τ	generalized time
S_{uts}	initial ultimate tensile strength
S_{ucs}	initial ultimate compression strength
S_r	residual strength
S_t	tensile residual strength
S_c	absolute value of the compressive residual strength
i	counter: the i^{th} load cycle
$A, A_t, A_c, C, C_t, C_c, x, y$	model curve fitting (material) constants
$G(z), H(z), I(z), J(z)$	functions of z
a	Power law S-N curve slope
b	Power law S-N curve intercept
Fa	normalized applied load
$Fa_t = \sigma_p/S_{uts}$	normalized applied tensile stress
$Fa_c = \sigma_v/S_{ucs}$	normalized applied compression stress

continued on next page

continued from previous page

Symbol	Description
$Fr = S_r/S_u$	normalized residual strength
$Fr_t = S_t/S_{utc}$	normalized residual strength
$Fr_c = S_c/S_{ucs}$	normalized residual strength

4.2 Experimental Data

Two publicly available fatigue data sets will be used in this study. The MD2 (R0400 geometry) material data set is part of the Optimat Blades database [136], and is publicly available electronically at [51]. In addition to initial quasi-static tension and compression strength and fatigue life data for a range of R-ratios, the data set includes tensile and compressive residual strength measurements for $R = 0.1$, $R = -1$ and $R = 10$ constant amplitude fatigue and spectrum fatigue measurements were made under the WISPER and WISPERX standard load spectra at various stress levels. The MD2 laminate is a multidirectional $[[\pm 45/0]_4/\pm 45]$ composite consisting of stitched E-glass with an epoxy matrix with and fiber volume fraction of 0.52 and is typical of wind turbine blade spars. The data was collected at several different laboratories and for the present study the results from all the laboratories were pooled for each test type. Fatigue frequencies ranged from about 1 to 10 Hz. The VT8084 data set was collected at Virginia Tech and is publicly available electronically at [5]. This material is a $[0/+45/90/\text{-}45/0]_s$ laminate consisting of 10 layers of woven roving E-glass with a rubber toughened vinyl ester matrix (Ashland Chemical Durakane 8084). The VT8084 material was primarily intended for naval ship hull construction. The data set includes quasi-static tension and compression strength measurements, constant amplitude fatigue life and tension and compression residual strength under $R = 0.1$, $R = -1$ and 10. Variable amplitude fatigue cases include Rayleigh distributed loading with 95% autocorrelation (degree of load ordering, see [2]) with a nominal $R = -1$. Fatigue frequency was held constant for all tests at 5 Hz.

4.3 Model development

The objective of this work is to develop a model that will simultaneously track the tension and compression residual strength under arbitrary variable amplitude fatigue loads. We start by observing the residual strength behavior of fiber dominated E-glass composite materials under constant amplitude fatigue loading.

4.3.1 Observation of residual strength under constant amplitude loading

Figures 4.1 through 4.6 plot the residual strength data including premature failures plotted in terms of the normalized cycles to failure for the MD2 and VT8084 data sets under $R = 0.1$, $R = -1$, and $R = 10$ constant amplitude fatigue. As expected, there is considerable scatter in the experimental data and there are relatively few replicates for each test. Along with the premature failures present, the scatter makes curve fitting to the data difficult. However, general observations of the trends may be made that will help in formulating a model. For $R = 0.1$ constant amplitude tension-tension (T-T) fatigue, the residual tension strength is observed to drop significantly in the first 10 to 20% of the life before leveling out. As indicated by the premature failures, the strength must again decrease rapidly near the end of the fatigue life. Under T-T loading, the compression strength decreases only slightly. Under $R = 10$ constant amplitude compression-compression (C-C) fatigue no significant change in the compression or tension residual strength is found over the life of the MD2 specimens while the compression strength decreases slightly for the VT8084 material. In both cases, a rapid sudden death behavior is present near the end of the C-C fatigue life. Under R=-1 tension-compression (T-C) fatigue, where failures are usually dominated by compression because the initial compression strength is significantly less than the initial tension strength, the data shows a significant reduction in the tensile residual strength, again occurring in the first 20% of the fatigue life. In contrast, change in the compression residual strength is not detectable in the MD2 data set although the large number of premature failures indicates that the residual compression strength must drop rapidly at the end of the fatigue life of a given specimen. An approximately linear reduction in residual compression strength is noted in the VT8084 material under T-C loading. Overall, lower stress levels appear to give slightly more damage (lower residual strength) for a given fraction of life, however, these differences are small compared to the scatter of the data.

The fatigue life of the MD2 material under $R = -1$ and $R = -0.4$ are compared to the life the laminate under $R = 0.1$ and $R = 10$ in terms of the peak applied tensile or compressive stress in Figure 4.7. The reversed loadings generate significantly more damage than the corresponding tensile or compressive stress fatigue under an equivalent peak stress indicating that the damage caused by tension and compression loading impacts the reduction of the compression and tension residual strength respectively. This observation is also supported by the previous observation of increased reduction in the residual strength over the life under $R = -1$. In particular, from Figure 4.7 it is apparent that the tensile component of the fully reversed $R = -1$ fatigue loading has a particularly important role in determining the fatigue life at lower stress levels and longer lives since the $R = -1$ fatigue data has a significantly steeper slope than $R = 10$.

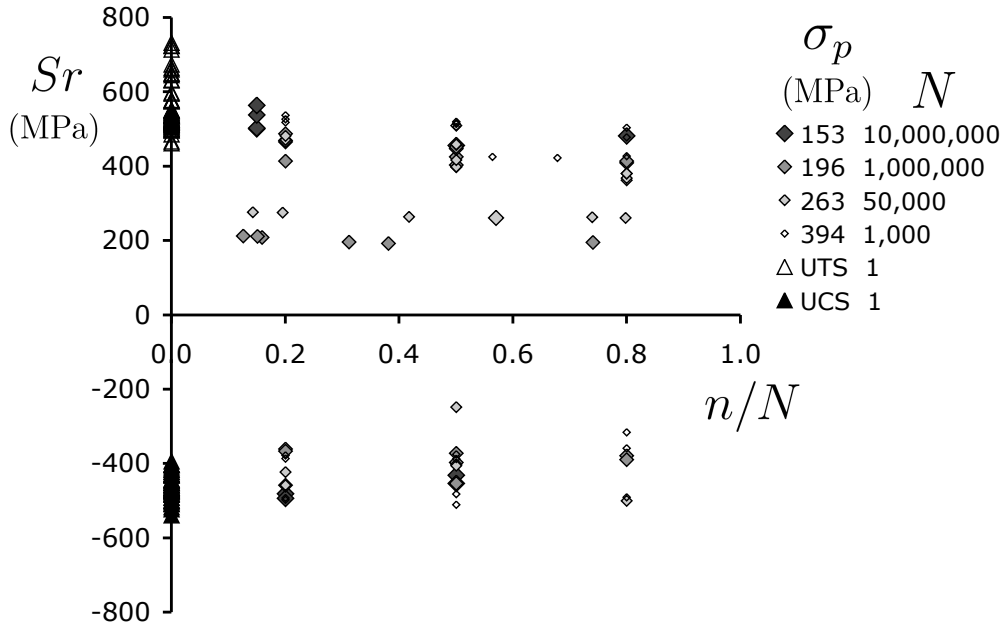

Figure 4.1: Tension and compression residual strength data for the MD2 laminate under $R = 0.1$ constant amplitude fatigue plotted as a fraction of the mean number of cycles to failure at each stress level as listed in the legend

4.3.2 Consideration of the phenomenon

Under an exclusively tensile fatigue load, the observed damage in a typical quasi-isotropic laminate includes off axis matrix cracks that can lead to meta-delaminations (where the cracks grow along the interface with another ply). The axial fibers that control ultimate tensile failure experience fiber/matrix debonding, and isolated axial fiber fractures. Ultimate failure is initiated by a group of axial fiber fractures leading to an increase in stress on the neighboring fibers such that they fail under the current global load and sudden catastrophic failure occurs. The global stress at which this catastrophic local failure occurs is the tensile (residual) strength of the material. The failure of off axis plies (non-critical elements) will increase the stress on the critical elements and accelerate the damage in the critical element.

Under an exclusively compressive fatigue load, the observed damage is primarily delamination initiation and growth and perhaps (although it is hard to detect) localized fiber micro-buckling. No matrix cracking is generally observed. Ultimate failure occurs as either micro-buckling of the fibers in the critical element, delamination leading to ply level buckling, or a combination of the two. Obviously if we consider ply level buckling, the compression strength is reduced when delaminations initiate and grow because the adjacent plies may now be susceptible to Euler buckling even if the original specimen was constrained to crushing failure. We can hypothesize that if individual or small groups of fibers buckle on the

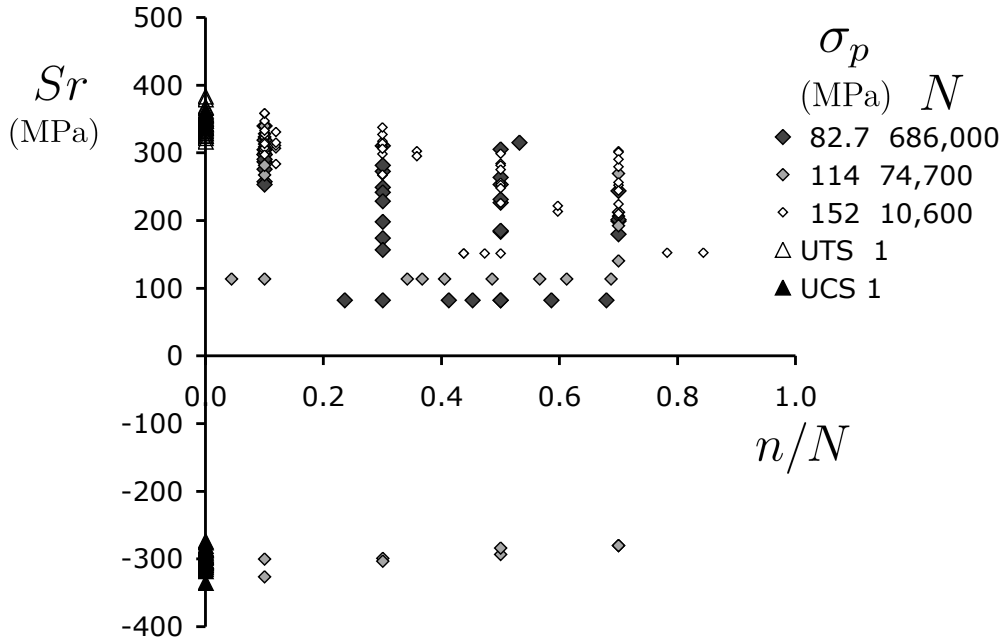

Figure 4.2: Tension and compression residual strength data for the VT8084 laminate under $R = 0.1$ constant amplitude fatigue plotted as a fraction of the mean number of cycles to failure at each stress level as listed in the legend

microscopic level, the compression stresses are increased and constraints decreased on adjacent fibers and they will be more likely to buckle as well. This damage mode propagation could lead to ultimate catastrophic failure by microbuckling.

To summarize, under tensile loading:

- Ultimate failure occurs by local density of fiber tensile breaks leading to catastrophic load concentration on adjacent fibers.
- Damage occurs in the form of fiber/matrix debonds and off axis ply cracking that increases the load on the critical elements

Under compressive loading

- Ultimate failure occurs by a combination of microbuckling of axial loaded fibers and ply level buckling of these lamina due to delamination with the rest of the material.
- Damage occurs in the form of delamination initiation and growth and localized microbuckling (or fiber matrix debond) of individual axial fibers.

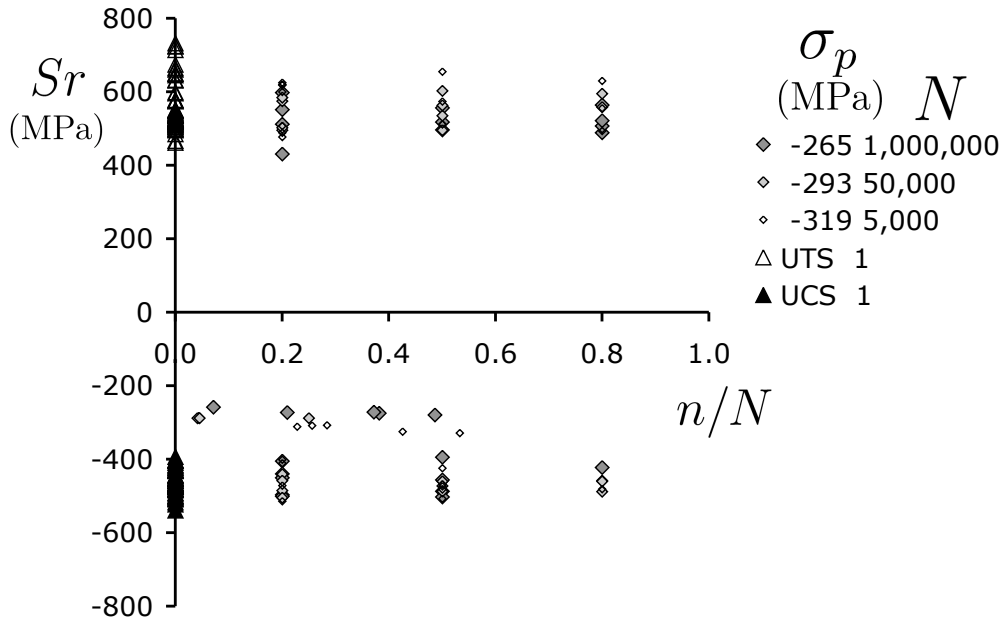

Figure 4.3: Tension and compression residual strength data for the MD2 laminate under $R = 10$ constant amplitude fatigue plotted as a fraction of the mean number of cycles to failure at each stress level as listed in the legend

Based on these observations, we note that the failure criteria of tensile and compressive residual strength are mechanistically different and they are primarily determined by different damage mechanisms/descriptions. We make the hypothesis that if it was possible to measure the strength of a composite without inducing damage prior to failure in the 0 degree fiber critical elements (this is of course not possible since the quasi-static loading process will cause damage prior to ultimate failure), then a delamination alone would not reduce the ultimate tensile strength of the material because that strength would rely entirely on the spacial density of broken fibers in the axial plies. Likewise, matrix cracks in off axis plies would not likely impact the compressive residual strength which would be dependent solely on the microbuckling of the 0 degree fibers or the ply level buckling of the corresponding critical elements.

Now consider the accumulation of damage over time, especially under a reversing fatigue load. It is reasonable to believe that damage induced by tensile loading (e.g. matrix cracks) will lead to an increase in the rate of reduction of the compressive strength under the next compression cycle (e.g. by initiating a delamination). Likewise, a compression cycle might increase the rate of reduction of tensile strength by creating damage that will increase the stress on the critical element in tension.

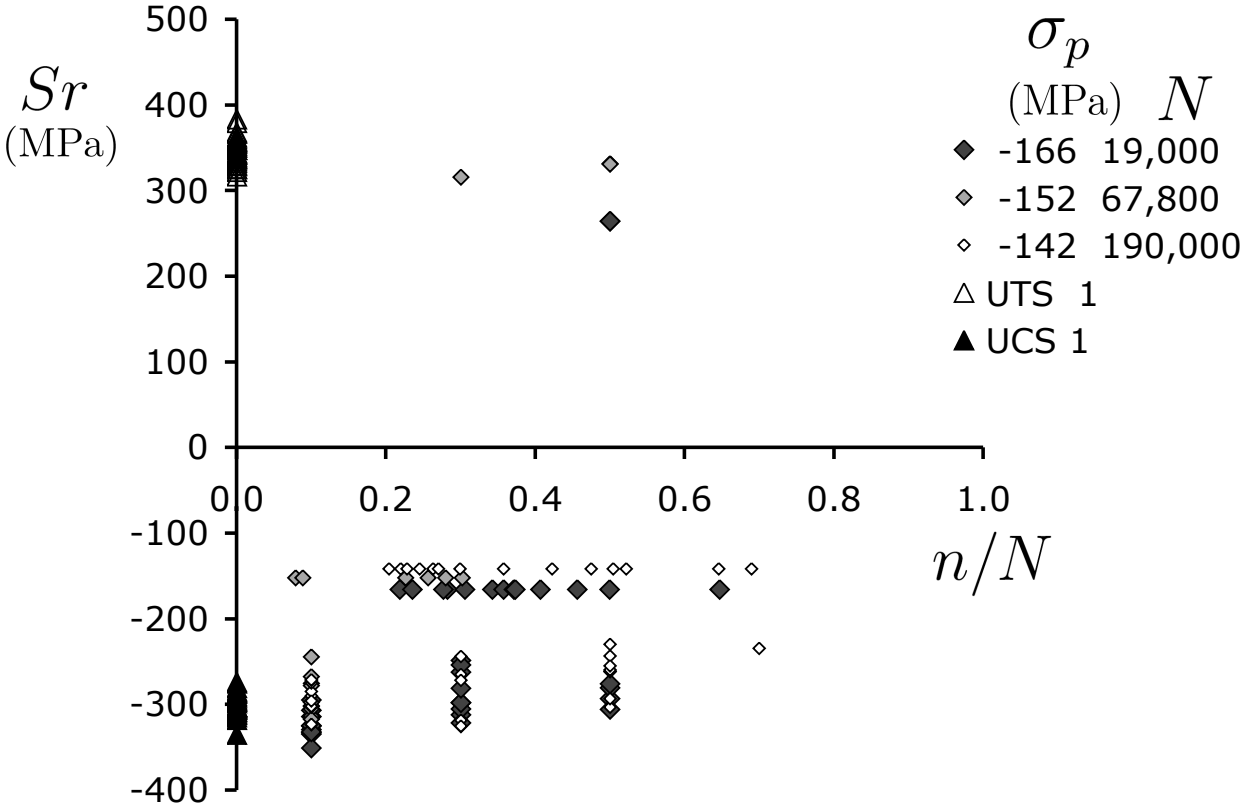

Figure 4.4: Tension and compression residual strength data for the VT8084 laminate under $R = 10$ constant amplitude fatigue plotted as a fraction of the mean number of cycles to failure at each stress level as listed in the legend

4.3.3 Formulation of the model

Developing a fatigue model that accounts for all of the damage and failure phenomena explicitly would be very difficult for a generalized composite material and would require knowledge of the fatigue behavior of the individual components, lamina, and their interaction with each other in the laminate. This information is generally not available and it is desirable to have a model that can be fit using data collected only on the entire laminate to make variable amplitude fatigue life predictions. Therefore, we propose a laminate level phenomenological fatigue model based on the concepts discussed, but incorporating several unknown parameters that will be determined by coupon level experimental data.

Sarkani et al. [14] noted that most laminate level residual strength models proposed in the literature are based on simplified versions of a generalized rate equation where the residual

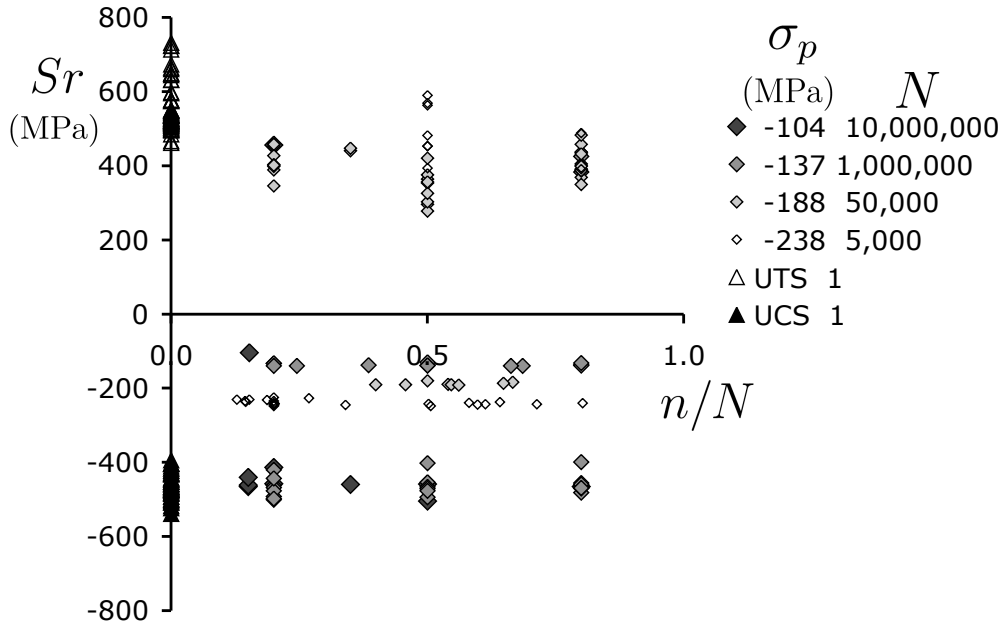

Figure 4.5: Tension and compression residual strength data for the MD2 laminate under $R = -1$ constant amplitude fatigue plotted as a fraction of the mean number of cycles to failure at each stress level as listed in the legend

strength S_r is assumed to be a monotonically decreasing function of the cycles applied:

$$\frac{dS_r(\tau)}{d\tau} = -H(\sigma(\tau))\frac{A\tau^{A-1}}{CS_r(\tau)^{C-1}} \tag{4.1}$$

where A and C are positive value parameters and may be functions of the applied stress and R-ratio, $H(\sigma(\tau))$ is an unknown function determined by the initial and final conditions and $S_r(\tau)$ is the residual strength as a function of a generalized time variable τ. These models can be used to calculate either the tensile residual strength or the absolute value of the compressive residual strength, but not both.

The new fatigue model starts with two versions of the standard rate equation, one for the tensile residual strength, S_t, and for the absolute value of the compressive residual strength, S_c, that each include a function coupling them together. We make the assumption that the tensile strength only decreases when the stress is increasing and is greater than zero. Likewise, we assume that the compressive strength only decreases when the stress is decreasing and is less than zero.

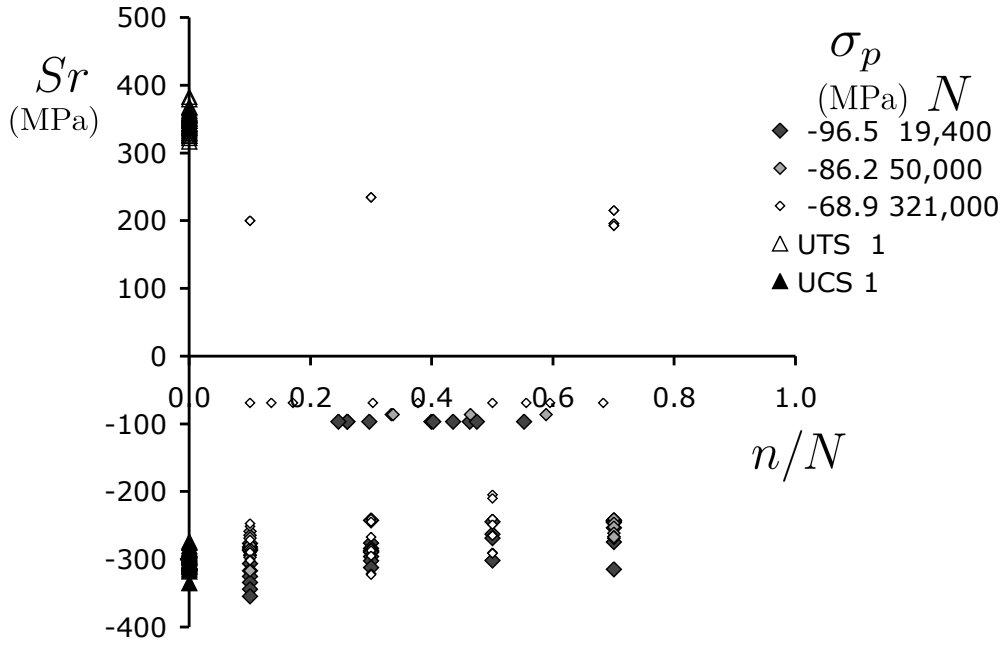

Figure 4.6: Tension and compression residual strength data for the VT8084 laminate under $R = -1$ constant amplitude fatigue plotted as a fraction of the mean number of cycles to failure at each stress level as listed in the legend

First defining a function:

$$\delta(\sigma(\tau)) = \begin{cases} 1 & \text{for} \quad \sigma > 0 \text{ and } \frac{d\sigma}{d\tau} > 0 \\ \\ 0 & \text{for} \quad \sigma \leq 0 \text{ or } \frac{d\sigma}{d\tau} \leq 0 \end{cases} \tag{4.2}$$

Then for tensile residual strength:

$$\frac{dS_t(\tau)}{d\tau} = -\delta(\sigma(\tau))G(S_c(\tau))H(\sigma(\tau))\frac{A_t\tau^{A_t-1}}{C_tS_t(\tau)^{C_t-1}} \tag{4.3}$$

and for compression residual strength:

$$\frac{dS_c(\tau)}{d\tau} = -\delta(-\sigma(\tau))I(S_t(\tau))J(\sigma(\tau))\frac{A_c\tau^{A_c-1}}{C_cS_c(\tau)^{C_c-1}} \tag{4.4}$$

where $G,\ H,\ I$, and J are positive valued functions. We will assume that $A_t,\ C_t,\ A_c$, and C_c are material constants. The tensile and compressive residual strengths, S_t and S_c, are treated as measures of the damage in the respective loading directions. Note that S_c represents the absolute value of the residual compression strength.

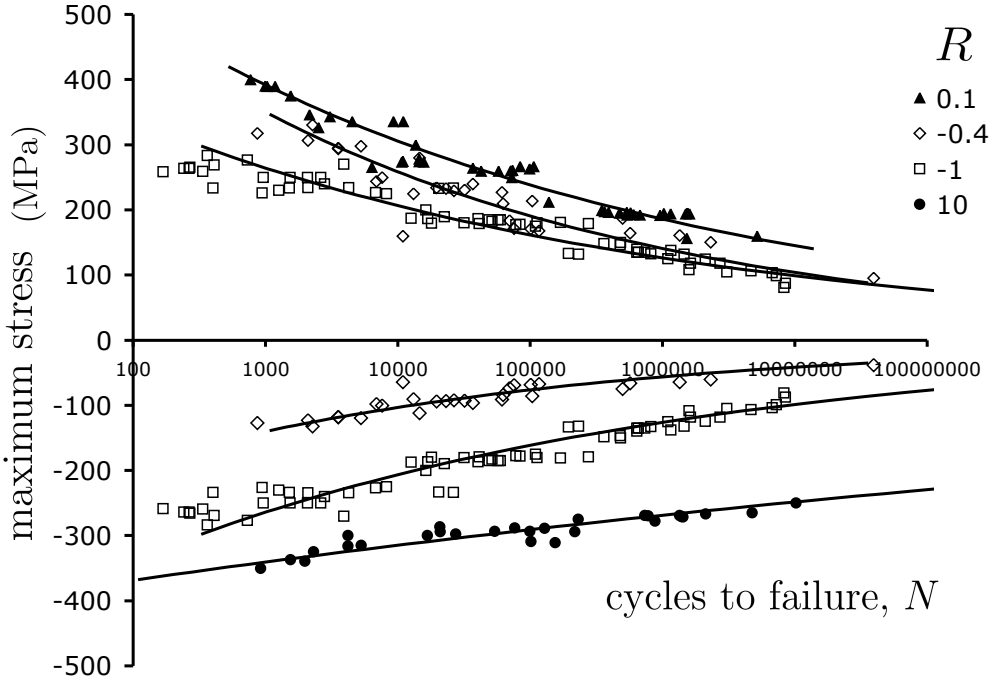

Figure 4.7: S-N curves in terms of the maximum peak or minimum valley stress for several R-ratios in the MD2 data base (note that R=-1 and R=-0.4 are plotted twice, once in terms of maximum tension stress and once in terms of maximum compression stress). Solid lines are a power law model fit to the experimental data using linear least squares with $\log(N)$ as the dependent variable.

By selecting this form of the equations, we are assuming that a tensile loading reducing the tensile strength does not directly reduce the compression strength. Instead the reduction of tensile residual strength accelerates the degradation of compression strength under a following compressive load. The compressive strength itself does not change until a compressive load is applied. Likewise the tensile strength is not directly reduced by a change in compressive strength, but the rate of tensile strength damage under a tensile load is increased by a change in compressive strength. This agrees with the phenomenological concepts previously discussed. The functions $G(S_c)$ and $I(S_t)$ relate how the current compressive or tensile strength impact the degradation rate of the other. Thus for an arbitrary loading history, Equations 4.3 and 4.4 are a system of coupled non-linear differential equations. However, because of the assumptions we have made, only one of the strengths, S_t or S_c can change at any given instant in time when $d\sigma/d\tau > 0$ or $d\sigma/d\tau < 0$ respectively. Thus, we can solve the equations iteratively by considering them in the context of a cyclic loading.

4.3.4 Determining the form of unknown functions

Consider a constant amplitude purely tensile loading ($0 \leq R < 1$). Because the valley stress, σ_v, is never negative, $dS_c/d\tau = 0$ and thus S_c is constant so $S_c = \|S_{ucs}\|$. It follows that the rate of tensile strength degradation will not be impacted by the compression strength and thus $G(S_{ucs}) = 1$. We further assume that the change in residual strength can be discretized cycles in terms of the maximum and minimum stresses without regard to the waveform. Each cycle contains the same segment of increasing stress from σ_v to σ_p and thus $H(\sigma(\tau)) = H(\sigma_p, \sigma_v)$, which is constant for a constant amplitude loading. Thus for this special case, we have reduced the coupled differential equations to the more standard form of the rate equation for constant amplitude loading where τ is in terms of cycles:

$$\frac{dS_t(\tau)}{d\tau} = -H(\sigma_v, \sigma_p)\frac{A_t \tau^{A_t - 1}}{C_t S_t(\tau)^{C_t - 1}} \tag{4.5}$$

Separating the variables and integrating:

$$\int_{\tau=0}^{\tau=n} C_t S_t(\tau)^{C_t - 1} dS_t = -H(\sigma_v, \sigma_p) \int_0^n A_t \tau^{A_t - 1} d\tau \tag{4.6}$$

yields

$$S_t(n)^{C_t} - S_t(0)^{C_t} = -H(\sigma_v, \sigma_p) n^{A_t} \tag{4.7}$$

Applying the initial condition that $S_t = S_{uts}$ at $n = 0$ gives $S_t(0) = S_{uts}$. Then applying the final condition for constant amplitude tensile fatigue failure $S_t = \sigma_p$ when $n = N_t(\sigma_p, \sigma_v)$ as defined by a constant life diagram for tensile fatigue life:

$$\sigma_p^{C_t} - S_{uts}^{C_t} = -H(\sigma_v, \sigma_p) N_t(\sigma_p, \sigma_v)^{A_t} \tag{4.8}$$

or

$$H(\sigma_v, \sigma_p) = \frac{S_{uts}^{C_t} - \sigma_p^{C_t}}{N_t(\sigma_p, \sigma_v)^{A_t}} \tag{4.9}$$

An identical procedure can be followed for the compressive residual strength under $R > 1$ constant amplitude fatigue to show that:

$$J(\sigma_v, \sigma_p) = \frac{\|S_{ucs}\|^{C_t} - \|\sigma_v\|^{C_t}}{N_c(\sigma_p, \sigma_v)^{A_c}} \tag{4.10}$$

where N_c is the fatigue life under the specific constant amplitude load with $R > 1$.

To define the form of the $G(S_c)$ and $I(S_t)$ we assume that a reduction in tensile or compressive strength is related to damage in the composite that will *increase* the rate of degradation of the other. Therefore, both functions must have values greater than or equal to one and monotonically increase as S_c and S_t decrease respectively. The form that fits this criteria

and the assumptions previously made for pure tensile loading where $G(S_c) = 1$ or pure compressive loading where $I(S_t) = 1$ is:

$$G(S_c) = \left(\frac{\|S_{ucs}\|}{S_c} \right)^x \tag{4.11}$$

$$I(S_t) = \left(\frac{S_{uts}}{S_t} \right)^y \tag{4.12}$$

where x and y are fitting parameters that will be treated as material constants.

4.3.5 A model for general loading

Because the general form of the model must apply to the special cases of $0 \leq R < 1$ and $R > 1$, we can rewrite Equations 4.3 and 4.4 for a general loading in terms of discrete cycle steps as:

$$\frac{dS_t(n)}{dn} = -\gamma(\sigma_p(n)) \left(\frac{\|S_{ucs}\|}{S_c(n-1)} \right)^x \frac{S_{uts}^{C_t} - \sigma_p(n)^{C_t}}{N_t(\sigma_p(n), \sigma_v(n-1))^{A_t}} \frac{A_t n^{A_t - 1}}{C_t S_t(n)^{C_t - 1}} \tag{4.13}$$

and

$$\frac{dS_c(n)}{dn} = -\gamma(-\sigma_v(n)) \left(\frac{S_{uts}}{S_t(n)} \right)^y \frac{\|S_{ucs}\|^{C_c} - \|\sigma_v(n)\|^{C_c}}{N_c(\sigma_p(n), \sigma_v(n))^{A_c}} \frac{A_c n^{A_c - 1}}{C_c S_c(n)^{C_c - 1}} \tag{4.14}$$

where

$$\gamma(\sigma) = \begin{cases} 1 & \text{for} \quad \sigma > 0 \\ 0 & \text{for} \quad \sigma \leq 0 \end{cases} \tag{4.15}$$

and

$$N_t(\sigma_p, \sigma_v) = \begin{cases} N(\sigma_p, \sigma_v) & \text{for} \quad \sigma_v > 0 \\ N(\sigma_p, 0) & \text{for} \quad \sigma_v \leq 0 \end{cases} \tag{4.16}$$

$$N_c(\sigma_p, \sigma_v) = \begin{cases} N(\sigma_p, \sigma_v) & \text{for} \quad \sigma_p < 0 \\ N(0, \sigma_v) & \text{for} \quad \sigma_p \geq 0 \end{cases} \tag{4.17}$$

$N(\sigma_v, \sigma_p)$ is the constant amplitude fatigue life defined in the normal way in terms of an S-N curve or more generally a constant life diagram.

In forming Equations 4.13 and 4.14 the standard definition of the n^{th} cycle as a peak, $\sigma_p(n)$, followed by a valley, $\sigma_v(n)$ was employed. However, because we assumed that only an increase in stress with a peak greater than 0 can cause a change in tensile residual strength, Equation 4.13 is actually dependent on the half cycle connecting $\sigma_v(n-1)$ and $\sigma_p(n)$. It is reasonable to take $\sigma_v(0) = 0$ for the initial condition prior to the first cycle.

Integration of Equations 4.13 and 4.14 for a reversing load or more generally any variable amplitude fatigue spectrum while assuming that $A_t,\ A_c,\ C_t,\ C_c,\ x$, and y are all material

constants and not dependent on the load applied gives:

$$S_t(n)^{C_t} = S_{uts}^{C_t} - \left[\sum_{i=1}^{n} \gamma(\sigma_p) \left(\frac{\|S_{ucs}\|}{S_c(i-1)}\right)^{x/A_t} \frac{\left(S_{uts}^{C_t} - \sigma_p(i)^{C_t}\right)^{1/A_t}}{N_t(\sigma_p(i), \sigma_v(i-1))}\right]^{A_t} \tag{4.18}$$

and

$$S_c(n)^{C_c} = S_{ucs}^{C_c} - \left[\sum_{i=1}^{n} \gamma(-\sigma_v) \left(\frac{S_{uts}}{S_t(i)}\right)^{y/A_c} \frac{\left(\|S_{ucs}\|^{C_c} - \|\sigma_v(i)\|^{C_c}\right)^{1/A_c}}{N_c(\sigma_p(i), \sigma_v(i))}\right]^{A_c} \tag{4.19}$$

These can be applied iteratively, first Equation 4.18 and then Equation 4.19 for each cycle, tracking the inner summation values at each step.

Alternatively, the model can be represented in terms of normalized strengths F_t and F_c as:

$$Fr_t(n)^{C_t} = 1 - \left[\sum_{i=1}^{n} \gamma(Fa_t(i)) \left(\frac{1}{Fr_c(i-1)}\right)^{x/A_t} \frac{\left(1 - Fa_t(i)^{C_t}\right)^{1/A_t}}{N_t(Fa_t(i), R_{i-1})}\right]^{A_t} \tag{4.20}$$

and

$$Fr_c(n)^{C_c} = 1 - \left[\sum_{i=1}^{n} \gamma(Fa_c(i)) \left(\frac{1}{Fr_t(i)}\right)^{y/A_c} \frac{\left(1 - Fa_c(i)^{C_c}\right)^{1/A_c}}{N_c(Fa_c(i), V_i)}\right]^{A_c} \tag{4.21}$$

In Equations 5.12 and 5.13 (hereafter "TC model"), $Fr_t = S_t/S_{uts}$ is the normalized tensile residual strength, $Fr_c = S_c/\|S_{ucs}\|$ is the normalized compressive residual strength, calculated in terms of the peak and valley normalized applied stresses, $Fa_t = \sigma_p/S_{uts}$ and $Fa_c = \sigma_v/S_{ucs}$. N_t and N_c are calculated using Fa_t and Fa_c, and $R_{i-1} = \sigma_v(i-1)/\sigma_p(i)$, or the reciprocal R-ratio, $V_i = \sigma_p(i)/\sigma_v(i)$ respectively for the i^{th} cycle. Using the reciprocal of the R-ratio, V, for compressive loads avoids numerical difficulties with evaluating equations at $R = \infty$. The normalized version of the model has the advantage being slightly simpler computationally.

4.4 Method of fitting parameters

For the residual strength approaches applied in the literature, typically either C or A in Equation 4.1 are taken to be 1. Post et al. [1] compared various versions of Equation 4.1 and showed little difference in the predictions for a range of spectrum loads and no significant improvement by treating both A and C as parameters over a simple linear model (Broutman-Sahu [9]) where $A = C = 1$. However those models were applied to spectra with a dominant R-ratio and only considered either the tensile or compressive residual strength for each case.

Initial experimentation found that the fatigue life under reversed loading ($R < 0$) predicted by the TC Model is very sensitive to the initial loss of strength. Thus the inclusion of

both A and C as parameters is important because it gives the model the ability to fit both an initial reduction of strength and the final rapid decline as observed in the composite material residual strength data in Section 4.3.1. The present model treats a reversing load as a variable amplitude loading with first a tensile stress cycle $\{0 \rightarrow \sigma_p \rightarrow 0\}$ followed by a compressive stress cycle $\{0 \rightarrow \sigma_v \rightarrow 0\}$ and thus accurate representation of the initial reductions in strength is critical to fitting the damage acceleration observed under $R < 0$ compared to T-T or C-C fatigue.

4.4.1 Determination of N_t and N_c

The first step will be to determine the functions for $N_t(\sigma_p, \sigma_v)$ and $N_c(\sigma_p, \sigma_v)$. These can be based on linear interpolation (similar to the Goodman approach) of the constant life diagram using the experimental S-N curves for $R_1 = 0.1$ and $R_3 = 10$ ($V_3 = 0.1$) as shown in Figure 4.8. Constant amplitude fatigue life data is typically fit to either a power law or exponential relationship. The choice of the form of this empirical model will influence the model results for variable amplitude loading because the predicted cycles to failure at low applied stresses can be very different. For the present analysis, a power-law model was selected:

$$\log N = a \log Fa + b \tag{4.22}$$

a and b are fit to the experimental fatigue data at each R by minimizing the linear least squares error in the $\log N$ direction.

The linear interpolation method shown graphically in Figure 4.8 enables the cycles to failure for any T-T R_2 to be calculated in terms of the $R_1 = 0.1$ S-N curve defined by a_1 and b_1 parameters. First, by shifting the horizontal axis by $-S_{uts}$ the ratio of rise to run must be the same for all points on a constant life line:

$$\frac{\sigma_{a,1}}{\sigma_{m,1} - S_{uts}} = \frac{\sigma_{a,2}}{\sigma_{m,2} - S_{uts}} \tag{4.23}$$

which in terms of peak stress σ_p and R for $0 \leq R < 1$ can be written as:

$$\frac{\frac{1}{2}\sigma_{p,1}(1 - R_1)}{\frac{1}{2}\sigma_{p,1}(1 + R_1) - S_{uts}} = \frac{\frac{1}{2}\sigma_{p,2}(1 - R_2)}{\frac{1}{2}\sigma_{p,2}(1 + R_2) - S_{uts}} \tag{4.24}$$

Solving for $\sigma_{p,1}$:

$$\sigma_{p,1} = \frac{\sigma_{p,2}(1 - R_2)S_{uts}}{\sigma_{p,2}(R_1 - R_2) + S_{uts}(1 - R_1)} \tag{4.25}$$

or in terms of normalized stress:

$$Fa_1 = \frac{Fa_2(1 - R_2)}{Fa_2(R_1 - R_2) + (1 - R_1)} \tag{4.26}$$

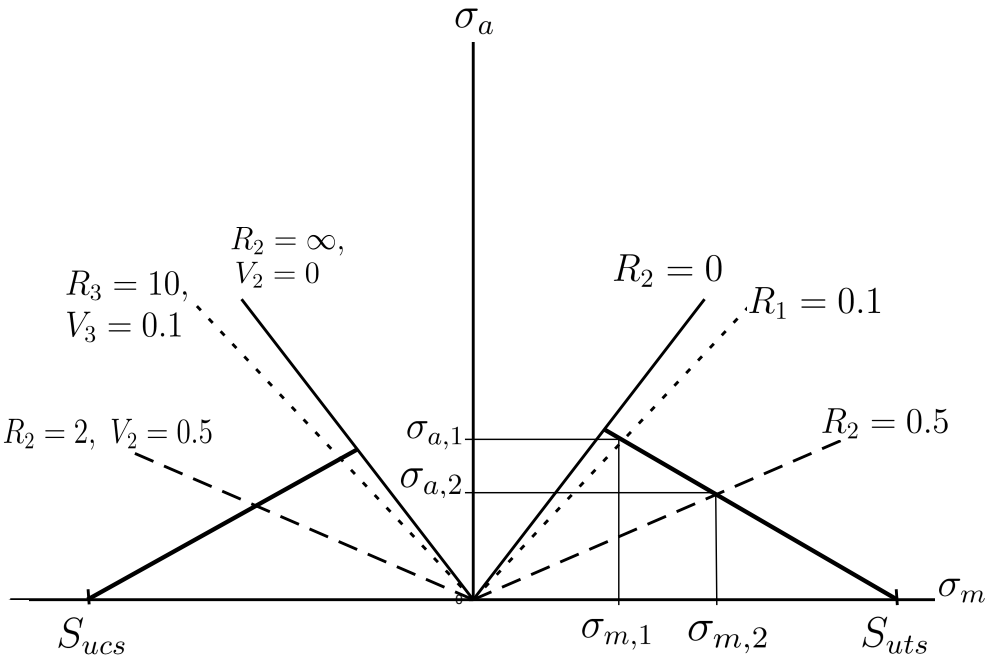

Figure 4.8: Schematic modified constant life (Goodman) diagram showing the linear interpolation of constant amplitude fatigue life lines in the T-T ($0 \leq R < 1$) and C-C ($1 < R$) ranges

Thus, in general:

$$N_t(Fa_2, R_2) = 10^{b_1} \left[\frac{Fa_2(1 - R_2)}{Fa_2(R_1 - R_2) + (1 - R_1)} \right]^{a_1} \tag{4.27}$$

where

$$R_2 = \gamma(\sigma_v(i-1)) \frac{\sigma_v(i-1)}{\sigma_p(i)} \tag{4.28}$$

and

$$Fa_2 = \frac{\sigma_p(i)}{S_{uts}} \tag{4.29}$$

Similar analysis for C-C fatigue ($1 < R \leq \infty$) results in an identical relationship in terms of V using the $V_3 = 0.1$ ($R = 10$) S-N curve defined by $\log N = a_3 \log Fa_3 + b_3$:

$$N_c(Fa_4, V_4) = 10^{b_3} \left[\frac{Fa_4(1 - V_4)}{Fa_4(V_3 - V_4) + (1 - V_3)} \right]^{a_3} \tag{4.30}$$

where

$$V_4 = \gamma(-\sigma_p(i)) \frac{\sigma_p(i)}{\sigma_v(i)} \tag{4.31}$$

and

$$Fa_4 = \frac{\sigma_v(i)}{S_{ucs}} \tag{4.32}$$

4.4.2 Determining material constants

Parameters A_t and C_t could theoretically be determined by fitting tensile fatigue to residual tensile strength data collected at $R = 0.1$ constant amplitude fatigue while A_c and C_c could be fit to compression residual strength under $R = 10$ constant amplitude fatigue. In reality, a wide range of pairs of A and C values will reasonably fit the residual strength data given the small number of replicates and the scatter present. Reversed loading fatigue is required to fit x and y. A_t, C_t, A_c and C_c may also be adjusted to while maintaining reasonable representation of the $R = 0.1$ and $R = 10$. For the demonstration of the model presented in this paper, values of A_t, C_t, A_c, C_c, x, and y were selected to provide a reasonable fit of the available constant amplitude fatigue data.

4.5 Results and discussion

To apply the TC model, the initial median (50^{th} percentile) tensile and compression strengths listed in Table 4.2 from each data set are used for the S_{uts} and S_{ucs} values. Thus, based on the Strength-Life Equal Rank Assumption, median residual strength and life values will be calculated. The $R = 0.1$ and $R = 10$ fatigue life data is normalized by the initial tension and compression strength respectively and fit to Equation 5.17 resulting in the parameters listed in Table 4.3 and the selected values for the remaining six parameters for each data set are listed in Table 4.4.

Table 4.2: Initial median strength calculated from the experimental data sets based on 30 or more replicates in each case

Data set	S_{uts} (MPa)	S_{ucs} (MPa)
MD2	535	-464
VT8084	348	-303

The fatigue life curve representations generated by the model for reversed loading conditions are compared to the experimental data in Figures 4.9 and 4.10. The results show that the model is capable of fitting reversed data reasonably well by treating it as a variable amplitude load of alternating tension and compression peaks.

Table 4.3: T-T and C-C normalized S-N power law parameters fit to experimental data sets

	$R_1 = 0.1$		$V_3 = 0.1$	
Data set	a_1	b_1	a_3	b_3
MD2	-9.267	1.749	-19.16	1.159
VT8084	-6.881	1.546	-14.60	0.4530

Table 4.4: TC model parameters selected for each fatigue data set

Data set	A_t	C_t	A_c	C_c	x	y
MD2	0.2	11	0.9	35	110	95
VT8084	0.2	7	0.6	10	2	25

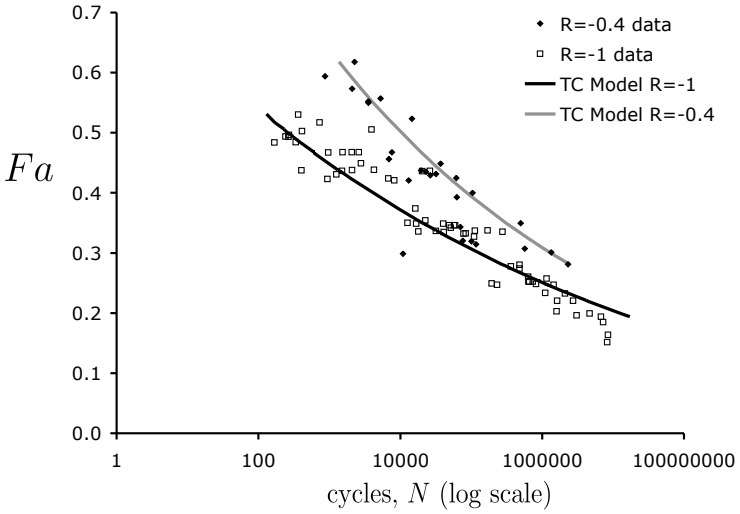

Figure 4.9: Normalized S-N data in terms of Fa_t compared to the TC model representation for the MD2 data set

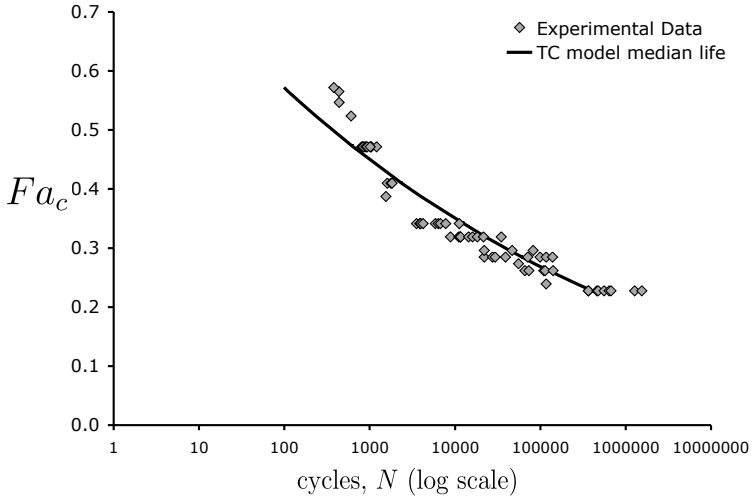

Figure 4.10: $R = -1$ normalized S-N data in terms of Fa_c compared to the TC model representation for the VT8084 data set

Using the selected parameters fit to the constant amplitude fatigue data, predictions were made for nominally fully reversed Rayleigh distributed fatigue loading with an autocorrelation of 0.95(see [2] for full description of the spectrum) tests in the VT8084 material system. As expected the model predicts compression failures. Results plotted in terms of the root mean square of the stress time history are shown in Figure 4.11 show excellent comparison between the model and experiments. Residual compression strength measurements were also available under the Rayleigh distributed loading and an example of the median predicted residual strength history for the middle stress level of 33 MPa RMS stress is compared to the data in Figure 4.12. The TC model appears to slightly overestimate the compression residual strength for most of the life under Rayleigh distributed loading. For the MD2 material, fatigue to failure under WISPER and WISPERX load spectra at various peak stress values was available. WISPER and WISPERX spectra are dominantly tension but contain a small percentage of reversing cycles. The results plotted in Figure 4.13 show good agreement for the WISPER spectrum while the TC model over predicted the WISPERX fatigue life at the higher stress levels.

4.6 Conclusion

This article presents the derivation of a phenomenological model for coupled calculation of the residual tensile and compressive strengths of a composite material subjected to an arbitrary loading history. The primary advantage of the TC model over previous residual strength and damage rule models for variable amplitude loading is that it explicitly handles both tension and compression failure modes and determines which type failure occurs. While

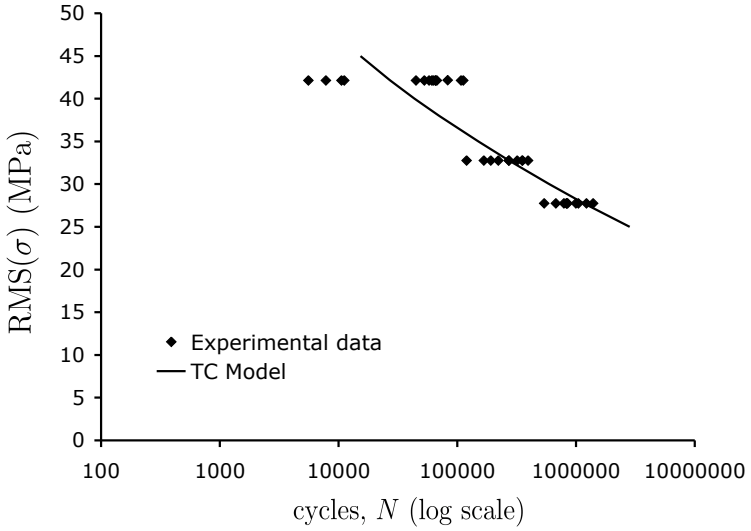

Figure 4.11: VT8084 data set Rayleigh distributed spectrum fatigue to failure data compared to TC model prediction in terms of time history RMS stress applied

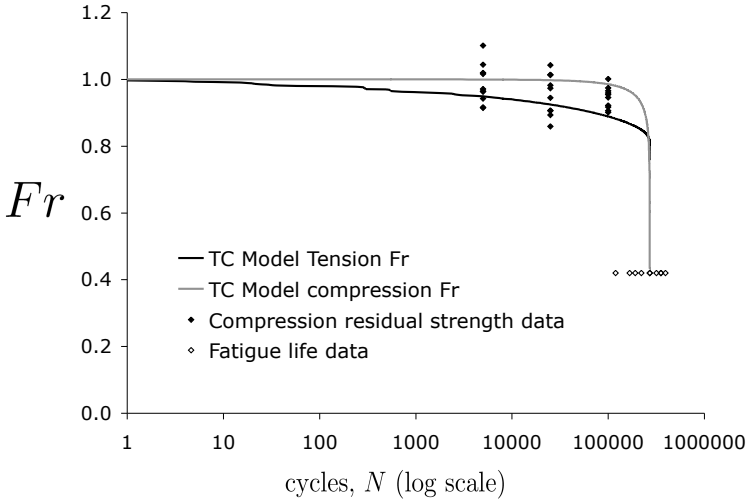

Figure 4.12: VT8084 data set Rayleigh distributed spectrum fatigue normalized residual strength compression data compared to TC model prediction for tensile and compressive residual strength at a time history RMS stress of 33 MPa

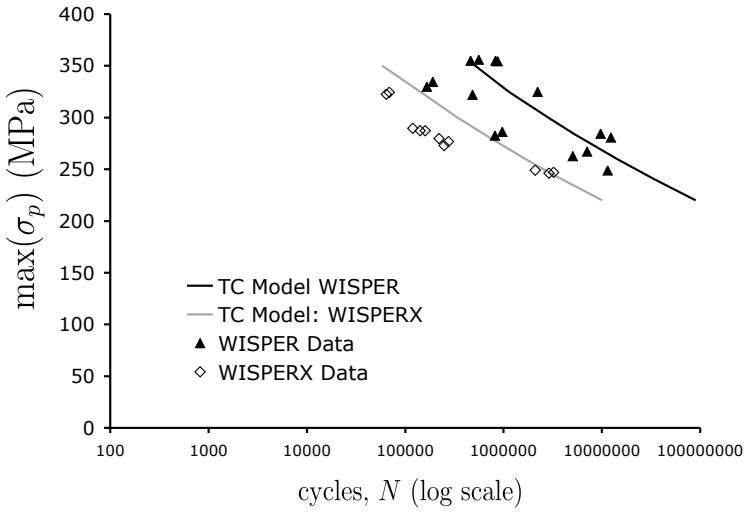

Figure 4.13: MD2 data set WISPER and WISPERX spectra fatigue to failure data compared to TC model predictions in terms of the maximum applied stress in the spectra

the new model appears to have more parameters than other spectrum fatigue models, it does not require a full constant life diagram as an input for modeling a general spectrum fatigue load (only T-T and C-C S-N curves are required). Additionally, most residual strength models treat A or C type parameters as function of R ratio while they are considered to be material constants in the TC model. Since the reversed loading cases can be used to help determine the remaining parameters, the data requirements for fitting are similar or possibly less than previous residual strength models. Once fit, application of the model to any fatigue loading sequence is straight forward because the model calculations are based on each increase in stress magnitude. Thus, rainflow or other traditional spectrum analyses of the load history are not required.

Application of the proposed model to two experimental data sets have shown that based on T-T and C-C fatigue life time data, it can be fit satisfactorily to constant amplitude reversed loading with dominant tension ($R = -0.4$) and compression ($R = -1$) failures. Predictions made for several variable amplitude loading cases showed good agreement with experimental lifetime results for Rayleigh distributed reversed loading and the WISPER spectrum. Thus the concept of treating tension and compression fatigue loading separately in a variable amplitude model has been shown to be a valid approach.

Acknowledgments
Financial support for this research was provided by the Office of Naval Research (Award #N00014-06-1-0812). Note: The opinions expressed herein are the views of the authors and should not be interpreted as the views of the Naval Surface Warfare Center or the Department of the Navy.

Chapter 5

Reliability based design of composites under high cycle variable amplitude fatigue: a new residual strength formulation

Reliability based design of composites under high cycle variable amplitude fatigue: a new residual strength formulation

N.L. Post, S.W. Case, J.J. Lesko
MC 219, Virginia Polytechnic Institute and State University, Blacksburg, VA 24061, USA

ABSTRACT

Reliability-based design of structural components is becoming the standard in many industries. Wind turbine blades and ship hulls are two examples of fiber reinforced composite applications where the material is subjected to high cycle, variable amplitude fatigue over its lifetime. In order to perform a reliability-based design analysis, the probability of failure must be computed for the expected design life. This research developed a reliability design methodology using a model for the tension and compression residual strength of a fiber reinforced composite subjected to any defined stress history. By first selecting an acceptable probability of failure and a series of characteristic loading histories, this approach enables load and resistance factor design (LRFD) knockdowns to be calculated with a computationally efficient procedure.

This paper will be prepared for submission to Composites Science and Technology.

5.1 Introduction

Reliability-based design methods are becoming the norm in many industries. In civil infrastructure, load and resistance factor design (LRFD) guidelines and specifications based on structural reliability analysis are commonplace [142, 143]. Winterstein and Lange et al. have discussed many aspects of fatigue-critical reliability-based design for wind turbine blades [57, 58, 59, 144, 145]. LRFD is currently under exploration for naval structural design as well where high cycle variable amplitude fatigue can be critical. For example, Assakkaf and Cárdenas-Garcia [63] discussed the application of LRFD design to doubler plates for ship structures.

The philosophy of reliability-based design accepts that all structures have a finite probability of failure over their design life and seeks to optimize the design in terms of the economic costs and value associated with selecting the probability of failure. Theoretically, by comparing the cost of improving the reliability (more materials, and reduced efficiency due to weight, increased environmental impact, etc.) relative to the cost and likelihood of a failure (including damage, replacement, injury or loss of life, etc.) an optimum design can be determined. In reality, this analysis is very complex because it may need to account for multiple failure modes and failure consequences, and can include analysis of hundreds of statistical variables. Thus, the desired reliability of a structure is often selected based on a combination of simplified statistical analysis and socially acceptable rates of failure. In civil engineering, the acceptable probability of failure has in many cases been determined by back-calculation of the probability of failure given by existing design guidelines [143, 146, 147, 148].

In this paper, we will assume that a desired reliability for a structural component has been determined and focus on methods to ensure that the selected design will meet that reliability. Fiber reinforced polymer (FRP) composite structures in the aircraft, naval architecture, and wind turbine blade industries are often subjected to high cycle variable amplitude fatigue loads that degrade the strength of the material over time, leading to fatigue failures at stresses well below the initial strength of the material. This accumulated damage can result in fatigue failure mode critical designs. Thus fatigue analysis must be incorporated into the reliability calculations. All current approaches to fatigue analysis in reliability-based design use linear damage accumulation (Palmgren Miner Rule) for determining the fatigue life distribution. These approaches have several significant disadvantages for design of composite materials. Palmgren-Miner rule has been shown to be highly non-conservative for predicting lifetimes in some cases and if the critical damage sum is taken as a variable, determining its distribution requires extensive spectrum fatigue experiments. Because the traditional approach involves calculating the average damage accumulation rate, rare extreme stress events and variation in load history order are not accounted for in the failure criteria and thus the probability of failure may be underestimated. This paper describes a new residual strength-based approach for calculating the probability of failure that overcomes the shortcomings of the traditional fatigue reliability methods.

Table 5.1: Nomenclature

Symbol	Description
R_n	nominal material resistance
L_n	nominal applied load
ϕ	resistance factor (for material uncertainty and fatigue)
γ	load factor (for load uncertainty)
P_f	probability of failure
$f_X(x)$	probability density function of X
$F_X(x)$	cumulative density function of X
$G(\mathbf{X})$	limit state function in terms of variables $\mathbf{X}$
τ	generalized time
τ_d	design life
f_0	average fatigue frequency
$n_d = f_0\tau_d$	design life in cycles
n	cycles applied
N	cycles to failure under a given loading condition
i	the i^{th} loading cycle
D	damage sum
Δ	critical damage value
$\overline{D}$	average damage accumulation rate
e	environmental condition or "operation cell"
σ	stress (general)
σ_p	maximum (peak) applied stress during a fatigue cycle
σ_v	minimum (valley) applied stress during a fatigue cycle
$R = \sigma_v/\sigma_p$	R-ratio (definition)
$V = 1/R = \sigma_p/\sigma_v$	reciprocal of the $R - ratio$
S_{uts}	initial ultimate tensile strength
S_{ucs}	initial ultimate compression strength
S_r	residual strength
S_t	tensile residual strength
S_c	absolute value of the compressive residual strength
Fa	normalized applied load
$Fa_t = \sigma_p/S_{uts}$	normalized applied tensile stress
$Fa_c = \sigma_v/S_{ucs}$	normalized applied compression stress
$Fr = S_r/S_u$	normalized residual strength
$Fr_t = S_t/S_{utc}$	normalized residual strength
$Fr_c = S_c/S_{ucs}$	normalized residual strength
δ	the heavy side function
$A, A_t, A_c, C, C_t, C_c, x, y$	model curve fitting (material) constants

continued on next page

continued from previous page

Symbol	Description
a	Power law S-N curve slope
b	Power law S-N curve intercept
α	Weibull distribution shape parameter
$S_0,\ N_0$	Weibull distribution scale parameters for stress and life
p	percentile of a probability distribution
j	integer counter
m	number of experimental or simulated replicates
u, v	random numbers on [0,1]
$\rho(x, y)$	correlation coefficient for two random variables, x and y
T-T	tension-tension loading ($0 < R < 1$)
C-C	compression-compression loading ($R > 1$)
T-C	tension-compression loading ($R < 0$). Fully reversed: $R = -1$

5.2 Background

5.2.1 Load and Resistance Factor Design

In Load and Resistant Factor Design (LRFD) a probabilistic framework is used to determine standard material knockdowns that can then be applied to nominal material properties as easily as allowable stress design [143, 146, 147]. Typically the LRFD design concept is presented as:

$$\phi R_n > \sum \gamma L_n \tag{5.1}$$

where the design problem has been reduced to a simple inequality for each failure mode in terms of the nominal material property, R_n, nominal applied load, L_n, and the resistance and load factors, ϕ and γ. These factors can be tabulated for various scenarios and probabilities of failure. The uncertainties in the applied loads are incorporated using γ, while ϕ accounts for the distribution of material properties and any change in that distribution over time due to fatigue, environmental degradation, etc. In the context of LRFD, the objective is to determine the values of ϕ and γ required for the desired reliability of the structure.

A conceptual representation of the reliability problem for a single loading peak, L, is shown in Figure 5.1. As γ increases > 1 and ϕ decreases < 1, the load and resistance distributions are shifted further from each other and the probability of failure is reduced. Analytically, the probability of failure is the integral of the product of the probability density of the maximum

applied stress, $f_L(x)$, and the cumulative density of resistance, $F_R(x)$:

$$P_f = \int_{-\infty}^{\infty} f_L(x) F_R(x) dx \tag{5.2}$$

In the case of fatigue loading $F_R(x)$ is a function of the past applied loads and thus the probability of failure must be integrated over the design life of the structure.

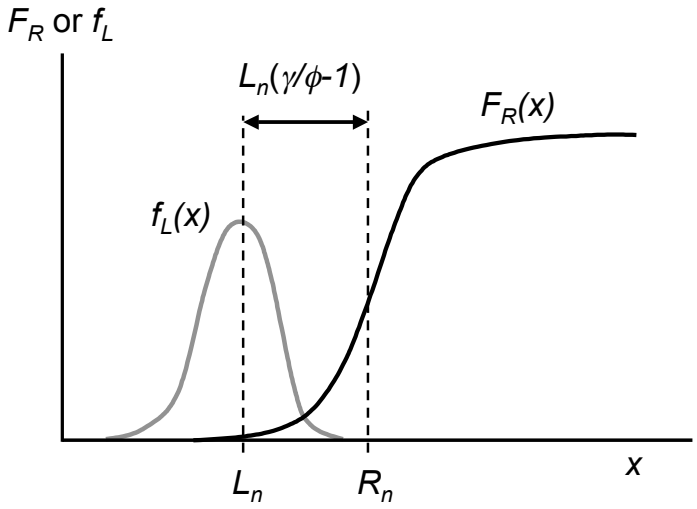

Figure 5.1: Conceptual representation of LRFD and the probability of failure given by the overlap of the probability density of loads, f_L and the cumulative probability of resistance F_R

Consideration of methods to determine ϕ for an FRP composite given a fatigue loading scenario, lifetime and desired reliability is the focus of this paper. There are many other aspects of a design including stress concentrations, non-axial stress states, and environmental degradation of the material that must also be included in complete reliability calculations. However, these considerations are beyond the scope of this present research which will focus on the problem of reliability calculations for axially loaded fiber dominated composites under spectrum fatigue loading.

5.2.2 Limit state function

Reliability problems are often defined in terms of a limit state function, $G(\mathbf{X})$, configured to give failure when $G < 0$ and safety for $G > 0$. $\mathbf{X}$ represents a vector of stochastic and deterministic variables that are relevant in the design problem. The limit state is $G = 0$ and

the reliability is given by the probability that $G \geq 0$: $P[G(\mathbf{X}) \geq 0]$. For example, a simple axial loading of a component in quasi-static tension might have the limit state:

$$G(\mathbf{X}) = S_{uts}(\mathbf{X}) - \sigma_{applied}(\mathbf{X}) \tag{5.3}$$

where both the strength of the material and the applied stress depend on a set of stocastic variables, $\mathbf{X}$.

For most problems, the functional form of the limit state equation is too complex to directly calculate the probability that the structure will fail, $P[G(\mathbf{X}) < 0]$. Instead, either numerical simulation techniques such as Monte-Carlo simulations, or approximations including the linear First Order Reliability Method (FORM) or Second Order Reliability Method (SORM) are employed [59, 149, 150]. The latter are more common because they are much less computationally intensive. In FORM or SORM analysis, the random variables of the initial limit state formulation are transformed to uncorrelated normally distributed random variables. For a given design point, a critical design case (random variable values most like to give failure) where the structure just fails is located using the gradients of $G(\mathbf{X}) = 0$. The limit state function $G(\mathbf{X}) = 0$ is approximated through this point as either a linear (FORM) or quadratic (SORM) function of the variables and the probability of failure is calculated based on this approximated failure surface. Often, finding the critical design point requires an iterative process where the limit state function is approximated, and a new design point that is closer to the original design is found. Then the limit state function is reevaluated and the process repeats until convergence is reached [149].

5.2.3 Limit state functions for fatigue

Current reliability-based design methodology for fatigue defines the limit state function in terms of the fatigue life [59, 62, 151]:

$$G(\mathbf{X}) = T_f(\mathbf{X}) - T_t(\mathbf{X}) \tag{5.4}$$

where T_f is the calculated time to failure and T_t is the target lifetime and $\mathbf{X}$ is a vector of stochastic parameters describing operation, loading and material behavior. For both wind turbines and ships [59, 62], T_f is calculated based on linear damage accumulation (Palmgren-Miner rule [8]) defined as:

$$D = \sum_i \frac{n_i}{N_i} \tag{5.5}$$

where n_i is the number of cycles applied at a stress level giving N_i constant amplitude cycles to failure and D is the damage sum for the loading. The main advantage to using Miner's rule in these calculations is that it enables the computation of an average damage rate based on the applied loading distribution, simplifying the final form of the limit state equation [59]. The average damage summation per unit time is given by:

$$\bar{D} = \int_0^\infty \int_0^\infty \frac{f_{\sigma|E}(\sigma|e) f_E(e)}{N(\sigma)} d\sigma de \tag{5.6}$$

where $f_{\sigma|E}(\sigma|e)$ is the conditional probability distribution of a fatigue cycle with stress σ given the environmental conditions e, $f_E(e)$ is the probability distribution of environmental conditions over the life and $N(\sigma)$ is the number of cycles to failure at applied cyclic stress σ [59]. Environmental conditions, also termed "operation cells," are typically defined in terms of constant wind speed and power demand for wind turbines, sea state and velocity for ships, etc. Linear damage accumulation defines failure to occur when the D reaches some critical value, Δ. Given an average response cycle rate f_0, the time to failure is:

$$T_f = \frac{\Delta}{f_0 \bar{D}} \tag{5.7}$$

Taking Miner's rule to be true, $\Delta = 1$. More generally Δ can be treated as a stochastic variable to reflect uncertainty in the accuracy of Miner's rule [59].

Typically for each environmental condition experimental data or simulations are used to define the stress time history. Then Rainflow cycle counting [55, 152, 153] of complete hysteresis loop cycles is used to reduce the time history to a histogram of applied cycles defined by the mean stress, σ_m, and stress amplitude, σ_a [154, 155, 156]. This analysis is repeated for each environmental condition and the relative frequency $f(e)$ of the environmental conditions are assessed. An S-N curve for zero mean stress (R-ratio$= -1$) and linear Goodman diagram are used to determine $N(\sigma)$. The $S - N$ curve parameters may be treated as stochastic variables to represent the variability in the material fatigue behavior [59].

Lange implemented the above approach in a computational package to calculate reliability of wind turbine blades based on several sets of example stochastic parameters [59, 145, 144]. Tang and Zhao considered a similar approach using the linear damage accumulation rule to calculate reliability under random cyclic loading for metals based on a gausian distribution of applied loads [151].

Murty et al. [157] proposed a method to calculate the reliability under constant amplitude loading where the applied stress level was a random variable by calculating the "fatigue strength" distribution at different lifetimes in terms of the fatigue life distribution at different stress levels. Kamiński [158] considered reliability of homogeneous material and composites in terms of damage accumulation and crack growth models. For the case of composite materials, limit state functions were derived in terms of Hill-Chamis, Hoffman and Tsai-Wu failure criterion for multi-axis loading in terms of the stress amplitude applied.

Ichikawa [159] considered a limit state function for fatigue reliability analysis where the "stresses" and "strengths" were defined in terms of the value of the applied and critical cumulative damage ratio (Miner's rule). This analysis used the constant amplitude fatigue life and the average damage rate to convert the limit state function to values with units of stress and strength. However, the failure criteria was still essentially in terms of the damage sum. The probability of failure was derived for the case where the spectrum is held constant and the maximum applied stress and critical cumulative damage ratio were both assumed to be log-normally distributed. The standard deviation of the critical cumulative damage

ratio was assumed to be the same as the standard deviation of fatigue life under constant amplitude loading to avoid requiring extensive variable amplitude fatigue data [159]. Chen [160] developed a similar approach to the one proposed by Ichikawa and gave several examples of the analysis using data on homogenous materials under variable amplitude loading.

Winterstein et al. discussed many aspects of fatigue-critical reliability-based design for wind turbine blades using a damage accumulation approach and more general definition of the loads in terms of wind velocity and other parameters [57, 58]. When applying LRFD in this context, Winterstein et al. defined L and R in terms of cycles. Thus, all of the current approaches to fatigue failure modes in reliability-based design consider calculations of the fatigue life and do not explicitly account for the change in strength of the material over time.

5.2.4 Residual strength in reliability-based design

Although residual strength models of composites under fatigue loading have been studied and tested over the last 30 years [1], their use in design analysis methodology has been non-existent to date, at least in the public literature. Despite the commonly reported advantages of residual strength approaches to variable amplitude lifetime prediction, the Palmgren-Miner linear damage accumulation law has been used exclusively in reliability-based design under fatigue loading.

In the case of the wind turbine WISPER and WISPERX spectra, the traditional fatigue analysis including use of a linear Goodman diagram and Palmgren-Miner rule method has been shown to overestimate the life by 1 to 2 orders of magnitude [139]. Nijssen et al. improved predictions for WISPER by modifying the Goodman diagram and S-N curve shape [49, 139]. These authors felt that such a method might be more readily accepted in the design community than replacing Miner's sum calculations with a nonlinear damage or residual strength equation. Although significantly better predictions were made with this modified approach, it's application is arbitrary (not backed by actual constant amplitude fatigue data) and thus the generality of the method is questionable.

In addition to often providing highly non-conservative estimates of fatigue life, using Miner's rule means predicting *lifetimes* in order to calculate the required *strength* knockdown for an acceptable probability of failure over the lifetime. Implicit in this approach is that the mean predicted lifetime must be much larger than the actual desired lifetime for an acceptable probability of failure. Philosophically, predicting *residual strength* distributions over the desired life of a structure to determine the appropriate *strength* material knockdown is more logical. This approach could also enable more accurate analysis of the structural reliability if rare large stress events that exceed the residual strength are present.

Another difficultly in calculating the probability of failure using linear damage accumulation is that the distribution of Δ is typically unknown and would require extensive variable amplitude fatigue test data on realistic loading scenarios to determine. Thus, most analyzes

have made assumptions about the shape and distribution of Δ that are not well supported experimentally. By comparison, residual strength models have often been extended to calculate the distribution of residual strength and, if the distribution of applied loads is already well characterized, the failure criterion can be easily defined in terms of the stochastic inputs.

A residual strength based limit state function takes the form:

$$G(\mathbf{X}, \tau) = S_r(\mathbf{X}, \tau) - \sigma(\mathbf{X}, \tau) \tag{5.8}$$

where $S_r(\mathbf{X}, \tau)$ is the residual strength, $\sigma(\mathbf{X}, \tau)$ is the applied stress and $\mathbf{X}$ contains parameters defining the time history of loads and the material response to those fatigue loads. G, S_r and σ are shown as explicit functions of generalized time, τ, to emphasize that the limit state, and thus the probability of failure, changes over time as the residual strength decreases. Failure can occur at any point in time when the applied stress exceeds the current strength.

A challenge to applying most residual strength models in reliability-based design is that they can only consider one dominant failure mode, either tension or compression, selected prior to the analysis. By comparison, linear damage accumulation does not consider the failure mode explicitly and the life is determined by when $D \geq \Delta$. For a residual strength model that calculates both the tension residual strength S_t and the compression residual strength, S_c, two limit state functions G_t and G_c are required to describe failure:

$$G_t(\mathbf{X}, \tau) = S_t(\mathbf{X}, \tau) - \sigma_t(\mathbf{X}, \tau) \tag{5.9}$$

and

$$G_c(\mathbf{X}, \tau) = S_c(\mathbf{X}, t) - \sigma_c(\mathbf{X}, \tau) \tag{5.10}$$

where S_t and S_c are the residual tensile and compressive strengths of the material subjected to applied tensile stresses σ_t and σ_c. The probability of failure in this case will be given by:

$$P_f = P[G_t < 0 \cup G_c < 0] = P[G_t < 0] + P[G_c < 0] \tag{5.11}$$

5.2.5 Tension and Compression Residual Strength Model

Recently, Post et al. [3] proposed a new residual strength model that calculates the tension and compression residual strengths of an FRP composite subjected to an arbitrary series of peak and valley stresses. The final version of this model (hereafter "TC model") as presented for deterministic analysis of residual strength was:

$$Fr_t(n)^{C_t} = 1 - \left[\sum_{i=1}^{n} \delta(Fa_t(i)) \left(\frac{1}{Fr_c(i-1)} \right)^{x/A_t} \frac{\left(1 - Fa_t(i)^{C_t}\right)^{1/A_t}}{N_t(Fa_t(i), R_{i-1})} \right]^{A_t} \tag{5.12}$$

and

$$Fr_c(n)^{C_c} = 1 - \left[\sum_{i=1}^{n} \delta(Fa_c(i)) \left(\frac{1}{Fr_t(i)} \right)^{y/A_c} \frac{\left(1 - Fa_c(i)^{C_c}\right)^{1/A_c}}{N_c(Fa_c(i), V_i)} \right]^{A_c} \tag{5.13}$$

where $Fr_t = S_t/S_{uts}$ is the normalized tensile residual strength, S_t, and $Fr_c = S_c/\|S_{ucs}\|$ is the normalized compressive residual strength, S_c. The residual strength is calculated in terms of the peak, σ_p, and valley, σ_v, normalized applied stresses, $Fa_t = \sigma_p/S_{uts}$ and $Fa_c = \sigma_v/S_{ucs}$. Tension failure is defined by $Fr_t < Fa_t$ and compression failure is defined by $Fr_c < Fa_c$.

In Equations 5.12 and 5.13, material constants A_t, C_t, A_c, and C_c control the shape of the tensile and compressive residual strength curves under constant amplitude while x and y are interaction parameters that control how changes in tensile and compressive strength accelerate the degradation of the other. The tensile strength is assumed to only decrease under an increasing tensile stress and compression strength is only reduced under a decreasing compressive stress so:

$$\delta(Fa) = \begin{cases} 1 & \text{for} \quad Fa > 0 \\ 0 & \text{for} \quad Fa \leq 0 \end{cases} \tag{5.14}$$

N_t and N_c are the constant amplitude cycles to failure under the component of the applied load that is pure tensile or pure compressive stress respectively and calculated based on Fa_t and Fa_c, and $R_{i-1} = \sigma_v(i-1)/\sigma_p(i)$, or the reciprocal R-ratio, $V_i = \sigma_p(i)/\sigma_v(i)$ respectively for the i^{th} cycle. Using V, the reciprocal of the R-ratio, for compressive loads avoids numerical difficulties with evaluating equations at $R = \infty$.

$$N_t(Fa_t, R) = \begin{cases} N_t^*(Fa_t, R) & \text{for} \quad R > 0 \\ N_t^*(Fa_t, 0) & \text{for} \quad R \leq 0 \end{cases} \tag{5.15}$$

$$N_c(Fa_c, V) = \begin{cases} N_c^*(Fa_c, V) & \text{for} \quad V > 0 \\ N_c^*(Fa_c, 0) & \text{for} \quad V \leq 0 \end{cases} \tag{5.16}$$

$N(Fa, R)$ is the constant amplitude fatigue life defined by linear interpolation (similar to the Goodman method) of the tension-tension and compression-compression fatigue regimes anchored using measured S-N curves (typically at $R_1 = 0.1$ and $V_3 = 0.1$ ($R_3 = 10$). Fatigue life curves are taken to follow a power law relationship

$$\log N = a_j \log Fa + b_j, \quad j = 1, 3 \tag{5.17}$$

where a and b are fit to the experimental fatigue data at each R by minimizing the linear least squares error in the $\log N$ direction. For linear interpolation of the constant life plot in the tension-tension and compression-compression regimes, we can show that:

$$N_t^*(Fa_2, R_2) = 10^{b_1} \left[\frac{Fa_2(1 - R_2)}{Fa_2(R_1 - R_2) + (1 - R_1)} \right]^{a_1} \tag{5.18}$$

where

$$R_2 = \delta(\sigma_v(i-1)) \frac{\sigma_v(i-1)}{\sigma_p(i)} \tag{5.19}$$

and

$$Fa_2 = \frac{\sigma_p(i)}{S_{uts}} \tag{5.20}$$

Likewise

$$N_c^*(Fa_4, V_4) = 10^{b_3}\left[\frac{Fa_4(1-V_4)}{Fa_4(V_3-V_4)+(1-V_3)}\right]^{a_3} \tag{5.21}$$

where

$$V_4 = \delta(-\sigma_p(i))\frac{\sigma_p(i)}{\sigma_v(i)} \tag{5.22}$$

and

$$Fa_4 = \frac{\sigma_v(i)}{S_{ucs}} \tag{5.23}$$

Although the mathematical description of the TC model is complex and requires the input of 12 material parameters $\{S_{uts}, S_{ucs}, a_1(R_1), b_1(R_1), a_3(V_3), b_3(V_3), A_t, C_t, A_c, C_c, x, y\}$, its application to any loading sequence of peak and valley stresses is straight forward by iterative computation of Equations 5.12 and 5.13 while keeping track of the inner summation. The R_1 T-T and V_3 C-C normalized S-N curve parameters, a_1, b_1, a_3, and b_3, may be fit to constant amplitude fatigue data using linear least squares on a log-log representation of the data. Reversed fatigue loads are treated as a variable amplitude fatigue with each tension followed by a compression cycle and then another tension cycle. A_t, C_t, A_c, C_c, x and y are selected to provide reasonable fits to constant amplitude T-T and C-C residual strength data and fatigue life data under reversed T-C fatigue. This has been demonstrated by Post et al. in [3]. Unlike the Palmgren-Miner rule and many earlier residual strength approaches, the TC model does not require a series of closed hysteresis loop cycles as its input. Instead, fatigue damage is effectively calculated based on half cycles, $\sigma_v(i-1) \rightarrow \sigma_p(i)$ and $\sigma_p(i) \rightarrow \sigma_v(i)$. Thus any load sequence, defined by its local maxima and minima points may be used as an input. Rainflow analysis is not required or desirable because the model will depend on the relative order of tension and compression stresses.

The present work extends this model to stochastic prediction and then considers the analysis in the context of a reliability-based design to determine the load and resistance factors.

5.3 Calculating the distribution of residual strength

The first step to including the TC residual strength model in a reliability analysis is to determine a method for calculating the distribution of residual strength under a given loading history. Potentially, all 12 material parameters could be treated as stochastic variables. However, determining the distributions and correlation of these parameters experimentally would be difficult so we simplify the approach by incorporating the strength-life equal rank assumption (SLERA). The results are compared to experimental data for reversed and spectrum fatigue loading to assess the accuracy of these assumptions.

The SLERA term was first used by Chou and Croman [70] and explicitly means that

$$F_{S_u}(S_k) = F_N(n_k) \tag{5.24}$$

where F_{S_u} and F_N are the cumulative distributions of initial strength and life, and the k^{th} percentile specimen has strength S_k and life n_k [70]. Several residual strength models have been introduced in probabilistic formulations that explicitly use both the distributions of fatigue life and initial strength including those by Yang and colleagues [80]. Schaff and Davidson [78] used the SLERA principle and chose to do an empirical curve fit of the spread of the residual strength distribution based on the initial strength and fatigue life distributions.

Post et al. [76, 77] showed that a reasonable prediction of the residual strength distribution was calculated for constant and variable amplitude fatigue loading cases with a normalized residual strength model by treating only the initial properties as stochastic variables. In this simple tensile fatigue loading under one R, Post et al.[77] used a residual strength model that can be derived as a simplification of the TC model:

$$Fr(n) = 1 - \left[\sum_{i=1}^{n} \left(1 - Fa(i)\right)^{1/A} \frac{1}{N(Fa(i))} \right]^{A} \tag{5.25}$$

where

$$N(Fa) = 10^{b} Fa^{a} \tag{5.26}$$

Parameters A, a and b were taken to be non-stochastic material constants and were given the best fit values to the data using the median initial strength in the calculation of Fr and Fa. Then the distribution of Fr for a given loading could be calculated by using the input of the initial strength distribution to define a series of trials with different S_{uts} and known cumulative probability rank values. Because N is a function of $Fa = \sigma_p / S_{uts}$ rather than just σ_p, the residual strength distribution will spread as the fatigue progresses and the distribution of fatigue life has been shown to approximate that of the data. Philippidis and Passipoularidis [16] also demonstrated this method of calculating the residual strength distribution for several residual strength models applied to constant amplitude fatigue.

A similar approach can be used with the TC model by taking the initial tension strength, S_{uts}, and initial compression strength, S_{ucs}, as stochastic variables and all other model parameters as deterministic material constants. Comparison of the model fatigue life distribution results to experimental data assess the effectiveness of this simplification. The statistical correlation, $\rho(S_{uts}, S_{ucs})$, of S_{uts} and S_{ucs} remains a significant unknown in this analysis. Unfortunately, it is impossible to determine $\rho(S_{uts}, S_{ucs})$ experimentally because each quantity can only be measured using a distractive test. As the damage and failure modes on a microscopic level are different for tension and compression loading of composites, it is likely that the tension and compression strength are not perfectly correlated, however the level of correlation remains unknown. As a first step to addressing this unknown, we will perform Monte-Carlo simulations to calculate the fatigue life distribution with $\rho \approx 1$ (S_{uts} and S_{ucs} perfectly correlated) and $\rho \approx 0$ (S_{uts} and S_{ucs} independent) for several reversed fatigue loads. The results are compared to estimates of the actual fatigue life distribution from experimental data.

We used a set of data collected at Virginia Tech that is publicly available at [5], hereafter called the "VT8084" data set. This material is a $[0/+45/90/\text{-}45/0]_s$ laminate consisting of 10 layers of woven roving E-glass with a rubber toughened vinyl ester matrix (Ashland Chemical Durakane 8084). The VT8084 material was primarily intended for naval ship hull construction. The data set includes quasi-static tension and compression strength measurements, constant amplitude fatigue life and residual strength under $R = 0.1$, $R = -1$ and 10. Variable amplitude fatigue cases include Rayleigh distributed loading with 95% autocorrelation (degree of load ordering, see [2]) and a nominal $R = -1$. The fatigue frequency was held constant for all tests at 5 Hz. In most cases, at least 10 replicates of each test have been performed so estimates of the underlying population distribution can be obtained.

The strength data was fit using a two parameter Weibull distribution [83] defined as:

$$F(x) = 1 - \exp\left[-\left(\frac{x}{S_0}\right)^{\alpha}\right] \tag{5.27}$$

where $F(x)$ is the cumulative density function, S_0 is the location parameter and α is the shape parameter. The values of α and S_0 are estimated by calculating a median rank $P_{0.50}$ of the strength of each specimen [161]:

$$P_{0.50} = \frac{j - 0.3}{m + 0.4} \tag{5.28}$$

where j is the sorted rank of the data and m is the total number of data points. Then a linear least squares fit is found for $\ln(\ln(1/(1-P)))$ vs. $\ln(S)$. The resulting slope is α and the S_0 may be calculated from the intercept, B as:

$$S_0 = \exp\left[\frac{-B}{\alpha}\right] \tag{5.29}$$

Because of the limited number of experimental samples, there will be some uncertainty in the calculated α and S_0 values for each set of results. A 95% confidence interval on α and S_0 was determined to provide a measure by which to compare them to simulated values. The range of this confidence interval can be calculated by:

$$\alpha^{+} = \alpha_{calc} \exp\left(\frac{-0.78 * 1.960}{\sqrt{m}}\right) < \alpha < \alpha_{calc} \exp\left(\frac{0.78 * 1.960}{\sqrt{m}}\right) = \alpha^{-} \tag{5.30}$$

$$S_0^{+} = S_{0,calc} \exp\left(\frac{-1.05 * 1.960}{\alpha_{calc}\sqrt{m}}\right) < S_0 < S_{0,calc} \exp\left(\frac{1.05 * 1.960}{\alpha_{calc}\sqrt{m}}\right) = S_0^{+} \tag{5.31}$$

where m is the number of data points used when calculating the distribution parameters α_{calc} and $S_{0,calc}$ [161].

The distribution parameters for initial tensile and compression strength are given in Table 5.2. The remaining model parameters were selected based on the fitting analysis performed in [3] and are given in Table 5.3

Table 5.2: Initial tensile and compressive strength distribution parameters calculated from experimental data

	# of replicates	α_{calc}	α^+	α^-	$S_{0,calc}$ (MPa)	S_0^+	S_0^-
S_{uts}	33	25.7	33.5	19.7	354	359	349
$\|S_{ucs}\|$	30	26.2	34.7	19.8	305	310	301

Table 5.3: TC model parameters for the VT8084 data set

Parameter	Value	Parameter	Value
R_1	0.1	A_t	0.2
a_1	-6.881	C_t	7
b_1	1.546	A_c	0.6
V_3	0.1	C_c	10
a_3	-14.60	x	2
b_3	0.4530	y	25

If S_{uts} and S_{ucs} are taken to be independent random variables that follow the distribution given in Table 5.2 then it is not possible to know the resulting rank of a residual strength or fatigue life calculation from the model explicitly and a Monte-Carlo style simulation is required to calculate the resulting fatigue life distribution. This simulation was implemented in Java, using the standard library *Math.random*() random number generator to create a series of initial strength values. For each simulated specimen, these strengths were calculated as:

$$S_{uts} = S_{0,uts} \exp\left[(-\ln(1-u))^{1/\alpha_{uts}}\right] \tag{5.32}$$

$$S_{ucs} = S_{0,ucs} \exp\left[(-\ln(1-v))^{1/\alpha_{ucs}}\right] \tag{5.33}$$

where u and v are uniform random numbers on [0,1]. For $\rho \approx 0$ separate random numbers are generated for u and v while $v = u$ for each specimen when $\rho \approx 1$. The correlation of the tensile and compressive strength for the simulated was always within 10% of the desired value. The fatigue life can then be calculated for each of these trials and the resulting distribution parameters α_N and N_0 are found by fitting the Weibull distribution to the fatigue life using the same method as for actual experimental data.

To give an example of the computational time required for this model, running on an Apple PowerBook G4 with a 1.8 GHz. processor, a TC model calculation of a variable amplitude fatigue life for approximately 10^6 cycles takes about 8 seconds. If we were to simulate fatigue

lives on the order of 10^9 cycles to failure, each model evaluation would take about 2 hours on this computer.

5.4 Simulation Results and Discussion

5.4.1 Monte-Carlo refinement

To determine the required number of simulated specimens, a series of constant amplitude fatigue life simulations were performed for $R = -1$ with a maximum stress of 97 MPa. For these simulations, the initial tension and compression strength were taken to be uncorrelated. The α_N and N_0 results calculated for each simulation run are plotted in Figure 5.2. While there is a large amount of scatter in the resulting distribution parameters for 10 and 50 simulated specimens, 100 or more provide fairly uniform results. Thus, to limit computational time, 100 simulated specimens will be used for the following comparisons.

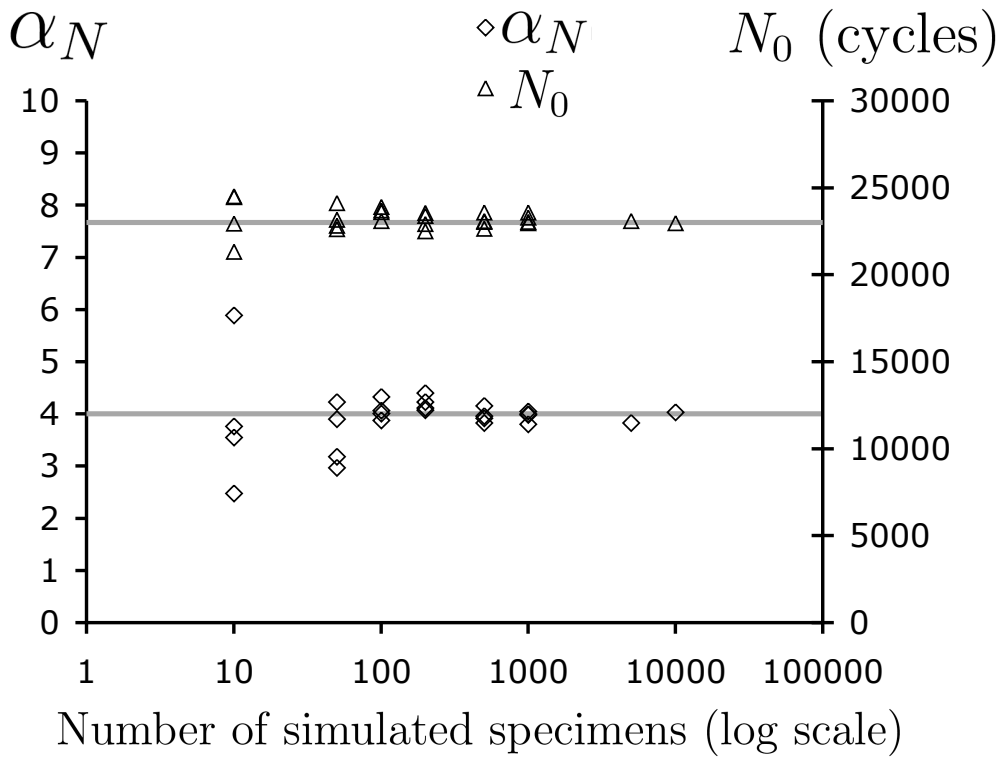

Figure 5.2: Monte-carlo simulation refinement for T-C model of R=-1 fatigue to failure with a peak stress of 97 MPa and $\rho \approx 0$. Horizontal lines are for reference only and show $\alpha_N = 4$ and $N_0 = 23000$)

5.4.2 Evaluation of initial strength correlation and model accuracy

To evaluate the effect of correlation between the initial tension and compression strengths, simulations with $\rho = 0$ and $\rho = 1$ were run to calculate the fatigue life at several stress levels for $R = -1$ constant amplitude loading. The predicted SN curves for 0.05, 0.50, and 0.95 probability of failure are shown in Figure 5.3 and the α_N and N_0 values for the simulations and experimental results are compared in Figures 5.4 and 5.5. Overall, both simulations provide results that are usually within the 95% confidence interval of the experimental distribution parameters. The simulation with $\rho = 1$ results in a broader distribution of fatigue lives and in general the α_N values are closer to the experimental results. As a result, assuming $\rho = 1$ also will result in a more conservative estimate of reliability because the lower life tail of the distribution will be greater as shown in Figure 5.6. We note that at the lowest stress levels, the correlation between the initial tensile and compressive strengths does not appear to have a significant effect on fatigue life and the model gives a conservative result compared to experimental data.

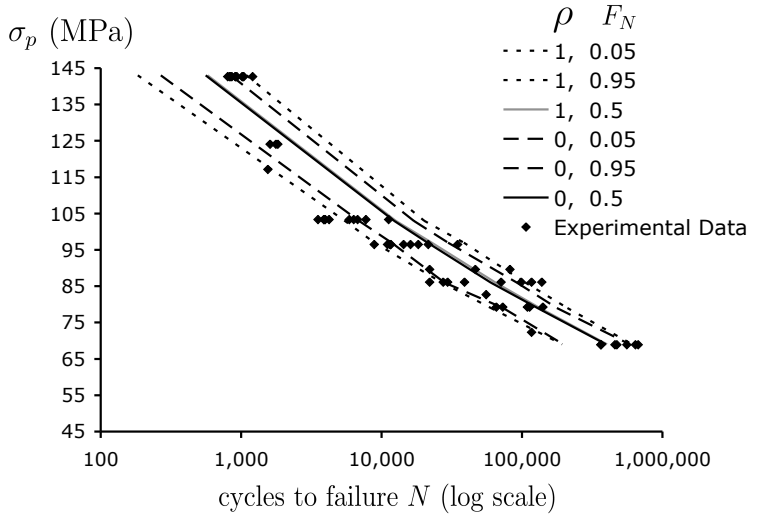

Figure 5.3: S-N curve plot of R=-1 constant amplitude fatigue data with TC model simulation results for 0.05, 0.5 and 0.95 probability of failure assuming $\rho = 0$ and $\rho = 1$

To ensure that this conclusion is also applicable to spectrum loading, we consider the case of a 5000 cycle Rayleigh distributed fatigue load with an autocorrelation of 0.95 (see [2] for details) repeated until failure at three time-history RMS stress levels. The RMS S-N curve is shown in Figure 5.7 and the experimental and simulated α_N and N_0 values are compared in Figures 5.8 and 5.9. Again, we find that the results generated by assuming 100% correlation between initial tensile and compressive strengths are the most satisfactory.

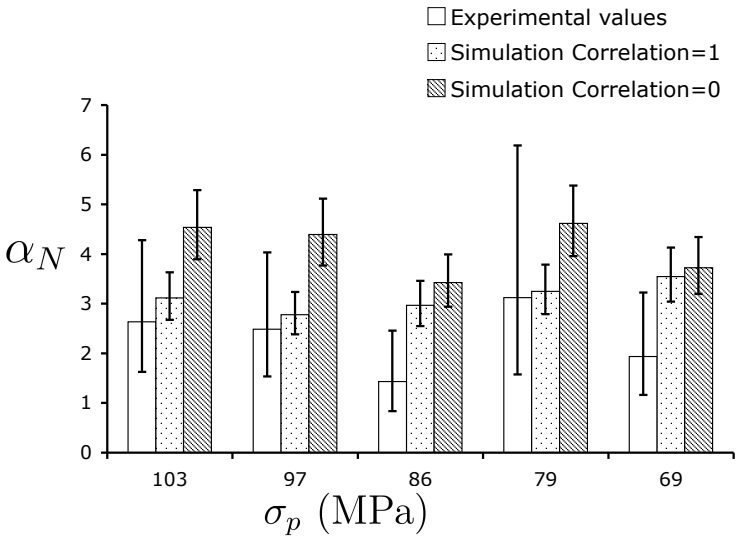

Figure 5.4: Comparison of experimental and simulated shape parameter, α_N, for $R = -1$ constant amplitude fatigue life distributions. Error bars indicate a 95% confidence interval on α_N.

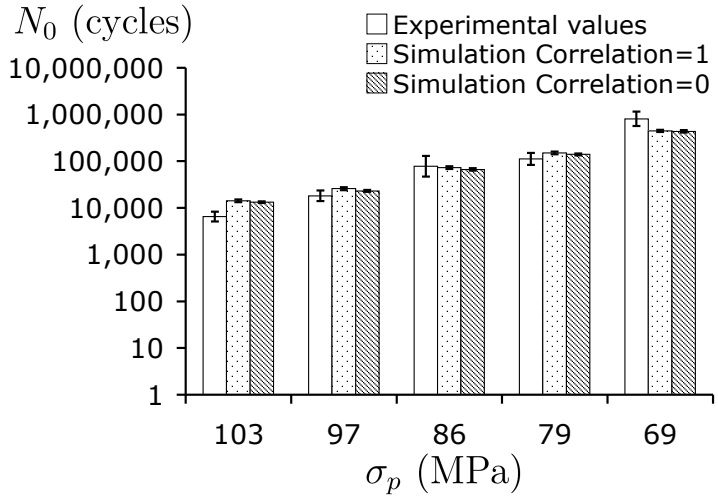

Figure 5.5: Comparison of experimental and simulated location parameter, N_0, for $R = -1$ constant amplitude fatigue life distributions. Error bars indicate a 95% confidence interval on N_0.

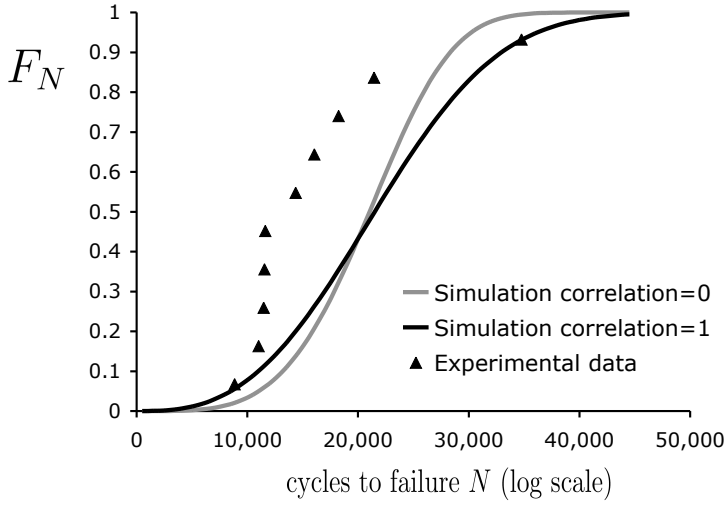

Figure 5.6: Example of cumulative probability of failure from each simulation and the experimental data for $R = -1$ constant amplitude fatigue

Based on this empirical evidence, it is acceptable to assume full correlation between the initial tensile and compressive strengths. It is conceivable that by including more variability in the model parameters, this conclusion would change; however as the model performs very well for both the reversed constant amplitude and Rayleigh distributed loading spectra, especially at lower stress levels, we conclude that this simple statistical application is adequate to describe the material behavior, at least for these types of loadings. Assuming that the ultimate strengths are correlated has a significant advantage for reliability calculations because the SLERA will now hold true for the tension-compression model. Thus, rather than simulating the entire range of initial strengths, we only need to perform calculations for the probability rank strengths that are expected to fail. This greatly reduces the computational time for calculating the probability of failure during long lifetimes.

5.4.3 Application to reliability analysis

Finding the LRFD parameters ϕ and γ for a specified design situation and required reliability is an iterative process. Values of ϕ and γ are selected, the probability of failure is calculated, and ϕ or γ is adjusted until the desired reliability is obtained. With the TC model approach, based on Equations 5.9 - 5.11, the analytical calculation for the probability of failure is:

$$P_f = \int_{\tau=0}^{\tau_d} \int_0^{\infty} \left[f_{Fa_t}(x) F_{Fr_t}(x,\tau) + f_{Fa_c}(x) F_{Fa_c}(x,\tau) \right] dx d\tau \tag{5.34}$$

where f_{Fa_t} and f_{Fa_c} are the probability density functions of the normalized applied peak and valley stresses, F_{Fr_t} and F_{Fr_c} are the cumulative probability functions of the tension

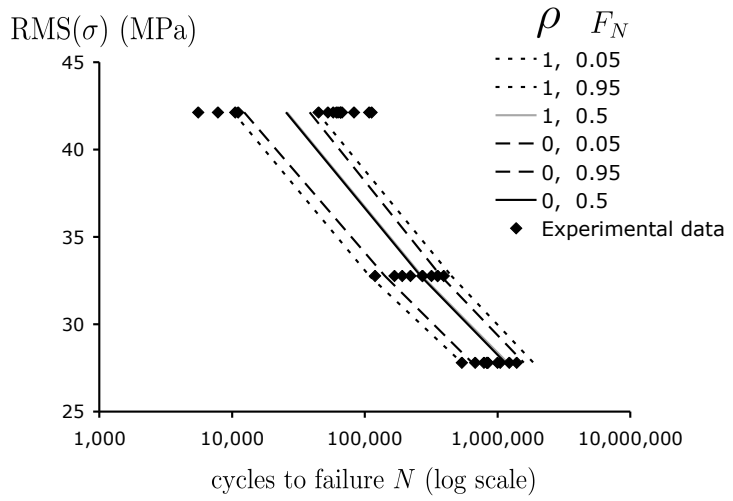

Figure 5.7: S-N curve plot of nominally $R = -1$ Rayleigh spectrum fatigue data with TC model simulation results for 0.05, 0.5 and 0.95 probability of failure assuming $\rho = 0$ and $\rho = 1$

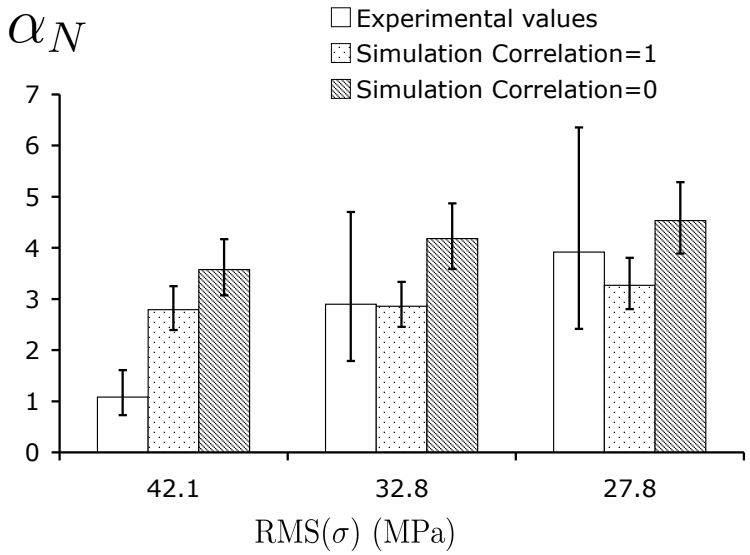

Figure 5.8: Comparison of experimental and simulated shape parameter, α_N, for nominally $R = -1$ Rayleigh spectrum fatigue life distributions. Error bars indicate a 95% confidence interval on α_N.

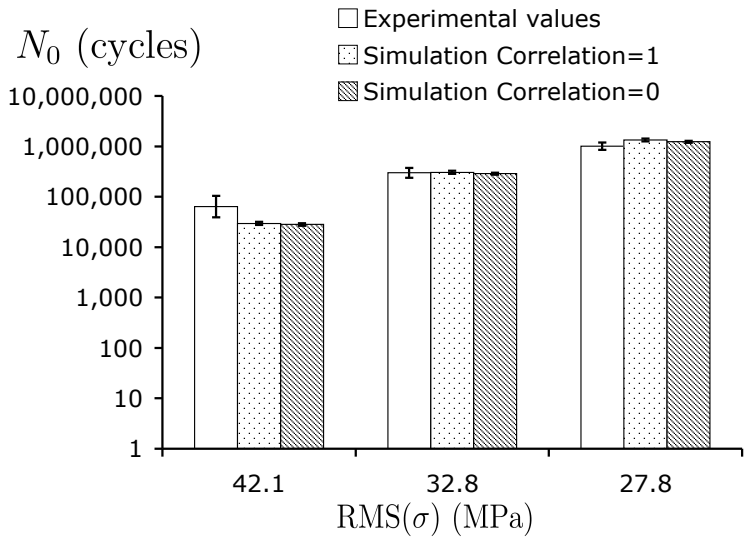

Figure 5.9: Comparison of experimental and simulated location parameter, N_0, for nominally $R = -1$ Rayleigh spectrum fatigue life distributions. Error bars indicate a 95% confidence interval on N_0.

and compression residual strength as a function of time, and τ_d is the design life of the component. If we assume an average applied frequency, f_0, then time can be measured in terms of cycles with the design cycles, $n_d = f_0\tau_d$.

It is reasonable to assume that the probability density function of applied loads is constant with respect to time. Interchanging the order of integration yields:

$$P_f = \int_0^\infty \left[f_{Fa_t}(x) \int_{n=1}^{n_d} F_{Fr_t}(x,n)dn + f_{Fa_c}(x) \int_{n=1}^{n_d} F_{Fa_c}(x,n)dn \right] dx \qquad (5.35)$$

Thus it is only necessary to simulate the specimens trials for the cycle range $1 < n < n_d$. In general, Fr_t and Fr_c depend on the load history in addition to the probability distribution of applied loads. Because of this interaction, exact calculation of the probability of failure from Equation 5.35 requires a Monte-Carlo simulation where both the percentile of initial strength and the spectrum load order sequence are considered random variables. First and second order reliability methods are not applicable because the limit state function is in terms of time as well as the design variables and depends on the loading sequence. Typical design lives for high cycle fatigue structures like ship hulls and wind turbines blades range from 10^7 to 10^9 cycles and desired probabilities of failure may be on the order of $P_f \leq 10^{-6}$. In order to accurately assess the probability of failure, a huge number of simulation runs ($> 10^8$) will be required. Due to the length of a realistic design life, the TC model fatigue calculations to determine if failure occurs for each simulated specimen and load history will take a minute to a few hours on a modern computer. Thus the computational time required for such a simulation would be very high and would require parallel processing on a supercomputer to

complete the analysis in a reasonable amount of time. Statistical sampling biasing techniques may be used to reduce the number of simulations required. Instead, we present an alternative approximate method that greatly reduces the number of model evaluations required.

The proposed method for determining ϕ and γ based on the TC model makes the assumption that the distribution of residual strength does not depend strongly on the location of occasional rare events in the time history. This assumption is supported empirically by experimental fatigue results including the high-to-low and low-to-high spectrum loading performed by Post et al. [2, 77] that resulted in statistically identical residual strength distributions. Also, the conclusion by Nijssen et al. [139] that the WISPER spectrum is considerably more damaging than WISPERX implies that the lower fatigue stress levels are significant and perhaps dominate in the fatigue degradation of the material because of their high occurrence frequency. Because fatigue failure is dependent on the current applied stress as well as the residual strength, the following approach will only be valid if all of the stress histories have an approximately constant distribution of extrema over the lifetime. This assumption was also previously included in deriving Equation 5.35.

The traditional LRFD approach only accounts for one failure mode at a time. Thus, if we consider both tensile and compressive failure, we need to consider both

$$\phi \overline{S}_{uts} \geq \gamma \overline{\sigma}_t \tag{5.36}$$

and

$$\phi \|\overline{S}_{ucs}\| \geq \gamma \|\overline{\sigma}_c\| \tag{5.37}$$

in the design process where the nominal tensile and compressive resistances are taken as the mean tensile strength, $\overline{S}_{uts}$, and mean compression strength, $\overline{S}_{ucs}$. The nominal load values $\overline{\sigma}_t$ and $\overline{\sigma}_t$ could be taken as the mean or the root mean square (RMS) of the peak and valley stress extrema distributions for the applied loading. As $\sigma_p < 0$ or $\sigma_v > 0$ do not contribute to the calculated tensile and compressive residual strength degradation respectively, such extrema points should be excluded from the calculation of the nominal loads. As only one design environment is considered, ϕ and γ will be the same for both tension and compression failure modes and will be calculated based on whichever failure mode is critical for the design and loading applied.

The previous discussion of Equation 5.35 leads us to consider the determination of the resistance factor ϕ and the load factor γ separately, reflecting variability in the material behavior and the effect of different load histories respectively. The TC model with $\rho(S_{uts}, S_{ucs}) = 1$ will obey the SLERA for a given applied load history so the percentile, p, of a fatigue failure is equal to the percentile of the initial strengths of that specimen. For example, the fatigue model analysis could be performed starting with the $F_{S_{uts}} = p = 10^{-6}$ percentile initial strength and the resulting life, N, will be the $F_N(N) = p = 10^{-6}$ percentile life. Thus, for a defined load sequence and desired reliability, we only need to run one model analysis to determine if the specimen fails prior to n_d given an initial strength percentile equal to the desired probability of failure, a starting value of ϕ. For this part of the analysis, we will

assume that $\gamma = 1$. If the specimen fails prior to n_d, then ϕ should be decreased and the model run again until $N \geq n_d$. If the specimen does not fail before n_d is reached, ϕ can be increased. This process is shown conceptually as a life vs. ϕ plot in Figure 5.10. Only a handful of iterations should be required to arrive at a value of ϕ that gives approximately the desired reliability. The calculation so far only applies to one load sequence and the ϕ that was determined is dependent on the material variability and the change in the residual strength over the fatigue life.

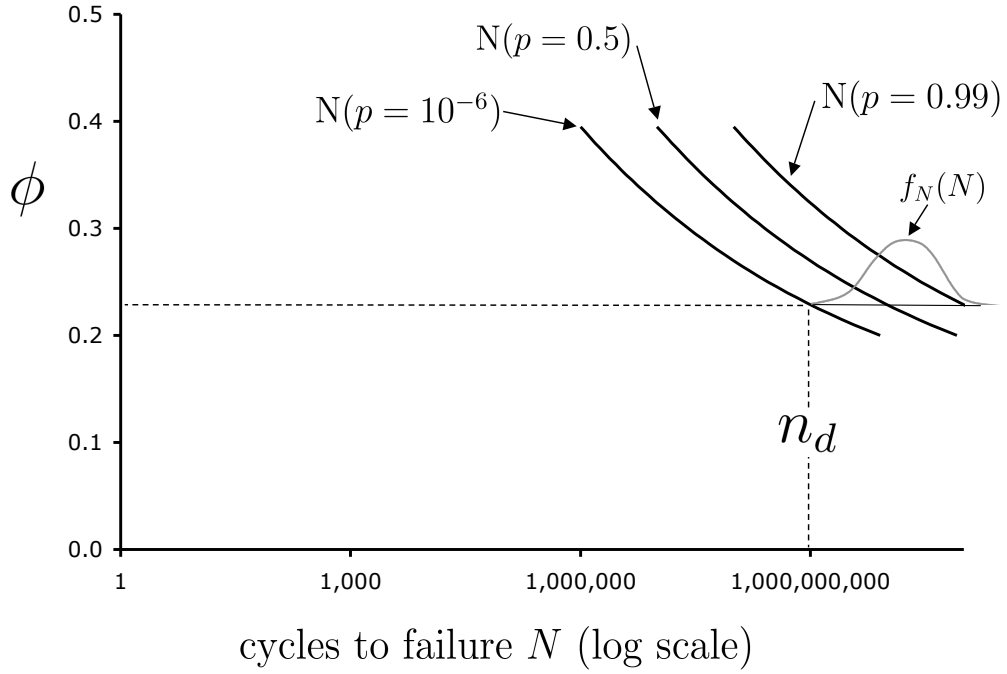

Figure 5.10: Conceptual representation of the first step in the reliability analysis to determine ϕ for the desired probability of failure p and life n_d. Values of n_d and ϕ are fictional and are provided to improve for clarity of the figure.

In general, there are an infinite number of possible load sequences, even if they all follow the same distributions, f_{Fa_t} and f_{Fa_c}, and have the same autocorrelation between the extrema. Because the TC model is load order dependent for reversing fatigue loads, and because the spectrum fatigue failure will be highly dependent on the occurrence of relatively rare extreme stress events, the probability of failure over the design life will vary as a function of the load history simulated. To assess the impact of the variability in load history, a series of load histories following the underlying distribution and autocorrelation should be simulated or potentially measured experimentally. For each load history, the probability of failure over the design life can be determined by iteratively selecting different percentiles of the initial strength distribution until the specimen fails at the design life. These P_f points will approximate the distribution of probability of failures for any load history sequence.

We envision that this distribution may be approximately Gaussian as depicted in Figure 5.11. The average probability of failure, $\overline{P_f}$, is the probability of failure for the design if each simulated load history has an equal probability of occurring. If $\overline{P_f}$ is less than the desired probability of failure then γ should be increased and the previous analysis repeated until the desired P_f is reached. Because only the mean of the distribution of P_f is required, only a small number of load sequence simulations (on the order of 10) are required and a suitable value of γ for the desired probability of failure could be found after a handful of iterations. Thus, the entire process of determining ϕ and γ for a desired probability of failure is performed using 100 to 200 model evaluations. Computationally, this entire process is reasonable and would take at most a few days on a single personal computer, even if each model evaluation lasted several hours to calculate failures over a design life of 10^9 cycles.

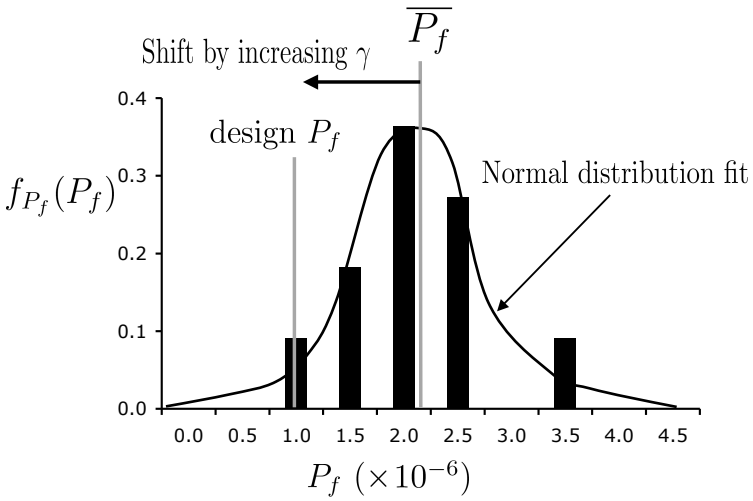

Figure 5.11: Conceptual representation of the distribution of P_f generated by repeated simulation of the load history. Values of P_f and f_{P_f} are fictional and are provided to give clarity to the figure. Comparison to the desired P_f enables γ to be determined.

The proposed method is an approximate calculation of the theoretical probability of failure given by Equation 5.35 because the interaction between the distribution of material properties and the relative reduction in strength caused by the simulated load histories is not included. Although the calculations are performed in terms of fatigue lives, occasional rare extreme stress events, even if they only occur in a fraction of the simulated load histories, will be accounted for because they will shift the distribution of P_f calculated in the second stage higher. Thus, care must be taken when selecting the underlying distribution of the applied loads, especially if very long stress histories are to be simulated. If an infinite distribution, (e.g. Rayleigh or exponential) is used, then for a long stress history, it is probable that a single peak exceeding even the initial strength will exist unless an extremely small ϕ is selected. Therefore, other design considerations should be taken into account before blindly applying such a load distribution to this analysis. For example, perhaps a different compo-

nent will fail first if a specific stress value is exceeded and relieve the stress on the component of interest in the design problem. Alternatively, the failure of a different component at an extreme load level might cause catastrophic failure of the entire structure in which case we are no longer concerned with the survival of the component of interest. Or perhaps there are some physical constraints on the maximum loads. In any of these cases, the distribution of applied loads might be truncated at an extreme value. In contrast, traditional fatigue reliability analysis only relies on the computation of the average damage rate and will not be affected significantly by rare extreme events so the use of an infinite distribution model for the applied loads does not significantly affect the resulting probability outcome.

5.5 Conclusions

This paper presented the probabilistic treatment of a model for calculating the residual strength distribution of tensile and compressive strength of a composite material as a function of an arbitrary load history. The application of this model to reliability-based design was discussed and a computationally efficient approximate method for calculating LRFD knockdowns was described. The proposed residual strength approach has several significant advantages over the traditional fatigue analysis for reliability-based design:

1. Any simulated or experimentally measured load history described as a series of local extrema can be used as input without Rainflow analysis.
2. The tension and compression failure modes are handled explicitly so rare extreme events are significant in determining the probability of failure. As a result, care must be taken when selecting an infinite theoretical distribution to represent the load distribution for a long stress history.
3. Variation in the load sequence is included in the assessment of the probability of failure.
4. The variability in material behavior is treated separately from variability in the load sequence.

Acknowledgments
Financial support for this research was provided by the Office of Naval Research (Award #N00014-06-1-0812). Note: The opinions expressed herein are the views of the authors and should not be interpreted as the views of the Naval Surface Warfare Center or the Department of the Navy.

Chapter 6

Conclusion

The four papers presented in this dissertation provide a logical progression toward an improved reliability-based design methodology for fatigue of composite materials subjected to in-plane axial spectrum fatigue loading.

6.1 Review and comparison of variable amplitude fatigue models

In Chapter 2 analysis of present models in the literature showed that several of the recent approaches for variable amplitude block loading fatigue are not applicable to generalized spectrum fatigue. A comparison of 12 approaches that could be applied to a generalized spectrum showed that the simple linear residual strength approach (Broutman and Sahu) provides an overall improvement in fatigue life prediction compared to the Palmgren Miner rule or other damage accumulation laws. More complex "non-linear" residual strength degradation models provided better results than Broutman and Sahu in some cases, but overall were not consistently better and the additional requirements for empirically fitting data are a disadvantage. We also noted that the the residual strength approaches previously available are only capable of calculations for one failure mode (either tension or compression) while the damage accumulation approaches do not explicitly consider a failure mode and thus they do not handle rare extreme stress events accurately.

6.2 Evaluation of load order effects by autocorrelation

Chapter 3 was focused on experimental evaluation of the impact of load order in the residual strength and life of FRP composites under spectrum fatigue. Evaluation of load history randomness by the first order autocorrelation of stress events was proposed. Because most of the models presented in Chapter 3 provide a load order independent calculation of the residual strength, understanding if and when the degree of randomness in the sequence of a spectrum load becomes significant is critical if these models are to be successfully employed. Previous experimental data and replicated fatigue tests as part of this research showed that for an extreme case of a totally ordered spectrum compared to a totally random sequence of the same loads under nominal $R = 0.1$ tension-tension fatigue load sequence, the randomization had a dramatic impact on the residual strength and fatigue life. The behavior of the highly random spectrum was not captured by residual strength models in this case. However, for fully reversed Rayleigh distributed spectrum loads over a wide range of autocorrelations and for the semi ordered primarily tension standard spectra like WISPER and WISPERX there was no evidence of load sequence impact on the fatigue results. While the factors that affect when load sequence is particularly detrimental to these composites remain unknown, this research did show that for approximately reversed fatigue under Rayleigh distributed loading, load sequence was not critical in the material behavior.

Thus we proceeded to consideration of a residual strength-based modeling approach that does not explicitly account for "cycle mix" events.

6.3 Development of the tension and compression residual strength model

Chapter 4 makes the case for a fatigue model that can track the change in both tension and compression residual strength under a general loading. Based on observations of empirical data and a discussion of the micro-mechanics deterioration and failure phenomena of FRP composites under fatigue loading, a new residual strength "TC model" was proposed. The model couples the rate of tensile residual strength degradation to the current residual compressive strength and vice versa. Reversed constant amplitude fatigue cycles are treated as spectrum fatigue cases containing first a tension cycle followed by a compression cycle and so on. For variable amplitude fatigue loads containing both tension and compression stresses, the model results will be dependent on the load history. The new model contains 12 material parameters that must be selected so that the model provides a good representation of experimental constant amplitude fatigue data. Then residual strength, fatigue life, and the final failure mode can be predicted for any load history based on the series of local stress extrema. Traditional Rainflow analysis to reduce a spectrum to a histogram of complete hysteresis loops is not required. As a result, the spectrum load order is maintained when performing analysis with the new model. Results showed very good agreement to experimental data in two material systems for a Rayleigh distributed spectrum and the WISPER spectrum.

6.4 Implementation of the TC residual strength model for reliability-based design

The final step toward reliability-based design was proposed in Chapter 5. First a stochastic implementation of the new TC model was considered. Based on Monte-Carlo simulation results compared to experimental data under constant amplitude and Rayleigh distributed reversed fatigue loads, it was found that the distribution of fatigue life could be adequately represented by taking the initial tension and compression strengths as 100% correlated stochastic variables and the remaining 10 model parameters as deterministic material constants. To precisely calculate the probability of failure over a design life for a given stochastic description of the applied loads, a computationally expensive Monte-Carlo simulation would be required because the fatigue response and failure criterion both depend on the history of applied loads which is itself randomly generated. Instead, an approximate method was proposed by separating the resistance knockdown factor required to compensate

for the fatigue degradation and variability in the material from the load factor required to compensate for variability due to the applied spectrum fatigue history. This method will enable calculation of the load and resistance factor design parameters with relatively few model evaluations while still accounting for the impact of rare extreme events. The proposed approach has several advantages over traditional lifetime damage sum accumulation reliability analysis, however, the definition of the applied load distribution will have to be considered carefully with regard to the occurrence of extreme stresses that may exceed the initial material strength.

6.5 Summary

This dissertation has developed a process for computing reliability-based design knockdown factors for an FRP composite under axial spectrum fatigue loading given a desired component reliability. The method proposed requires readily collected constant amplitude fatigue data for the laminate of interest to fit model parameters and a stochastic definition of the applied loads and load history order that the structure is expected to experience. Thus, a new methodology based was proposed that could provide a significant step forward for reliability-based design of composite material structures. Future work will be required to evaluate the accuracy of this approach in various situations and to provide specific applied examples.

6.6 Future work

Although it is impossible to prove the accuracy of an empirically fit model for all possible load cases, further experiments on load spectra designed to evaluate the impact of tension and compression damage and failure mode will help to build confidence in the TC model approach. These experiments could include spectra with primarily compression cycles that include occasional tension cycling, broadband (multiple frequency) and non-Gaussian distributed fatigue loading, and further measurements of both tension and compression residual strength under various spectra loads. The results of these experiments will serve to extend the range where we have confidence in the TC model or bound that range by determining situations where the model is less effective.

We know that the TC model, like its simpler tension only version used in previous efforts, does not adequately describe the fatigue process for a long histogram spectra when it is applied in a random order. It is still unclear why the randomized loads cause so much more fatigue damage than the order loading in this case while under a shorter repeated spectra, load order did not make a detectable difference in fatigue life. Future experiments on mid-length spectra and different histograms may provide information that will help to explain these observations.

Simulations for various example cases will be required to assess the accuracy of the approximate method for calculating reliability knock-downs proposed in Chapter 5. For a given load spectra (for example, Rayleigh distributed reversed loading) and desired probability of failure the load and resistance factors can be calculated using the proposed method. Then a Monte-Carlo simulation can be performed to calculate the probability of failure with those load and resistance factors and the result compared to the desired probability of failure. For unrealistically high probabilities of failure and shorter lifetimes, experiments might also be run to empirically verify the probability of failure.

There are many other factors including moisture, temperature, UV exposure, biaxial stress states, out-of-plane loading, stress concentrations, etc. that were not considered in the present analysis but may impact the composite degradation and thus the probability of failure. Inclusion of these additional impacts and the possibility of interaction with fatigue damage progression will need to be considered in the development of comprehensive composite structure reliability calculations. The proposed residual strength approach is well suited to extension for the inclusion of other degradation phenomenon.

Bibliography

[1] N L Post, J J Lesko, and S W Case. Modeling the variable amplitude fatigue of composite materials: a review and evaluation of the state of the art for spectrum loading. *In review, Int J Fatigue*, 2008.

[2] N L Post, J J Lesko, and S W Case. Fatigue durability of E-glass composites under variable amplitude loading: the importance of load sequence. In *Accepted for publication: Scientific Track proceedings of the European Wind Energy Conference*, 2008.

[3] N L Post, S W Case, and J J Lesko. A new phenomenological model fo rthe tension and compression residual strength of fiber dominated composite materials. *In review, Composites Science and Technology*, 2008.

[4] N L Post, S W Case, and J J Lesko. Reliability based design of composites under high cycle variable amplitude fatigue: a new residual strength formulation. *In review, Composites Science and Technology*, 2008.

[5] N L Post. *Reliability based design methodology incorporating residual strength prediction of structural fiber reinforced polymer composites under stochastic variable amplitude fatigue loading*. PhD thesis, Virginia Polytechnic Institute and State University, 2008.

[6] A Fatemi and L Yang. Cumulative fatigue damage and life prediction theories: a survey of the state of the art for homogeneous materials. *Int. J. of Fatigue*, 20(1):9–34, 1998.

[7] M S Found and M Quaresimn. Two-stage fatigue loading of woven carbon fibre reinforced laminates. *Fatigue Fract Engng Mater Struct*, 26:17–26, 2003.

[8] MA Miner. Cumulative damage in fatigue. *J. Applied Mechanics*, 12:A159–A164, 1945.

[9] L J Broutman and S Sahu. A new theory to predict cumulative fatigue damage in fiberglass reinforced plastics. In *Composite Materials: Testing and Design (Second Conference) ASTEM STP 497*, pages 170–188. American Society for Testing and Materials, 1972.

[10] S M Marco and W L Starkey. A concept of fatigue damage. *Trans. ASME*, 76:627–632, 1954.

[11] Z Hashin and A Rotem. A cumulative damage theory of fatigue failure. *Mat Sci and Eng*, 34:147–160, 1978.

[12] J A Epaarachchi. A study on estimation of damage accumulation of glass fibre reinforced plastic (GFRP) composites under a block loading situation. *Composite Structures*, 75:88–92, 2006.

[13] J A Epaarachchi and P D Clausen. A new cumulative fatigue damage model for glass fibre reinforced plastic composites under step/discrete loading. *Composites: Part A*, 36(9):1236–1245, 2005.

[14] S Sarkani, G Michaelov, D P Kihl, and D L Bonanni. Comparative study of nonlinear damage accumulation models in stochastic fatigue of frp laminates. *J. of Structural Engineering*, 127(3):314–322, 2001.

[15] P A Filis, I R Farrow, and I P Bond. Classical fatigue analysis and load cycle mix-event damage accumulation in fibre reinforced laminates. *Int. J. of Fatigue*, 26:565–573, 2004.

[16] T P Philippidis and V A Passipoularidis. Residual strength after fatigue in composites: theory vs. experiment. *Int. J. Fatigue*, 29:2104–2116, 2007.

[17] Z Hashin. Cumulative damage theory for composite materials: residual life and residual strength methods. *Composites Science and Technology*, 23:1–19, 1985.

[18] W Hwang and K S Han. Statistical study of strength and fatigue life of composite materials. *Composites*, 18:47–53, 1987.

[19] H A Whitworth. Cumulative damage in composites. *J. of Engineering Materials and Technology*, 112:358–361, 1990.

[20] M H R Jen, Y S Kau, and I C Wu. Fatigue damage in a centrally notched composite laminate due to two-step spectrum loading. *Int. J. of Fatigue*, 16:193–201, 1993.

[21] T Adam, N Gathercole, H Reiter, and B Harris. Life prediction for fatigue of T800/5245 carbon-fibre composites: II. variable-amplitude loading. *Int. J. of Fatigue*, 16(8):533–547, 1994.

[22] N Gathercole, H Reiter, T Adam, and B Harris. Life prediction for fatigue of T800/5245 carbon-fibre composites: I. constant amplitude loading. *Int. J. of Fatigue*, 16(8):523–532, 1994.

[23] B L Lee and D S Liu. Cummulative damage of fiber-reinforced elastomer composites under fatigue loading. *J. of Composite Materials*, 28(13):1261–1286, 1994.

[24] H Noguchi, Y H Kim, and H Nisitani. On the cumulative fatigue damage in short carbon fiber reinforced poly-ether-ether-ketone. *Engineering Fracture Mechanics*, 51(3):457–468, 1995.

[25] N Otani and D Y Song. Fatigue life prediction of composites under two-stage loading. *J of Materials Science*, 32:755–760, 1997.

[26] B Harris, N Gathercole, H Reiter, and T Adam. Fatigue of carbon-fiber-reinforced plastics under block-loading conditions. *Composites Part A*, 28A:327–337, 1997.

[27] J Bartley-Cho, S G Lim, H T Hahn, and P Shyprykevich. Damage accumulation in quasi-isotropic graphite epoxy laminates under constant-amplitude fatigue loading. *Composites Science and Technology*, 58:1535–1547, 1998.

[28] W vanPaepegem and J Degrieck. Effects of load sequence and block loading on the fatigue responce of fiber-reinforced composites. *Mechanics of Advanced Materials and Structures*, 9:19–35, 2002.

[29] C H Lee and M H R Jen. Fatigue responce and modeling of variable stress amplitude and frequency in AS-4/Peek composite laminates, part 1: Experiments. *J. of Composite Materials*, 34(11):906–929, 2000.

[30] E K Gamstedt and B A Sjögren. An experimental investigation of the sequence effect in block amplitude loading of cross-ply composite laminates. *Int. J. Fatigue*, 24:437–446, 2002.

[31] S Sarkani and L D Lutes. Fatigue experiments for welded joints under pseudo-narrowband loads. *J. Structural Engineering*, 114(8):1901–1916, 1988.

[32] D P Kihl, S Sarkani, and J E Beach. Stochastic fatigue damage accumulation under broadband loadings. *Int. J. Fatigue*, 17(5):321–329, 1995.

[33] T Svensson. Prediction uncertainties at variable amplitude fatigue. *Int. J. Fatigue*, 19(1):S295–S302, 1997.

[34] R Sunder. Spectrum load fatigue - underlying mechanisms and their significance in testing and analysis. *Int. J. of Fatigue*, 25:971–981, 2003.

[35] S Sarkani, G Michaelov, D P Kihl, and J E Beach. Stocastic fatigue damage accumulation of FRP laminates and joints. *J. of Structural Engineering*, 125(12):1423–1431, 1999.

[36] D P Kihl, D L Bonanni, S Sarkani, and G Michaelov. A comparative study of non-linear damage accumulation models in stochastic fatigue of glass fiber reinforced laminates and joints. Technical Report NSWCCD-66-TR-2000/27, US Navy: Naval Surface Warfare Center Carderock Division, West Bethesda, MD 20817, 2001.

[37] M Aboussaleh and R Boukhili. Life prediction for composite laminates submitted to service loading spectra. *Polymer Composites*, 19(3):241–245, 1998.

[38] N Himmel. Fatigue life prediction of laminated polymer matrix composites. *Int. J. Fatigue*, 24:349–360, 2002.

[39] T P Philippidis and A P Mouritz. Life prediction methodology for GFRP laminates under spectrum loading. *Composites: Part A*, 35:657–666, 2004.

[40] C M Sonsino and E Moosbrugger. Fatigue design of highly loaded short-glass-fiber reinforced polyamide parts in engine components. *Int. J. Fatigue*, 2007.

[41] J F Mandell. DOE/MSU composite material fatigue database. Technical report, Sandia National Laboratories, Albuquerque, NM 87185, 2004.

[42] D Schultz and J J Gerharz. Fatigue strength of a fibre-reinforced material. *Composites*, 8:245–250, 10 1977.

[43] I P Bond. Fatigue life prediction for GRP subjected to variable amplitude loading. *Composites: Part A*, 30:961–970, 1999.

[44] I P Bond and I R Farrow. Fatigue life prediction under complex loading for XAS/914 CFRP incorporating a mechanical fastner. *Int. J. of Fatigue*, 22:633–614, 2000.

[45] T Nyman, H Ansell, and A Blom. Effects of truncation and elimination on composite fatigue life. *Composite Structures*, 48:275–286, 2000.

[46] J Schon and A Blom. Fatigue life prediction and load cycle elimination during spectrum loading of composites. *Int. J. of Fatigue*, 24:361–367, 2002.

[47] N Wahl, D Samborsky, J Mandell, and D Cairns. Spectrum fatigue lifetime and residual strength for fiberglass laminates in tension. In *ASME Wind Energy Symposium*, number AIAA-2001-0025. ASME/AIAA, 2001.

[48] N Wahl, D Samborsky, J Mandell, and D Cairns. Effects of modeling assumptions on the accuracy of spectrum fatigue lifetime predictions for a fiberglass laminate. In *AIAA-2002-0023*, pages 19–26. AIAA/ASME, 2002.

[49] N K Wahl and J F Mandell. Spectrum fatigue lifetime and residual strength for fiberglass laminates. Contractor Report SAND2002-0546, Sandia National Laboratories, Albuquerque, NM 87185, 2001.

[50] J Schon. Spectrum fatigue loading of composite bolted joints-small cycle elimination. *Int. J. of Fatigue*, 28:73–78, 2006.

[51] Knowledge Center WMC, Optimat Blades Optidat material database.

[52] A A tenHave. WISPER and WISPERX final definition of two standardized fatigue loading sequences for wind turbine blades. Technical Report NLR TP 91476 U, National Aerospace Laboratory NLR, Netherlands, 09 1992.

[53] A A tenHave. WISPER and WISPERX: a summary paper describing their backgrounds, derivation and statistics. *Wind Energy*, 14:169–178, 1993.

[54] A P Vassilopoulos, E F Georgopoulos, and V Dionysopoulos. Artifical neural networks in spectrum fatigue life prediction of composite materials. *Int. J. of Fatigue*, 29:20–29, 2007.

[55] N E Dowling. A review of fatigue life prediction methods. Technical Paper Series 871966, SAE Technical Paper Series, 400 Commonwealth Drive, Warrendale, PA 15096, 10 1987.

[56] P S Veers, T D Ashwill, H J Sutherland, D L Lairda, D W Lobitz, D A Griffin, J F Mandell, W D Musial, K Jackson, M Zuteck, A Miravete, S W Tsai, and J L Richmond. Trends in the design, manufacture and evaluation of wind turbine blades. *Wind Energy*, 6:245–259, 2003.

[57] S R Winterstein and C H Lange. Load models for fatigue reliability from limited data. In *Wind Energy*, volume 16. ASME SED, 1995.

[58] S R Winterstein and T Kashef. Moment-based load and response models with wind engineering applications. In *ASME Wind Energy Symposium*, 1999.

[59] C H Lange. Probabilstic fatigue methodolgy and wind turbine reliability. Contractor Report SAND96-1246, Sandia National Laboratories, Albuquerque, NM 87185, 5 1996.

[60] H J Sutherland. On the fatigue analysis of wind turbines. Technical Report SAND99-0089, Sandia National Laboratories, Albuquerque, NM 87185, 6 1999.

[61] J F Mandell, R M Reed, and D D Samborsky. Fatigue of fiberglass wind turbine blade materials. Contractor Report SAND92-7005, Sandia National Laboratories, Albuquerque, NM 87185, 8 1992.

[62] D P Kihl. Stocastic fatigue concepts in welded surface ship structures. Departmental Report SSPD-90-173-25, US Navy: David Taylor Research Center, Bethesda, MD 20084, 1990.

[63] I A Assakkaf and J F Cardenas-Garcia. Reliability-based design of doubler plates for ship structures. In *Proceedings of the Fourth International Symposium on Uncertainty Modeling and Analysis (ISUMA'03)*. The Computer Society, IEEE, 2003.

[64] L Minnetyan and C C Chamis. Cyclic fatigue degradation responce of composite structures. In *47th Internationall SAMPE Symposium*, pages 1632–1646, 2002.

[65] P H Miller. Fatigue prediction varification of fiberglass hulls. *Marine Technology*, 38(4):278–292, 2001.

[66] V M Harik and T A Bogetti. Low cycle fatigue of composite laminates: A damage-mode-sensitive model. *J. of Composite Materials*, 37(7):597–609, 2003.

[67] W Hwang and K S Han. Fatigue of composites - fatigue modulus concept life prediction. *J. of Composite Materials*, 20:154–165, 1986.

[68] C H Lee and M H R Jen. Fatigue responce and modeling of variable stress amplitude and frequency in AS-4/Peek composite laminates, part 2: Analysis and formulation. *J. of Composite Materials*, 34(11):930–953, 2000.

[69] M J Owen and R J Howe. The accumulation of damage in a glass-reinforced plastic under tensile and fatigue loading. *J. Phys. D: Appl. Phys.*, 5:1637–1649, 1972.

[70] P C Chou and R Croman. Residual strength in fatigue based on the strength-life equal rank assumption. *J. Composite Materials*, 12:177–194, 1978.

[71] H T Hahn and R Y Kim. Proof testing of composite materials. *J. Composite Materials*, 9:297–311, 1975.

[72] J M Whitney. Fatigue characterization of composite materials. In *Fatigue of Fiberous Composite Materials, ASTM STP 723*, pages 133–151, 1981.

[73] K L Reifsnider and W W Stinchcomb. A critical-element model of the residual strength and life of fatigue loaded composite coupons. In H T Hahn, editor, *Composite Materials: Fatigue and Fracture, ASTM STP 907*, pages 298–313. American Society for Testing and Materials, 1986.

[74] K L Reifsnider. The critical element model: A modeling philosophy. *Engineering Fracture Mechanics*, 25:739–749, 1986.

[75] S W Case and K L Reifsnider. Fatigue of composite materials. *Comprehensive Structural Integrity*, 4:1–38, 2002.

[76] N L Post, J Bausano, S W Case, and J J Lesko. Modeling the remaining strength of structural composite materials subjected to fatigue. *Int. J. of Fatigue*, 28:1100–1108, 2006.

[77] N L Post, J Cain, K J McDonald, S W Case, and J J Lesko. Residual strength prediction of composite materials: Random spectrum loading. *Engineering Fracture Mechanics*, 75(9):2707–2724, 2008.

[78] J R Schaff and B D Davidson. Life prediction methodology for composite structures. part 1 - constant amplitude and two-stress level fatigue. *J. of Composite Materials*, 31(2):128–157, 1997.

[79] J R Schaff and B D Davidson. Life prediction methodology for composite structures. part ii - spectrum fatigue. *J. of Composite Materials*, 31(2):158–181, 1997.

[80] J N Yang and M D Liu. Residual strength degredation model and theory of periodic proof tests for graphite/epoxy laminates. *J. Composite Materials*, 11:176–203, 1977.

[81] R P L Nijssen, D D Samborsky, J F Mandell, and D R V vanDelft. Strength degredation and simple load spectrum tests in rotor blade composites. In *ASME Wind Energy Symposium*, number AIAA-2005-0197, pages 28–38. ASME/AIAA, 2005.

[82] H T Hahn. Fatigue behavior and life prediction of composite laminates. In S W Tsai, editor, *Composite Materials: Testing and Design (Fifth Conference)*, STP 674, pages 383–417. ASTM, American Society for Testing and Materials, 1979.

[83] W Weibull. *A statistical theory of the strength of materials*. Number N64 81687. National Technical Information Service, Springfield, VA 22161, 1939.

[84] P C Chou and R Croman. Degradation and sudden-death models of fatigue of graphite/epoxy composites. In S W Tsai, editor, *Composite Materials: Testing and Design (Fifth Conference)*, STP 674, pages 431–454. ASTM, American Society for Testing and Materials, 1979.

[85] J N Yang. Fatigue and residual strength degradation for graphite/epoxy composites under tension-compression cyclic loadings. *J. Composite Materials*, 12:19–39, 1978.

[86] J N Yang and D L Jones. Effect of load sequence on the statistical fatigue of composites. *AIAA Journal*, 18(12):1525–1531, 1980.

[87] J N Yang, R K Miller, and C T Sun. Effect of high laod on statistical fatigue of unnotched graphite/epoxy laminates. *J. Composite Materials*, 14:82–94, 1980.

[88] J N Yang and S Du. An exploratory study into the fatigue of composites under spectrum loading. *J. of Composite Materials*, 17:511–526, 1983.

[89] A Rotem. Residual strength after fatigue loading. *Int. J. Fatigue*, 10(1):27–31, 1988.

[90] A Rotem and H G Nelson. Residual strength of composite laminates subjected to tensile-compressive fatigue loading. *J. of Composites Technology and Research*, 12(2):76–84, 1990.

[91] T Adam, R F Dickson, C J Jones, H Reiter, and B Harris. A power law fatigue damage model for fibre-reinforced plastic laminates. *Proc Instn Mech Engrs*, 200:155–165, 1986.

[92] J A Epaarachchi and P D Clausen. An emperical model for fatigue behavior prediction of glass fibre-reinforced plastic composites for various stress ratios and test frequencies. *Composites: Part A*, 34:313–326, 2003.

[93] R W Hertzberg and J A Manson. *Fatigue of Engineering Plastics*. Academic Press, New York, 1980.

[94] P Qiao and M Yang. Fatigue life prediction of pultruded e-glass/polyurethane composites. *J. of Composite Materials*, 40(9):815–837, 2006.

[95] K L Reifsnider and R Jamison. Fracture of fatigue-loaded composite laminates. *Int. J. Fatigue*, page 187, 10 1982.

[96] W X Yao and N Himmel. A new cumulative fatigue damage model for fibre-reinforced plastics. *Composites Science and Technology*, 60:59–64, 2000.

[97] K L Reifsnider and Z Gao. A micromechanics model for composites under fatigue loading. *Int. J. of Fatigue*, 13(2):149–156, 1991.

[98] Z-M Huang. Micromechanical modeling of fatigue strength of unidirectional fibrous composites. *Int. J. of Fatigue*, 24:659–670, 2002.

[99] Z-M Huang. Fatigue life prediction of a woven fabric composite subjected to biaxial cyclic loads. *Composites: Part A*, 33:253–266, 2002.

[100] Z-M Huang. Simulation of the mechanical properties of fibrous composites by the bridging micromechanics model. *Composites: Part A*, 32:143–172, 2001.

[101] Y A Dzenis, S P Joshi, and A E Bogdanovich. Behavior of laminated composites under monotonically increasing random load. *AIAA Journal*, 31(12):2329–2334, 1993.

[102] Y A Dzenis, A E Bogdanovich, and C M Pastore. Stocastic damage evolution in textile laminates. *Composites Manufacturing*, 4(4):187–193, 1993.

[103] Y A Dzenis and S P Joshi. Long-term strength damage analysis of laminated composites. *AIAA Journal*, 35(6):1057–1063, 1997.

[104] Y A Dzenis. Cycle-based analysis of damage and fatigue in advanced composites under fatigue. 1. Experimental observation of damage development within loading cycles. *Int. J. of Fatigue*, 25:499–510, 2003.

[105] Y A Dzenis. Cycle-based analysis of damage and fatigue in advanced composites under fatigue. 2. Stocastic mesomechanics modeling. *Int. J. of Fatigue*, 25:511–520, 2003.

[106] N V Akshantala and R Talreja. A micromechanics based model for predicting fatigue life of composite laminates. *Mat Sci and Eng*, A285:303–313, 2000.

[107] SP Pantelakis, Em Ch Kyriakakis, and P Papanikos. Non-dstructive fatigue damage characterization of laminated thermosetting fibrous composites. *Fatigue Fract Engng Mater Struct*, 24:651–662, 2001.

[108] P Papanikos, K I Tserpes, and SP Pantelakis. Modeling of fatigue damage progression and life of CFRP laminates. *Fatigue Fract Engng Mater Struct*, 26:37–47, 2003.

[109] Z Sun, I M Daniel, and J J Luo. Modeling of fatigue damage in a polymer matrix composite. *Mat Sci and Eng*, A361:302–311, 2003.

[110] K Yoshioka and J C Seferis. Modeling of tensile fatigue damage in resin transfer molded woven carbon fabric composites. *Composites: Part A*, 33:1593–1601, 2002.

[111] Z Hashin and A Rotem. A fatigue failure criterion for fiber reinforced materials. *J. Composite Materials*, 7:448–463, 1973.

[112] S W Tsai and E M Wu. A general theory of strength for anisotropic materials. *J. Composite Materials*, 5:58, 1971.

[113] X Diao, L YE, and Y-W Mai. Statistical prediction of fatigue failure of fiber reinforced composite materials. *Applied Composite Materials*, 2:153–173, 1995.

[114] Jacob Aboudi. Micromechanics prediction of fatigue failure of composite materials. *Reinforced Plastics and Composites*, 8:150–166, 1989.

[115] Z Fawaz and F Ellyin. A new methodology for the prediction of fatigue failure in multidirectional fiber reinforced laminates. *Compos Sci Technol*, 53:47–55, 1995.

[116] Y Miyano, M Nakada, and N Sekine. Accelerated testing for long-term durability of GFRP laminates for marine use. *J. of Composite Materials*, 39(1):5–20, 2005.

[117] R Christensen and Y Miyano. Stress intensity controlled kinetic crack growth and stress history dependent life prediciton with statistical variability. *Int J Fracture*, 137:77–87, 2006.

[118] R Christensen. A physically based cumulative damage formalism. *Manuscript draft, International Journal of Fatigue.*

[119] M M Shokrieh and L B Lessard. Progressive fatigue damage modeling of composite materials, Part I: Modeling. *J. of Composite Materials*, 34(13):1056–1080, 2000.

[120] M M Shokrieh and L B Lessard. Progressive fatigue damage modeling of composite materials, Part II: Material chatracterization and model verification. *J. of Composite Materials*, 34(13):1081–1116, 2000.

[121] Y Gowayed and H Fan. Fatigue behavior of textile composite materials subjected to tension-tension loads. *Polymer Composites*, 22(6):762–769, 2001.

[122] W Hwang and K S Han. Cummulative damage models and multi-stress fatigue life prediction. *J. of Composite Materials*, 20:125–153, 1986.

[123] H A Whitworth. Modeling stiffness reduction of graphite/epoxy composite lamiantes. *J. of Composite Materials*, 21:362–373, 1987.

[124] R Talreja. *Yielding, Damage, and Failure of Anisotropic Solids, Ed. J. P. Bochler*, chapter Internal variable damage mechanics of composite materials, pages 509–533. Number EGF5. Mechanical Engineering Publications, 1990.

[125] L J Lee, J N Yang, and D Y Sheu. Prediction of fatigue life for matrix-dominated composite laminates. *Composites Science and Technology*, 46:21–28, 1993.

[126] H S Kim and J Zhang. Fatigue damage and life prediction of glass/vinyl ester composites. *J. of Reinforced Plastics and Composites*, 20(10):834–848, 2001.

[127] K Momenkhani, S Sarkani, and D L Jones. Development and application of a model using center of gravity of hysteresis loops to predict fatigue damage accumluation in fiber-reinforced plastic laminates. *J. of Composite Materials*, 39(6):557–575, 2005.

[128] K Momenkhani and S Sarkani. A new method for predicting the life of fiber-reinforced plastic laminates. *J. of Composite Materials*, 40:1971–1982, 2006.

[129] W vanPaepegem and J Degreck. Coupled residual stiffness and strength model for fatigue of fibre-reinforced composite materials. *Composites Science and Technology*, 62(687):696, 2002.

[130] W vanPaepegem and J Degrieck. A new coupled approach of residual stiffness and strength for fatigue of fibre-reinforced composites. *Int. J. of Fatigue*, 24:747–762, 2002.

[131] J N Yang, Se H Yang, and D L Jones. A stiffness-based statistical model for predicting the fatigue life of graphite/epoxy laminates. *J. of Composites Technology and Research*, 11(4):129–134, 1989.

[132] W-F Wu, L J Lee, and S T Choi. A study of fatigue damage and fatigue life of composite laminates. *J. of Composite Materials*, 30(1):123–137, 1996.

[133] R Tang, Y-J Guo, and Y J Weitsman. An appropriate stiffness degradation parameter to monitor fatigue damage evolution in composites. *Int. J. of Fatigue*, 26:421–427, 2004.

[134] J F Mandell, D D Samborsky, and D S Cairns. Fatigue of composite materials and substructures for wind turbine blades. Technical Report SAND2002-0771, Sandia National Laboratories, Albuquerque, NM 87185, 2002.

[135] J F Mandell, D D Samborsky, L Wang, and N K Wahl. New fatigue data for wind turbine blade materials. In *41st Aerospace Sciences Meeting and Exhibit*, number AIAA-2003-0692, pages 1–13. AIAA, 2003.

[136] J Wedel-Heinen, J K Tadich, C Brokopf, L G J Janssen, A M vanWingerde, D R V Delft, Ch W Kensche, Th P Philippidis, P Brondsed, A G Dutton, and R P L Nijssen. Reliable optimal use of materials for wind turbine rotor blades. Technical Report OB-TG6-R002-000 R8, Implementation of OPTIMAT in technical standards, 2006.

[137] P Johannesson, T Svensson, and J deMaré. Fatigue life prediction based on variable amplitude tests - methodology. *Int. J. of Fatigue*, 27:954–965, 2005.

[138] W X Yao and N Himmel. Statistical analysis of data from truncated fatigue life and corresponding residual strength experiments for polymer matrix composites. *Int. J. of Fatigue*, 21:581–585, 1999.

[139] R P L Nijssen, D R V vanDelft, and A M vanWingerde. Alternative fatigue lifetime prediction formulations for variable-amplitude loading. *J of Solar Engineering*, 124:396–403, 2002.

[140] P S Veers and S R Winterstein. Applicaiton of measured loads to wind turbine fatigue and reliability analysis. In *ASME Wind Energy Symposium*. ASME/AIAA, 1 1997.

[141] S Sarkani. Feasibiilty of auto-regressive simulation model for fatigue studies. *J. Structural Engineering*, 116(9):2481–2495, 1990.

[142] AASHTO. *LRFD Bridge Design Specification*. American Association of State Highway and Transportation Officials, 2nd edition, 1998.

[143] B Ellingwood. Lrfd: implementing structural reliability in professional practice. *Engineering Structures*, 22:106–115, 2000.

[144] C H Lange and S R Winterstein. Fatigue design of wind turbine blades: load and resistance factors from limited data. In *ASME Wind Energy Symposium*. ASME/AIAA, 1996.

[145] C H Lange and S R Winterstein. Effect of load models and limited data on load and resistance factors for fatigue design. In *ASCE Specialty conf.*, 1996.

[146] B Ellingwood and T V Galambos. Probability-based criteria for structural design. *Strctural Safety*, 1:15–26, 1982.

[147] T V Galambos, B Ellingwood, J G Macgregor, and C A Cornell. Probability based load criteria: Assessment of current design practice. *J. of the Structural Division*, 108(5):959–977, 1982.

[148] B R Ellingwood. Toward load and resistance factor design for fiber-reinforced polymer composites structures. *J. of Structural Engineering*, 129(4):449–458, 2003.

[149] M Shinozuka. Basic analysis of structural safety. *J. of Structural Engineering*, 109(3):721–740, 1983.

[150] D G Robinson. A survey of probabilistic methods used in reliability, risk and uncertainty analysis: analytical techniques i. Technical Report SAND98-1189, Sandia National Laboratories, Albuquerque, NM 87185, 6 1998.

[151] J Tang and J Zhao. A practical approach for predicting fatigue reliability under random cyclic loading. *Reliability Engineering and System Safety*, 50:7–15, 1995.

[152] N E Dowling. Fatigue failure predictions for complicated stress-strain histories. *J. of Materials*, 7(1):71–87, 1972.

[153] S D Downing and D F Socie. Simple rainflow counting algorithms. *Int. J. Fatigue*, pages 31–41, January 1982.

[154] H J Sutherland and R M Osgood. Frequency-domain synthesis of the fatigue load spectrum for the nps 100-kw wind turbine. In *Proceedings of WindPower 92*, Washington, D.C., 1992. AWEA.

[155] H J Sutherland. Fatigue case study and loading spectra for wind turbines. In *IEA Fatigue Experts Meeting*, pages 77–87, 4 1994.

[156] H J Sutherland and P S Veers. Effects of cyclic stress distribution models on fatigue life predictions. *Wind Energy*, 16:83–90, 1995.

[157] A S R Murty, U C Gupta, and A R Krishna. A new approach to fatigue strength distribution for fatigue reliabiltiy evaluation. *Int. J. Fatigue*, 17(2):85–89, 1995.

[158] M Kaminski. On probabilistic fatigue models for composite materials. *International Journal of Fatigue*, 24:477–495, 2002.

[159] M Ichikawa. An extension of the reliability-based design method for variable amplitude fatigue. *Reliability Engineering*, 17:181–187, 1987.

[160] D Chen. New approaches to the estimation of cumulative fatigue reliability. *Reliability Engineering and System Safety*, 33:231–247, 1991.

[161] R B Abernethy, J E Breneman, C H Medin, and G L Reinman. Weibull analysis handbook. Final Report AFWAL0TR083-2079, Pratt and Whitney Aircraft, P. O. Box 2691, West Palm Beach, FL 33402, 1982.

Appendix A

Fatigue experiments for generation of data set at Virginia Tech

This appendix describes the material system, and test methods used in making and comparing model predictions for the VT8084 material system. The data has been compiled as a Microsoft Excel workbook and is publicly available for download along with this dissertation [5].

A.1 Material

The composite material used was manufactured at Virginia Tech by vacuum assisted resin transfer molding (VARTM). The fiber reinforcement was Vetrotex 324 woven roving E-glass which has a 5:4 bias in the warp direction and the layup (denoted by warp direction in each layer) was $[0/+45/90/\text{-}45/0]_s$. The matrix material was Ashland 8084 vinyl ester resin (30% styrene) with the cure package by weight consisting of Norox MEKP-925H peroxide initiator (1.5%), Cobalt napthenate catalyst (0.3%) and N, N-dimethyl aniline retarder (0.025%) resulting in a gel time of 50-70 minutes. Following a 24 hour cure period under ambient conditions, the material was post-cured for 4 hr at 82℃. Material was manufactured in a series of batches under identical procedure, each producing a 0.9 m by 0.9 m panel 0.613 cm thick that was then cut into specimens. A diamond tile saw was used for initial cutting of the specimens to nominal 2.6 cm wide by 15.2 cm long blanks. These blanks were then ground on the long edges to provide parallel sided specimens 2.540 +/- 0.002 cm wide. All specimens were cut so that the loading was in the 0 fiber direction. The cross sectional area of all the specimens was taken to be 1.558 cm^2 based on the average of area of 40 randomly selected specimens (very little variation was noted).

A.2 Experimental procedure

Testing took place using several 90 KN (20 kip) MTS servo-hydraulic load frames with hydraulic wedge grips. The load-frame servo-valves were controlled by MTS 407 controllers operated in external input mode. The desired load voltage signals were created by a custom LabView program and National Instruments PCI-6221 M series DAQ card that also recorded the load and strain response data. The gage length between the grips was maintained at 5.0 cm to insure that compression failures would occur by crushing rather than global buckling.

The distribution of initial quasi-static stiffness and strength were determined by breaking about 30 specimens each in monotonic tension and compression using load control with a loading rate of 667 N/s. Subsequent constant amplitude fatigue to failure tests were performed with T-T, T-C, and C-C R-ratios of 0.1,-1, and 10 respectively. The frequency was maintained at 5 Hz. for constant and variable amplitude fatigue testing. In all cases, a continuous sinusoidal driving fatigue loading waveform was created by fitting a cosine curve

between each peak and valley and then that valley and subsequent peak such that the slope of the curve was zero at each load reversal point.

The LabView program used for driving constant amplitude fatigue tests incorporated a feedback loop that monitored the resulting peaks and valleys and adjusted gain factors to multiply the driving signal peak and valley until the desired maximum and minimum loads were achieved. As the specimen stiffness degraded and the machine response changed, the program continuously updated the gains to maintain the desired loads. The MTS 407 PID gain tuning parameters were adjusted manually until the resulting load waveform was as close to a sinusoidal shape as possible. For variable amplitude loading, it was found that the required gain was a nonlinear function of the load applied. An algorithm was developed that dynamically adjusted gain functions, defined as continuous and piecewise linear on 2.22 KN intervals, based on how close the past cycles were to the desired loads. Using this algorithm, the peak and valley loads were generally maintained within +/- 133 N of the desired loads, a level of error that was considered acceptable as it is on the order of the noise in the load signal.

A.3 Fatigue modulus data

During fatigue, the peak and valley stress and corresponding strains are recorded for each cycle. Then the secant fatigue modulus, E_f, is calculated as:

$$E_f(n) = \frac{\sigma_p(n) - \sigma_v(n)}{\epsilon_p(n) - \epsilon_v(n)} \tag{A.1}$$

where $\sigma_p(n)$ and $\sigma_v(n)$ are the peak and valley stresses of the n^{th} cycle and $\epsilon_p(n)$ and $\epsilon_v(n)$ are the strain recorded at those peak and valley stress. Then a normalized modulus is calculated for selected fractions of the fatigue life (or applied cycles for a residual strength measurement):

$$E_{norm}\left(\frac{n}{N}\right) = \frac{E(n)}{E(1)} \tag{A.2}$$

where N is the maximum number of cycles applied during the test and $E(1)$ is the secant modulus of the first cycle. These values are tabulated in the data set for most of the fatigue tests at various fractions of life.

A.4 Experimental data

The experimental test types are described as follows. Details of the applied spectrum fatigue loads are provided on separate worksheets within the data workbook. The random version

of the POST2007 spectrum is provided in terms of normalized values as a text file because the 735,000 cycles exceed the limit of an Excel Workbook.

- STT Quasi-static tension loading to failure
- STC Quasi-static compression loading to failure
- CA Constant amplitude fatigue to failure
- RST Tensile residual strength after constant amplitude fatigue
- RSC Compressive residual strength after constant amplitude fatigue
- PRST Premature fatigue failure of specimen intended for RST measurement
- PRSC Premature fatigue failure of specimen intended for RSC measurement
- RAY_#.## Nominally fully reversed Rayleigh distributed spectrum loading fatigue to failure where #.## is the autocorrelation of the absolute value of extrema
- RAYRSC_0.95 Residual compression strength measurement under nominally fully reversed Rayleigh distributed spectrum fatigue to failure with a 95% autocorrelation of successive extrema.
- POST2007HL Highest to lowest histogram stress spectrum residual strength measurement based on [77]
- POST2007LH Lowest to highest histogram stress spectrum residual strength measurement based on [77]
- POST2007R Randomized version of the histogram spectrum residual strength measurement based on [77]
- RAYr0.1_#.## Nominally $R = 0.1$ spectrum fatigue with Rayleigh distributed peaks equal to the corresponding RAY_#.## spectrum and following valleys fixed at $R = 0.1$
- N2CHIST An additional ordered histogram fatigue loading case
- N2CHISTRSC Residual compression strength measurements under the N2CHIST spectrum fatigue

Appendix B

VT8084 Data

The entire fatigue data is provided in Microsoft Excel Workbook format and can be downloaded along with this dissertation from [5].

Vita

Nathan Post grew up in central Vermont. He was home-schooled prior to attending Vermont Technical College in place of his senior year of high-school. In 2003, Nathan received a Bachelors of Science with University Honors degree in Mechanical Engineering from Clarkson University, Potsdam NY. Following this, he enrolled at Virginia Tech as a graduate student in the Engineering Science and Mechanics Department, earning his M.S. (2006) and Ph.D. (2008) degrees in Engineering Mechanics. Nathan's interests and hobbies outside of his academic research include sailing, contra dance and country waltzing, horsemanship, skiing, bicycling, and environmental philosophy.